

In presenting the dissertation as a partial fulfillment of the requirements for an advanced degree from the Georgia Institute of Technology, I agree that the Library of the Institute shall make it available for inspection and circulation in accordance with its regulations governing materials of this type. I agree that permission to copy from, or to publish from, this dissertation may be granted by the professor under whose direction it was written, or, in his absence, by the Dean of the Graduate Division when such copying or publication is solely for scholarly purposes and does not involve potential financial gain. It is understood that any copying from, or publication of, this dissertation which involves potential financial gain will not be allowed without written permission.

7/25/68

AN EXPERIMENTAL INVESTIGATION OF INDIVIDUAL
AUDITORY NERVE FIBER ACTIVITY

A THESIS

Presented to

The Faculty of the Graduate Division

by

Huey Neal Nunnally

In Partial Fulfillment

of the Requirements for the Degree

Doctor of Philosophy

in the School of Electrical Engineering

Georgia Institute of Technology

March, 1971

AN EXPERIMENTAL INVESTIGATION OF INDIVIDUAL
AUDITORY NERVE FIBER ACTIVITY

Approved:

Chairman

Date approved by Chairman March 25, 1971

ACKNOWLEDGMENTS

Dr. Roger P. Webb, my advisor, participated in much of the experimentation, provided much appreciated encouragement throughout the research, and carefully reviewed and criticized the manuscript.

Dr. Jay H. Schlag, who served as a member of my reading committee, provided invaluable assistance in setting up the data system and also assisted in many of the experiments.

Dr. Benjamin J. Dasher, past Director of the School of Electrical Engineering, provided financial support through a NASA Traineeship.

Dr. Demetrius T. Paris, Director of the School of Electrical Engineering, provided financial support with a Graduate Research Assistantship.

Dr. John W. Hooper served as a member of my reading committee.

Dr. Marton Majoros, Adjunct Professor of Electrical Engineering, helped me master the necessary surgical procedures and also provided the use of a precision high-speed drill.

Dr. Robert F. Thompson, Adjunct Professor of Electrical Engineering, also assisted in setting up surgical procedures and helped secure financial support for the project through private grants.

Dr. Walter L. Bloom, Associate Vice President for Academic Affairs, was instrumental in establishing the Bio-Acoustics Laboratory and helped obtain initial equipment grants from the Ferst Foundation.

Mr. Bill Goodner, a Research Assistant in the School of Electrical Engineering, learned from me the tricky art of microelectrode fabrication

and maintained a supply ready for data taking.

To all the above people I am sincerely grateful, but my deepest appreciation goes to my wife, Shirley, who typed much of the rough draft and helped me endure the unavoidable frustrations inherent in experimental work.

TABLE OF CONTENTS

	Page
ACKNOWLEDGMENTS	ii
LIST OF TABLES	vi
LIST OF ILLUSTRATIONS	vii
SUMMARY	x
Chapter	
I. INTRODUCTION	1
Objective I - Response Characterization	
Objective II- A Test of the Cochlear Microphonic	
Trigger Hypothesis	
General Anatomical and Physiological	
Background	
Specific Related Research	
The Characterization of Fiber Response	
Summary of the Experimental Methods and	
Apparatus	
II. INSTRUMENTATION AND EQUIPMENT.	26
Stimulus Presentation	
Data Acquisition	
Data Processing and Reduction Equipment	
III. PROCEDURES	47
Animal Preparation	
Cochlear Microphonic Modification	
Data Acquisition	
Stimulus Presentation	
Data Processing and Reduction	
IV. RESULTS	62
Part I - The Characterization of	
Response Patterns	
Part II - Effects of Microphonic	
Modification	
Summary of Results	

TABLE OF CONTENTS (Continued)

	Page
V. CONCLUSIONS AND RECOMMENDATIONS	137
BIBLIOGRAPHY	139
VITA	143

LIST OF TABLES

Table	Page
1. Listing of Procedures and Apparatus Used in the Research.	23

LIST OF ILLUSTRATIONS

Figure	Page
1. Schematic Diagram of Ear Structures.	5
2. Schematic Diagram of Cochlea Cross Section (one turn)	6
3. Magnitude of Transfer Function Relating Basilar Membrane Displacement to Stapes Displacement	10
4. Overall View of Equipment Located Outside Experiment Room.	27
5. Layout of Major Equipment Items Used Inside Experiment Room	28
6. Block Diagram of Waveform Generator and Acoustic Transducer.	30
7. Cross Section of Capacitor Microphone, Acoustic Coupler, and Mounting Hardware.	33
8. Calibration Curve for Acoustic Transducer.	34
9. Electrical Model of a Microelectrode	38
10. Block Diagram of Data Processing and Reduction System	43
11. Schematic Diagram of Alternating Current Stimulating System	55
12. Spike Response of a Single Fiber to Tone Bursts	57
13. PST Histogram Drawn by the Calcomp Plotter.	60
14. PST Histogram for Data of Figure 13 Drawn with Strip Chart Recorder.	61
15. Definition of Tone Burst Parameters.	64
16. PST and ISI Histograms for Unit 115-6 as Burst Duration is Increased	66
17. PST Histograms for Unit 115-5 as Burst Duration is Increased.	70

LIST OF ILLUSTRATIONS (Continued)

Figure	Page
18. PST Histograms for Unit 122-2 as Burst Duration is Increased.	73
19. PST and ISI Histograms for Unit 104-5 as Burst Intensity is Increased	75
20. PST and ISI Histograms for Unit 122-3 as Burst Repetition Rate is Increased.	79
21. Average Spike Rates During "Burst On" Periods for Data of Figure 20 Plotted Against Burst Rate	83
22. PST and ISI Histograms Showing Phase Locking of a Low-CF Unit	84
23. Tuning Curves for 6 Units from 5 Animals	90
24. PST Histograms for a Low-CF Unit (161-5) as Click Level is Increased.	92
25. PST Histograms for a High-CF Unit (163-3) as Click Level is Increased.	94
26. CF for 17 Units Plotted Against T_1	96
27. PST Histograms, Unit 153-4, for which Interpeak Intervals are not Constant	98
28. Latencies of the Histogram Peaks of Figure 27 Plotted Against Click Level.	100
29. PST Histograms, Unit 161-7, for Rarefaction and Condensation Clicks as Functions of Click Level.	102
30. PST Histograms, Unit 153-4, for Low-Level Rarefaction and Condensation Clicks.	104
31. PST Histograms, Unit 110-13, for Several Combinations of Current, I_c , and Tone Burst Stimulus Level	109
32. Average Spike Rates, Q(6:16), Q(20:30), and Q(40:50) for Data of Figure 31	111

LIST OF ILLUSTRATIONS (Continued)

Figure	Page
33. Effect of I_c on Q(60:100) for the Data of Figure 31.	113
34. PST Histograms Showing the Effect of Pulse Current, I_p , on Tone Burst Response.	116
35. PST Histograms Showing the Effect of Pulse Current, I_p , on Spontaneous Activity for Two Units.	118
36. PST Histograms Showing the Effect of I_p on Response to Tone Bursts at High and Low Levels Relative to Threshold.	120
37. PST Response Patterns as CM is Modified by Cochlear Heating	126
38. Average Spike Rates Q(0:50) and Q(60:100) for Histograms of Figure 37.	129
39. Effect of Heat Applied to Cochlea on CM and Average Fiber Response Rate.	131

SUMMARY

This dissertation describes an experimental investigation of the transformation relating acoustic signals at the ear drum to the action potential voltage spikes in individual primary auditory nerve fibers. This study was centered around two objectives, both of which were accomplished by locating microelectrodes in the auditory nerve bundles of anesthetized guinea pigs, monitoring single fiber sound responses, and processing spike occurrence times with on-line and off-line automated techniques.

The first research objective was to characterize the manner in which single auditory fibers in the guinea pig respond to selected acoustic stimuli, and to compare those response patterns to patterns that have previously been obtained from cat and monkey fibers. This was done by presenting repeated identical stimuli and processing the resulting spike occurrence times to obtain graphical displays of how the fiber behaves, on the average, during one presentation. Stimuli used were clicks of varying polarity and level, and tone bursts of controllable level, duration, frequency, and rate. Results of these experiments indicate that response patterns for the guinea pig with these stimuli are very similar to those that have been shown for the other species.

The second research objective pertained to the problem of identifying the inner ear process ultimately responsible for triggering electrical activity of individual fibers. It was desired to obtain an

experimental verification of the cochlear microphonic trigger hypothesis. This theory holds that the cochlear microphonic, a time-varying voltage that can be measured in the inner ear fluids, acts on the nerve fiber endings either directly or via a chemical mediator to initiate the single fiber responses. This hypothesis was examined by obtaining fiber sound responses as microphonic levels were varied independently of acoustic stimulation by two methods -- the passing of electric currents across the cochlear partition, and the application of heat directly to the cochlea. Depending on current polarity, the first procedure is known to increase or decrease microphonic response, but the heating procedure was found to produce only microphonic attenuation. Fiber response in either case was found to change in a manner consistent with the microphonic trigger hypothesis. That is, when the cochlear microphonic is increased in magnitude by current passage, fibers whose endings are near the site of current action show generally increased levels of activity. Likewise, when the microphonic is decreased by the reverse current or by the action of heat on the cochlea, fiber response to a given sound generally decreases.

CHAPTER I

INTRODUCTION

The two objectives of the research described in this dissertation were as follows:

I. To characterize individual guinea pig auditory nerve fiber responses to certain selected sound stimuli through the use of automated data processing methods, and to correlate those response patterns with patterns obtained for similar stimuli with other species.

II. To generate data to provide an experimental test of the cochlear microphonic trigger theory of auditory nerve spike initiation.

In the last thirty years quantitative measurements of many of the underlying phenomena associated with audition have been made practical through the application of electronic techniques. Such methods have provided fairly complete descriptions of the dynamics of middle and inner ear mechanical motions. Also, several electrical phenomena have been shown to originate in the inner ear and these have been examined with varying degrees of completeness. Certainly, one of the most important electrical effects is the voltage spike potential measurable in single primary auditory neurons, since these signals constitute the true "output" of the end organ. A thorough understanding of the processes involved in the production of these spikes is desirable not only from the standpoint of ultimate clinical treatment for nerve deafness, but also for the purpose of applying the signal processing

methods which operate in the ear to electronic communication systems. In this research, an investigation was made to examine the transformation from sound input at the ear drum to the spike activity of single primary auditory neurons by performing experiments related to two specific aspects of that transformation -- the coding of sound stimulation into fiber spike trains, and the actual process of spike initiation.

Objective I -- Response Characterization

The first research objective was to ascertain, with modern data reduction techniques, some of the characteristics of the coding that exists between carefully controlled acoustic inputs and the manner in which single fibers in the guinea pig auditory nerve respond, and to compare those response patterns to data generated under comparable conditions (of stimulation and analysis) from other species. Auditory nerve spike responses to controlled stimuli have previously been obtained with automated analysis primarily in the cases of cats and monkeys. By accomplishment of the first objective, the present study extended those results by securing spike patterns from another species and by correlating guinea pig responses with cat and monkey data. Experiments for this objective consisted of presenting acoustic stimuli while simultaneously monitoring and recording action potential responses from single near fibers. These spike trains were then used in both on-line and off-line computing modes to generate a characterization of fiber response, usually in the form of histograms, which give an estimate of the probability of a nerve firing during a given

portion of a stimulus. Stimuli investigated were: tones of variable frequency and level; tone bursts of variable frequency, level, burst duration, and period between bursts; and clicks of variable polarity and level.

Objective II -- A Test of the Cochlear Microphonic Trigger Hypothesis

The second objective was to obtain a test of one theory of auditory nerve fiber spike initiation. The hypothesis examined holds that the cochlear microphonic, an electrical analog signal that can be measured throughout the inner ear, functions as an electrical "trigger" of spike activity. In experiments relative to this objective, sound stimuli were presented and various inner ear parameters (e.g. ac or dc voltage levels, or temperature) were varied to alter microphonic activity independently of acoustic stimulation. Before and after response patterns were then compared to determine if microphonic alteration alone could produce changes comparable to those that would occur if the microphonic had been changed by altering the acoustic stimulation.

In order to place the problem of individual fiber activity in perspective, a few basic facts concerning auditory anatomy, physiology, and electrophysiology are surveyed below. Detailed accounts may be found in Wever (1), von Békésy (2), or Davis (3). Following this discussion, the research objectives are amplified and additional background material is presented, after which the quantitative basis for the characterization of fiber responses is given. Finally, an

experiment summary, which indicates the motivation for the various experimental procedures and apparatus employed in obtaining data, is presented.

General Anatomical and Physiological Background

Figure 1 shows a schematic representation of the ear structures. Sound pressure waves are transmitted through the air of the external auditory meatus until they are transformed into mechanical displacements by the middle ear system composed of the tympanic membrane (ear drum), malleus, incus, and stapes. Connection with the inner ear, or cochlea, is made through an opening called the oval window, in which the stapes is rather loosely held. In addition to transmitting sound signals, the middle ear provides some protection against overdriving of the cochlea through a set of muscles which contract under high intensity sound stimulation, making energy transfer less efficient. In the guinea pig all of these structures are situated in a bony capsule called the auditory bulla.

Cochlear Structure

The guinea pig cochlea may be visualized as a long narrow tube (about 19 mm long by about 1.5 mm in diameter) coiled into four turns ($2\frac{1}{2}$ in the human) and divided lengthwise into three fluid-filled channels, the scala vestibuli, the scala tympani, and the scala media, as indicated in the cross-section of Figure 2. The scala media, separating the other two, is defined from above by Reissner's membrane and from below by the basilar membrane and its associated structures. The scala vestibuli is mechanically linked to the stapes via the oval

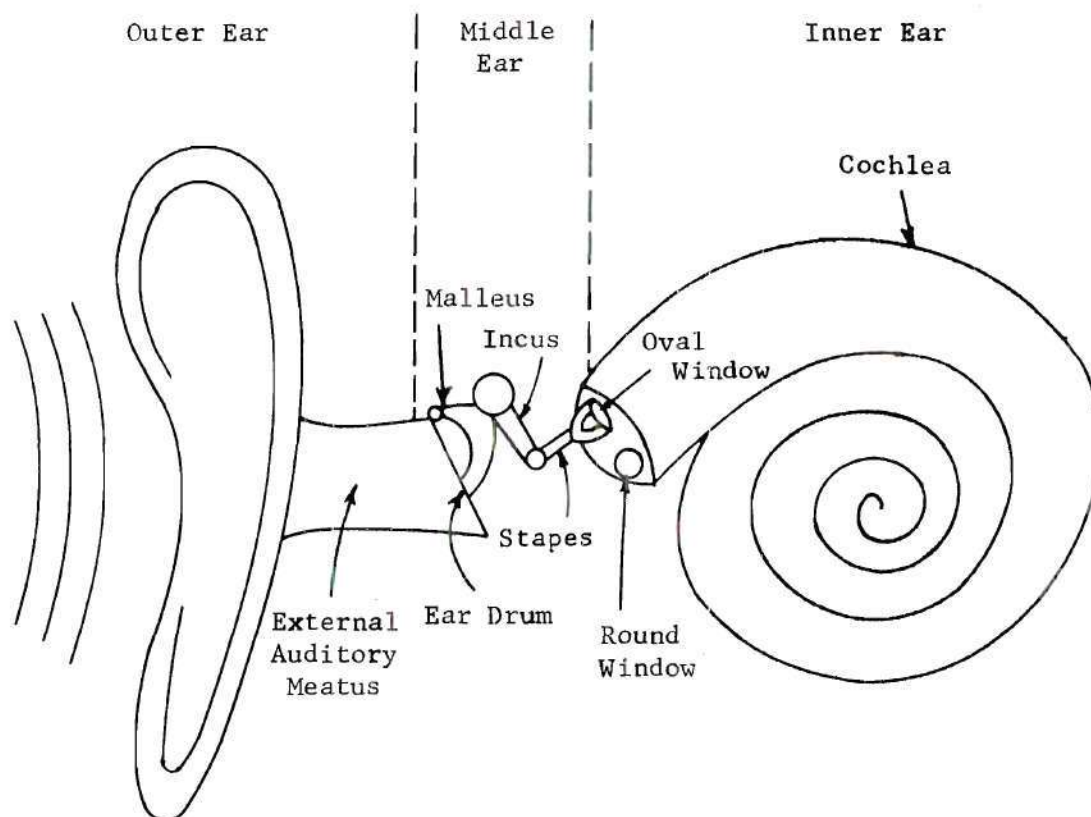


Figure 1. Schematic Diagram of Ear Structures

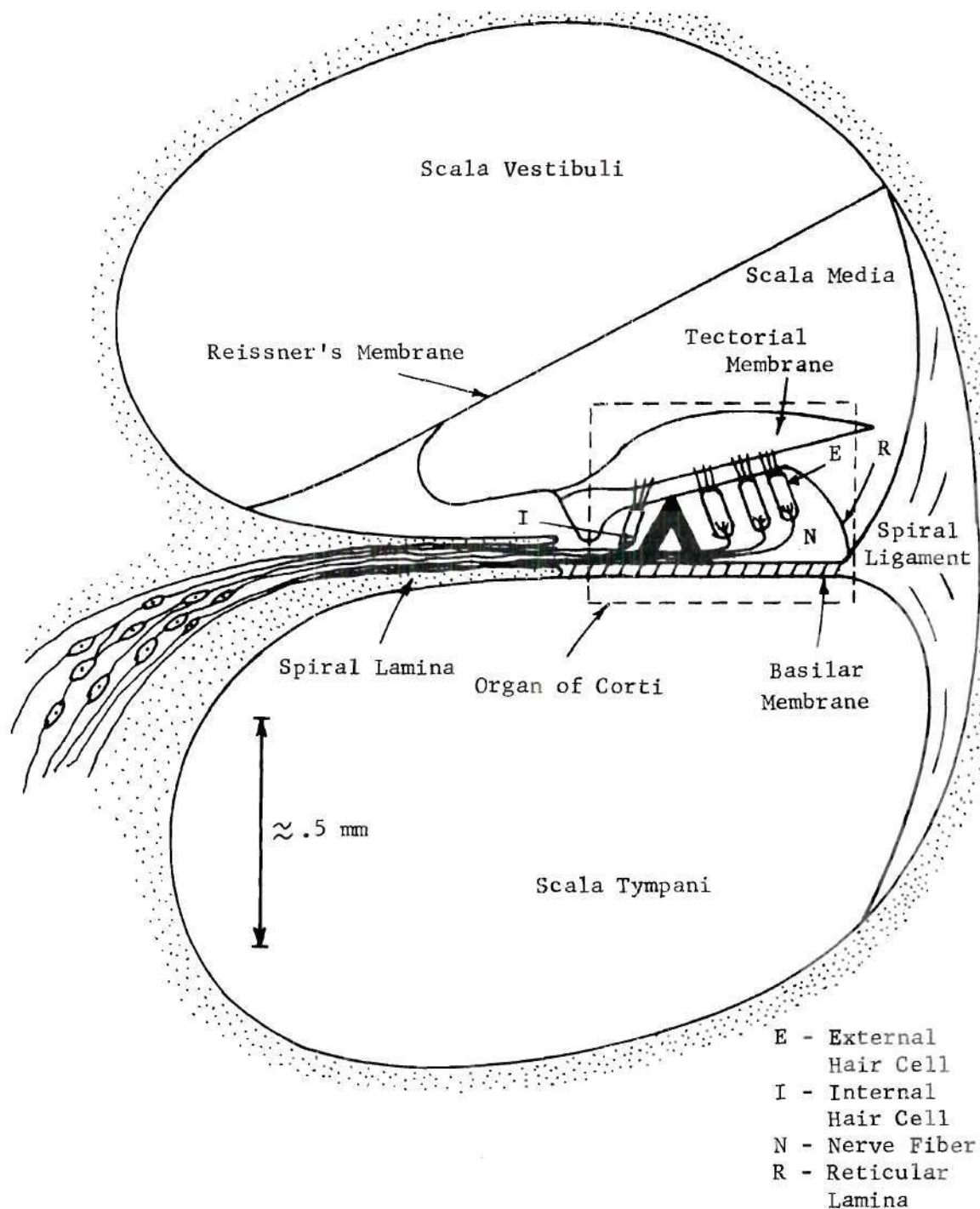


Figure 2. Schematic Diagram of Cochlea Cross Section (one turn)

window located at one end of the cochlear channels, termed the basal end; in the corresponding position in the scala tympani is situated another opening, the round window, which is capped with a flexible membrane. At the opposite end of the cochlea, the apex, the vestibuli and tympani are connected through a small opening called the helicotrema. (There is no communication with the scala media.) Through the action of the oval and round windows, and the helicotrema, acoustic pressure waves in the scalae fluids act to produce in the basilar membrane, movements which stimulate the auditory nerve through its nerve endings distributed along the membrane.

The Organ of Corti

The complete system of nerve fiber endings and supporting structures resting on the basilar membrane is called the organ of Corti (Figure 2). It contains supporting cells that hold three rows of outer and one row of inner hair cells, so called because the ends of these cells contain small fibers, or hairs, that protrude through the reticular lamina membrane and are anchored in the tectorial membrane. Imbedded in the hair cells are the peripheral endings of the auditory nerve fibers. These nerve fibers exit the organ of Corti through the spiral lamina (the internal bony support for the basilar membrane) and form the auditory nerve bundle which runs through the center of the cochlea (the modiolus). At the base of the cochlea, the bundle enters a small circular canal (about 1 mm in length and 1 mm in diameter) called the internal auditory meatus, from which they emerge to form synaptic connections with higher order auditory neurons in the brain at the cochlear nucleus. Any auditory units encountered

outside the internal meatus are not likely to be primary and would have firing characteristics different from primary units (4). Therefore, in all the experiments of this study, care was taken to record only from units either inside or peripheral to the internal meatus.

Close examination of Figure 2 shows that the tectorial and basilar membranes are pivoted at different points; hence, motion of the basilar membrane in response to sound causes relative motion between the tectorial membrane and reticular lamina. This produces a shearing effect on the hair cell hairs, and such deformation of the hair cells is thought to give rise (by processes not completely understood) to the action potential spikes of individual auditory neurons. Individual voltage spikes in a given fiber are alike in shape and amplitude (typical amplitude about 1 mv with respect to neutral tissue and 0.5 ms typical duration). Thus, all information about an audible signal must be coded in the time patterns of the spike sequences of the affected neurons.

The Fundamental Determinants of Neural Firings

From the above discussion, it may be inferred that the manner in which a primary nerve fiber responds to sound stimuli is determined in large part by the motion of the basilar membrane in the region where the fiber endings are located and by the mode of innervation of the fiber.

Basilar Membrane Mechanics. Von Békésy (1) stimulated cochleas from human cadavers with sinusoids and measured the amplitude and phase angle of the resulting basilar membrane movement at several points along its length. More recently, similar measurements have

been obtained for the guinea pig by Johnstone et al. (5). Such studies indicate that for a wide range of moderate intensities, sound pressure waves at the ear drum are transformed linearly into basilar membrane displacements. That is, for each point on the membrane there exists a transfer function which relates stapes movement to membrane movement. The characteristic features of this transfer function are illustrated in Figure 3. For each membrane point there is some frequency, f_c , for which maximal response occurs, and the response diminishes continuously as stimulation frequency is changed from f_c . The frequency f_c is a monotonic function of position on the membrane; at the basal end (near the stapes), f_c is high, and at the apex it is low. Flanagan (6) and Seibert (7), using von Békésy's data, calculated the impulse response of points on the membrane and showed that it consists of underdamped ringing at f_c which lasts only a few cycles. For the following discussions, it is sufficient to remember that ringing at f_c can occur, and that high-frequency stimulation is associated with the basal end of the cochlea and low-frequency stimulation with the apical end. Hence, if membrane movement ultimately causes nerve responses, fibers arising in the basal end should show high sensitivity for high-frequency stimulation, whereas apical fibers should show maximal sensitivity for low frequencies. All present research indicates this to be the case.

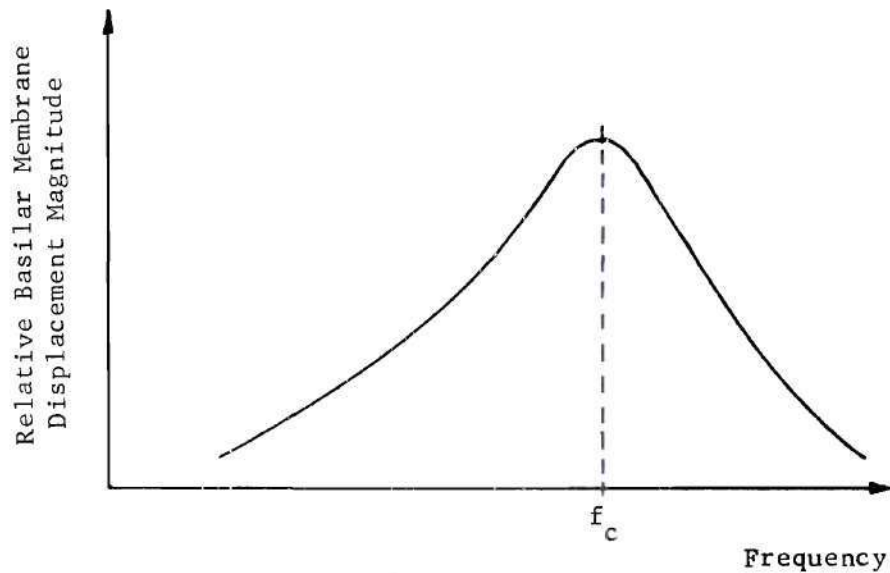


Figure 3. Magnitude of Transfer Function Relating Basilar Membrane Displacement to Stapes Displacement

Hair Cell Innervation. The other major physiological factor in determining nerve firing patterns is the manner in which individual fibers are associated with the hair cells and with each other. Unfortunately, the situation is not so simple as the schematic indication of one-to-one pairing of hair cells and fiber endings in Figure 2. Present knowledge concerning cochlear innervation is summarized by Spoendlin (8). All details are not completely known, but it is certain that single afferent fibers may innervate one or several cells, and likewise, a single hair cell may have as many as ten to twenty fibers impinging on it. Further clouding the issue is the presence of the endings of the efferent fibers of the olivo-cochlear bundle. (Efferent

fibers transmit signals from the brain as opposed to afferent fibers which conduct from an end-organ to the central nervous system.) Even though there are only about 500 efferent fibers (compared to approximately 50,000 afferent fibers), the number of efferent nerve endings seems to be only slightly smaller than the number of afferent endings, and the total contact area of efferent endings with hair cells is actually greater than that for afferents. Thus the response of a single fiber depends in a complicated way on events in many hair cells, with the efferent fibers providing the possibility for significant feedback effects.

Specific Related Research

With the above information providing a general description of the mammalian auditory system, additional background pertinent to the two objectives of the present research is now given.

Studies in Response Characterization -- Objective I

Research concentrated on stimulus coding in single primary auditory neurons may be separated, according to the instrumentation used in data analysis and reduction, into two classes. The first comprises those experiments in which relatively small amounts of data were obtained by non-automated means, and the second includes those in which large amounts of spike data were handled with data processing methods.

Non-Automated Analysis. Several studies of unit activity in auditory nerves have been conducted in the last twenty-five years without benefit of modern data analysis techniques. The first attempts were by Galambos and Davis with cats in 1943 (9), but it was later

shown that the responses measured had come not from primary neurons but from secondary units. In 1953, however, Tasaki (10) did successfully record from primary units in the guinea pig. His methods consisted of introducing various sound stimuli (continuous tones, tone pips, and clicks) and recording the fiber discharges photographically from an oscilloscope. (Clearly, the analysis of data in this format was a most time-consuming process.) Similar studies were done later with cats by Katsuki et al. (11) and Rupert et al. (12), and with monkeys by Katsuki et al. (13). Katsuki et al. (14) and Nomoto et al. (15) extended such experiments by utilizing multiple stimuli for cats and monkeys, respectively. All these studies employed a data reduction scheme essentially like Tasaki's with perhaps the addition of an electronic counter to record the number of nerve impulses occurring during selected portions of the stimulus period.

From the works cited above, some general characteristics of primary nerve fiber response became apparent and may be summarized as follows: (1) Even in the absence of sound stimulation, primary auditory nerve fibers show spontaneous activity which consists of irregularly spaced spikes occurring at average rates that may vary from less than one per second up to more than one hundred per second. (2) Application of an acoustic stimulus causes an increase in the unit's spike activity, and for a range of stimulus intensities of about 20-40 dB, increases in intensity result in continued increases in firing rate. (3) For sinusoidal stimulation of less than about 4 kHz, a fiber appears to fire during a "preferred" portion of the input wave cycle,

even though it will not in general respond during each cycle. (This phenomenon is referred to as "phase locking.") (4) Also for sinusoidal stimulation, there is a characteristic frequency (CF) which causes a change in spontaneous firing rate with a minimum of sound input. Only the nearest frequencies above the CF can cause a detectable response, but almost all frequencies below the CF can cause a response if made intense enough. (Recalling von Békésy's results concerning basilar membrane mechanics, these last two observations imply that nerve firings reflect in a reasonable manner the motion of the cochlear partition.) (5) A fiber clearly responding to one tonal stimulus can have its activity inhibited by a second with properly selected parameters. Likewise, two tonal stimuli may be picked so as to elicit a response when presented simultaneously, even though neither causes a response alone.

Automated Studies. During the past ten years, modern, computer-aided data recording and processing techniques have been applied in experiments similar to those mentioned above to produce histogram response characterizations of auditory unit activity. With such instrumentation, Rose et al. (16) demonstrated very clearly the low-frequency "phase-locking" of responses to individual cycles of the input wave and the effects of low-frequency, two-tone stimulation in monkeys (17). In 1965, Kiang et al. (18), using cats, published the most comprehensive study on single fiber activity that has appeared. Stimuli included clicks of variable level, polarity, duration, and rate; tone bursts of variable frequency, duration, level and rate; continuous tones of variable frequency and level; and, combinations of clicks, tone bursts, and noise. Since this study is fairly complete and agrees

with most others, portions of it were used as a main source of comparison for the guinea pig data of the present research.

The studies mentioned above (and others from Kiang's laboratory) have not only tended to confirm quantitatively the conclusions listed earlier under "Non-automated Studies," which in many cases were arrived at somewhat qualitatively, but they have also provided new basic information. For instance, by properly conditioning his data, Gray (19) was able to remove refractory effects from firing patterns to show that such effects do not account for certain temporal characteristics of the fiber response. Such results are possible because the use of automated analysis permits firing patterns to be obtained over thousands of neural events as opposed to the relatively small number that can be examined manually. For example, in a histogram display, phase-locked activity is unmistakable, but it may be difficult to identify from spikes observed on an oscilloscope.

It is believed that at the time of initiation of the present research, only one investigator, Hanna (20), had published results obtained from computer analysis of unit activity in the guinea pig. However, his stimulus conditions were not enough like those used in the cat and monkey experiments cited earlier to draw direct comparisons, and he states that not all of his recordings were from primary fibers. Furthermore, the time resolution of Hanna's data displays was not great enough to show neural events phase-locked to individual stimulus cycles.

Therefore, the first research objective was undertaken to establish computer-generated primary fiber response patterns in such

a manner as to allow more direct comparison to previously generated cat and monkey data. Such patterns were obtained for click stimuli as click level and click polarity were varied; and, for tone bursts as duration, frequency, intensity, and period between bursts were varied.

Motivation for the Cochlear Microphonic Trigger

Hypothesis -- Objective II

Besides the classification of fiber responses to specific stimuli, another problem of interest in auditory theory is to identify the process that ultimately causes action potential spikes to be initiated in individual nerve fibers. Early explanations described the process in purely mechanical terms, but modern evidence has led to more complicated theories. One line of reasoning has indicated that chemical effects in the organ of Corti are responsible. Another holds that an electrical signal in the cochlea, the cochlear microphonic, is the ultimate excitatory agent, either through direct action on fiber endings or through the liberation of a chemical mediator which then stimulates nerve fibers. Extensive comments of the merits of these theories may be found in Wever (21) and Davis (22). The second research objective was concerned with the microphonic trigger theory.

Definition of Cochlear Microphonic. There are several classes of electrical phenomena that are measurable in the cochlea in response to sound stimulation (21). Only two of these, though, are capable of responding at stimulation frequencies. One is the gross action potential of the entire collection of auditory nerve fibers, which can follow input frequencies up to about 3 kHz. The other is the so-called cochlear microphonic (CM), a voltage measurable with small wire probes

from either inside or outside the cochlea and on the surface of the round window membrane. For input sound of intensities less than about 80 dB (reference level to be defined in Chapter II), CM at a given point appears to be a linear transformation of the input sound signal, the exact transformation being a function of the recording location and method of recording. In general, the transformation results in low-pass filtering, but CM responses at 100 kHz have been reported (21), and CM responses to speech are quite intelligible when amplified and reproduced with a loudspeaker. The maximum value that CM may reach under intense stimulation is a function of stimulus frequency and recording location, but in guinea pigs, peak values (measured from the round window) are about 1000 μv (p-p) in the neighborhood of 1 kHz and about 100 μv (p-p) at 15 kHz (21).

Relationship of Cochlear Microphonic to Basilar Membrane

Mechanics. Two striking aspects of the relationship of CM to basilar membrane movements have caused the microphonic to be implicated in the spike triggering process.

In the first place, it has been shown by Tasaki et al. (23) that CM (referenced to neck muscle tissue) undergoes a reversal in sign in the region of the reticular lamina. This phenomenon was demonstrated by pushing a small electrode up through the scala vestibuli, into and through the organ of Corti, through the reticular lamina, and into the scala media while simultaneously recording CM response to sinusoidal stimulation. Such an effect has not been demonstrated for any other cochlear location, so it appears probable that the microphonic is generated at or near the reticular lamina, i.e., near the hair-bearing

ends of the hair cells. Since the nerve fiber endings are also located in the same area, the notion that microphonic voltage variations play an active role in spike initiation seems reasonable.

Secondly, Tasaki et al. (24) have demonstrated that amplitude and phase characteristics for CM measured throughout the cochlea are very similar to those for mechanical movements of the basilar membrane as obtained by von Békésy and others; i.e., low-frequency stimulation tends to give CM response associated with the upper turns, while high- and low-frequency CM response tends to be measured in the lower turns of the cochlea. Therefore, there certainly exists the possibility that basilar membrane movements are able to trigger nerve responses by the action of the cochlear microphonic; i.e., that the microphonic plays an active role in the triggering of individual fiber spikes.

In addition to the considerations mentioned above, Wever (21) states several other points in favor of the microphonic trigger theory, one of which is that CM is always present when an ear is working normally; and when CM is absent, the animal is completely unresponsive to sound. In other words, the presence of CM is a necessary condition for hearing.

A Test of the Microphonic Trigger Theory. The second objective of the present research was to perform experiments that would provide a test of the CM trigger theory. The basic experiment consisted of modifying microphonic response to sound by non-auditory means (so that basilar membrane motions are constant) and searching for resultant firing pattern changes, even though sound stimuli are unchanged. The presence of such concomitant variations would be good evidence in

favor of the microphonic theory (in the same sense that Tasaki's amplitude and phase characteristics for CM are good evidence). Nevertheless, they could not be interpreted as proving absolute causality for CM since one could not rule out the possibility that CM derives from some other unknown mechanism that is the actual fiber trigger. However, if no fibers were found to be sensitive to CM manipulation, there would be real reason to doubt the microphonic trigger hypothesis.

Several procedures are known to modify CM response independently of sound input, some of which require the administration of certain drugs or gross changes in the animal's oxygen intake. For the purposes of this research, however, procedures were needed that were both rapid in effect (so that significant changes in CM would occur during the few minutes of recording time generally available for a given fiber) and rapid in reversability (so that before and after conditions could conveniently be obtained from a number of units in the same animal). Two procedures were selected; these were CM modification by currents forced across the cochlear partition, and modification by the effect of heat applied directly to the cochlea. In either case, the experimental plan was to compare fiber sound responses with and without CM modification and to interpret any response changes in terms of the microphonic trigger theory. Details of implementation for the current and temperature procedures will be given in Chapter II.

Modification of CM sound-evoked response by the application of direct currents across the cochlear partition was first demonstrated by Tasaki and Fernandez (25), who placed current stimulating electrodes in the scala tympani and the scala vestibuli opposite each other across

the basilar membrane. CM response was measured by another electrode pair adjacent to the current electrodes. Their results were that currents directed across the partition in the direction vestibulotympani result in CM and whole nerve action potential increase, and that an opposite current causes attenuation, the effect on CM being approximately linear for polarization currents with absolute values less than about 200 μ a. They further demonstrated that the CM changes were localized to about three or four millimeters of basilar membrane on either side of the current electrodes.

For the present research, three different modes of cochlear current stimulation were used. These were:

1. Simple application of direct currents of varying levels and changing polarity.
2. Application of positive and negative 40-msec current pulses during a repeated acoustic stimulus.
3. Application of alternating currents (i.e., an attempt to generate an "artificial CM").

During the final stages of execution for this research, Konishi, Teas, and Wernick (26) and Teas, Konishi, and Wernick (27) published results also dealing with the effects on nerve firing patterns of currents placed across the cochlear partition. They studied the effects of current modes 1 and 3 listed above and reached conclusions concurrent with those of the present study. They also investigated the effects of short-term dc stimulation by much longer current pulses of 5-sec duration. However, because of the artifact produced by the make and break of current, they deliberately excluded from analysis any

fiber responses occurring within one second of the switching times. In the present research, though, it was desired to determine the time structure of responses to current pulses and sound within a few milliseconds of current initiation and termination in order to compare these responses with nerve response patterns for sudden sound level changes (e.g. tone bursts). Thus, current mode 2 was employed, with special precautions being taken to reduce artifacts so that reliable measurements were made within one millisecond or less of the current switching.

The second method employed for CM modification was direct heating of the cochlea. Motivation for this procedure, however, came from reports of the effects of cochlear cooling by reduction in the animal body temperature (28). Those results showed that hypothermia reduces CM, but that 60 to 80 minutes of body cooling is needed for sizeable effects to be seen. Therefore, it was decided to try a temperature modification scheme which would bring about alterations more rapidly by affecting only the cochlea. Since it was felt that CM would also respond to temperature increase, and since infrared radiation may be easily produced and focused on a small area, cochlear heating by directed radiation was adopted for temperature experiments.

The Characterization of Fiber Responses

Action potential spikes representing a fiber's response to sound are highly non-deterministic in that repetitions of a stimulus give generally different spike sequences. Therefore, any quantitative measure of fiber response must be based on some kind of averaging carried out over many responses to repeated, identical stimuli. A

particularly convenient type of analysis (and the type primarily used in this study) is the histogram, or frequency of occurrence diagram, the mathematical basis of which is given by Gerstein et al. (29). Two types of histograms, post-stimulus time (PST) and interspike-interval (ISI), are now discussed.

Post Stimulus Time Histograms

For PST calculations, a stimulus is presented to the ear at a regular interval (called the stimulus period) for a certain total time (usually 30 or 60 seconds for the present research), and the time of occurrence for each spike, referenced to the beginning of the most recent stimulus, is recorded. Then a bar graph is constructed in which the abscissa is the stimulus period divided into time bins of width Δt , and the height of the k^{th} bar, y_k , is the number of spikes over all stimulus presentation occurring between $k\Delta t$ and $(k + 1)\Delta t$. Thus, this type of display shows neural events synchronized with the stimulus; e.g., a peak on the PST histogram indicates a preferred firing time relative to the stimulus. Mathematically, if N represents the number of stimulus presentations, then y_k/N is an estimate of the probability of firing in the interval $(k\Delta t, (k + 1)\Delta t)$, over all presentations.

Interspike-Interval Histograms

The only difference in ISI and PST histograms is that in the former, the time of spike occurrence is referenced not to the most recent stimulus, but instead to the previous spike, so that the height of the k^{th} bar is the number of spike intervals of duration between $k\Delta t$ and $(k + 1)\Delta t$. Hence a peak on the ISI histogram indicates a

preferred interval between firings. If M is the number of spikes, then for the ISI histogram, y_k/M is an estimate of the probability of an interspike-interval between $k\Delta t$ and $(k + 1)\Delta t$.

Summary of the Experimental Methods and Apparatus

The two research objectives described above required that single primary auditory nerves be instrumented and their response patterns obtained. For the first objective, this was done under conditions of varying sound stimulus parameters, while the second required also the modification of cochlear microphonics. To accomplish these goals, a collection of experimental procedures and techniques, many involving specialized apparatus, was developed. The procedures were: (1) animal preparation; (2) cochlear microphonic modification; (3) stimulus presentation; (4) data acquisition; and (5) data processing and reduction. Table I lists the main procedures and gives major equipment items used in executing them. The table entries are summarized in the following discussion, while complete descriptions are given in Chapters II and III.

Extensive preparation of experimental subjects was necessary because the desired data sources, auditory nerve fibers and the cochlea itself, are extremely small and covered by anatomical obstructions around the guinea pig's neck. Such structures had to be removed with surgical techniques, which required the use of anesthesia. However, anesthetic agents usually disturbed the animal's respiratory and temperature control systems so that artificial respiration and closed-loop body temperature control were administered. (A useful measure of

Table 1. Listing of Procedures and Apparatus Used in the Research

Procedures	Major Equipment Employed
A. Animal Preparation - Anesthetization - Artificial respiration - Preliminary surgery - Body temperature control - Drilling of nerve access hole	Respirator Head-holder Closed-loop temperature controller Operating microscope, high-speed drill
B. Cochlear microphonic modification	DC stimulator, AC stimulator, stimulating electrodes, nichrome heating coil and reflector, electrode manipulator
C. Stimulus presentation	Stimulus waveform generator, acoustic transducer, sound-attenuated room
D. Data acquisition - CM measurement - Nerve fiber response measurements	CM amplifier, wave analyzer, microelectrodes, microdrive, floated platform, microelectrode amplifier
E. Data processing and reduction (On-line and off-line characterization of response patterns)	Signal conditioner for nerve signals, digital and analog tape recorders, on-line computer (GRI 909), off-line computer (Univac 1108)

the animal's general physiological condition was obtained by electrocardiogram measurements.)

After the cochlea was exposed, access to the auditory nerve was gained by drilling a small hole at the base of the cochlea to intersect the nerve bundle. Mechanical stability for this process (and, also for nerve measurements) was achieved by mounting the animal in a rigid head-holding frame. Drilling and all succeeding manipulation on the subject had to be accomplished under magnification with an operating microscope due to the small size of the involved structures.

For the experiments with microphonic modification by electric currents, direct and alternating currents were forced across the organ of Corti with electrodes placed into holes drilled in the cochlea. Again, because of the small size of the cochlea, these electrodes were positioned (under the operating microscope) with a mechanical manipulating system attached to the head holder. CM temperature alteration was obtained by heating the cochlea with radiation from a nichrome loop focused with a spherical reflector.

After a subject was prepared, experiments commenced with the presentation of controlled stimuli and the acquisition of data through monitoring of CM and nerve fiber responses. Stimuli were produced by driving a transducer (mounted in one of the earbars of the head-holder) with signals from a stimulus waveform generator. To minimize effects of uncontrollable ambient sound, the experiments were conducted in a sound attenuated chamber, which was also electrically shielded to eliminate interference with low level (about 1 mv) CM and fiber signals. CM measurements were straightforward, requiring only

a wire electrode inserted through a hole in the cochlea and connected to an amplifier. Signals from this amplifier were used in conjunction with a recording wave analyzer to obtain CM frequency response data, which was routinely used to monitor the performance of the subject's ear during experimentation.

Action potential (AP) measurements from nerve fibers required more elaborate measures than for CM, since single fibers are only a few microns in diameter. Therefore, AP recordings were made using microelectrodes, which have $0.5\ \mu$ or less tip diameters and exhibit impedances of greater than 20 megohms. Therefore, the AP amp had extremely high input impedance to prevent signal attenuation, and minimal input capacitance for maximum bandwidth. To contact and hold single fibers, microelectrode movement in the nerve bundle was governed with a microdrive system which allowed tip motion in steps of less than $1\ \mu$. To reduce relative motion between electrode tips and fibers due to mechanical vibration, the entire preparation was located on a heavy platform supported with springs.

After a fiber was contacted and was responding to sound, fiber spike responses occurred at average rates as great as two or three hundred per second. To analyze these responses, a data processing system was configured to encode the occurrence time of each spike and either record that time in digital form for later off-line computations or to use the data in real time calculations performed with an on-line digital computer.

CHAPTER II

INSTRUMENTATION AND EQUIPMENT

This chapter presents a discussion of the apparatus utilized in conjunction with the stimulus presentation, data acquisition, and data processing and reduction procedures listed in Table 1 of Chapter I. A treatment of devices used in animal preparation and cochlear microphonics modification is incorporated into the description of those procedures in Chapter III, which also indicates how the equipment detailed in the present chapter was used in obtaining data. The general layout for equipment located outside the sound-attenuated room is shown in Figure 4, and Figure 5 shows most of the apparatus used inside.

Stimulus Presentation

Since an important aspect of this research was the correlation of nerve fiber responses with acoustic stimuli, it was essential to present to test subjects precisely defined, repeatable stimuli. To accomplish this a stimulus presentation system, consisting of an electronic waveform generator coupled to a capacitor microphone transducer (used as an earphone), was assembled. The system was capable of producing the following acoustic stimuli:

- (1) Pure tones of controllable frequency and level.
- (2) Uniform onset-phase tone bursts of controllable exponential rise-fall time, burst duration, period between bursts, and frequency and level of the tone.
- (3) 100- μ sec clicks of controllable polarity, period, and level.

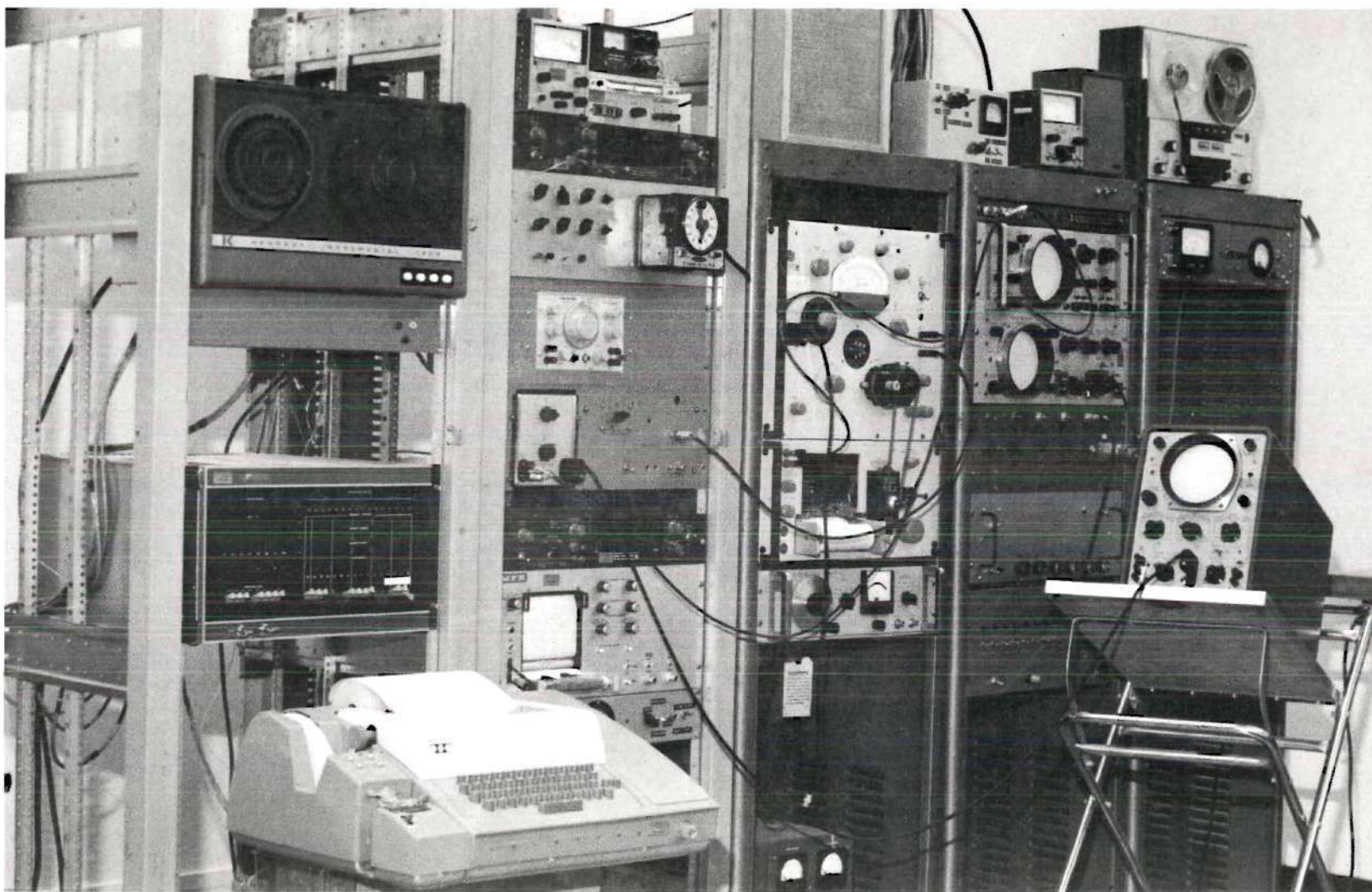


Figure 4. Overall View of Equipment Located Outside Experiment Room

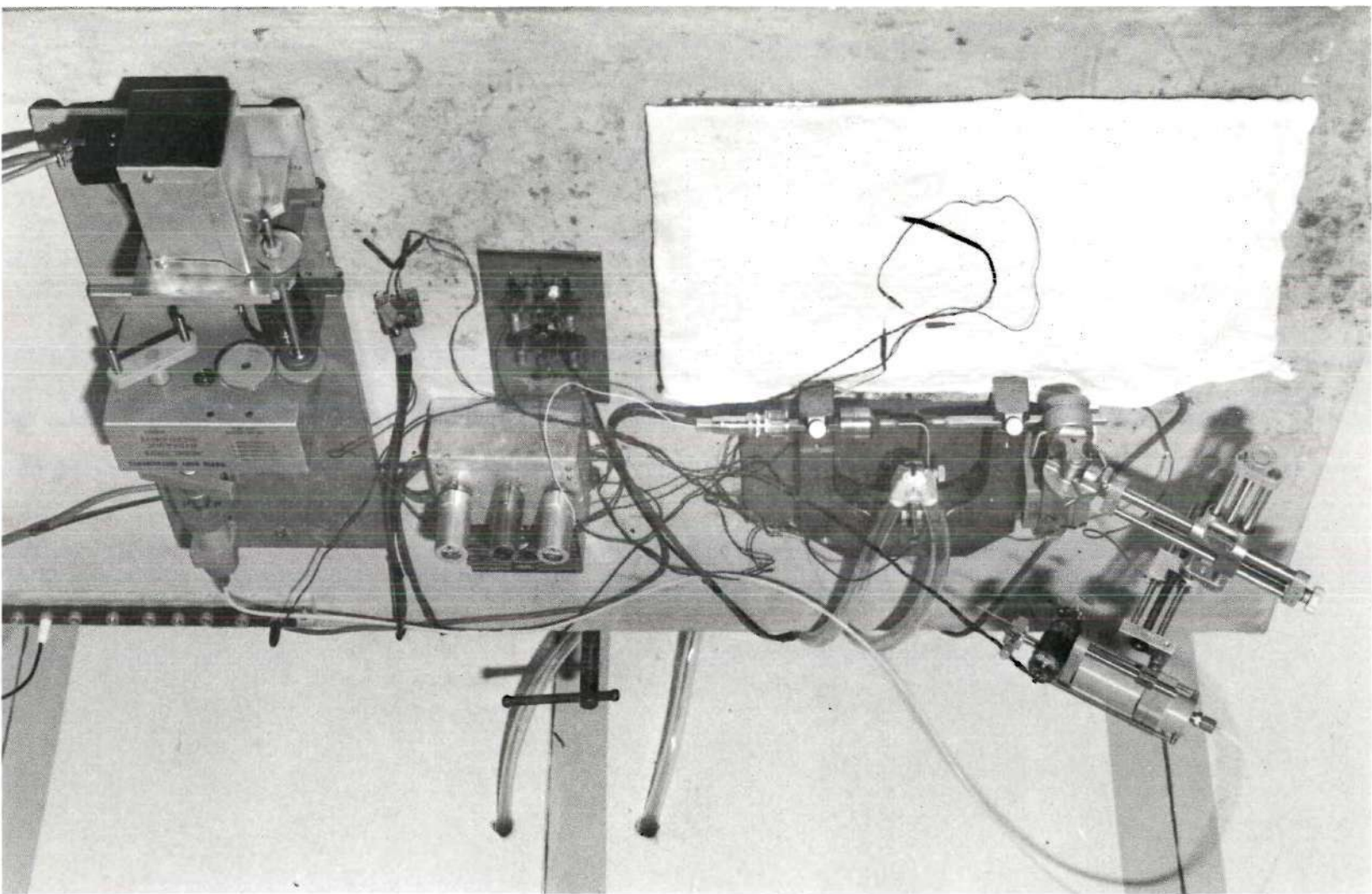


Figure 5. Layout of Major Equipment Items Used Inside Experiment Room

Tone bursts and clicks were employed to obtain histogram response characterizations, so that both these stimuli had to be synchronized with the data processing system, and for the same reason all tone bursts in a given data run had to begin with the same phase. Continuous tones, though, were used mostly in CM measurements, independently of the data processing equipment, so no particular timing was necessary for them. The electronic waveform generator and the acoustic transducer are now described.

Waveform Generator

A block diagram of the stimulus presentation system is given in Figure 6. This particular configuration resulted mainly from the uniform phase and exponential rise-fall requirements of the tone burst stimuli. Operation of the waveform generator for burst production was as follows: Stimulus period and duration were set with rotary switches into a digital control logic system, equipped with a 100-kHz, crystal-controlled time base. (Both period and duration could be set from 0 to 999 msec in 1-msec steps.) The logic system produced outputs W and E which controlled a Wave-Tek Model 112 sine wave generator and an exponential envelope generator with variable time constant. Control logic outputs R and S were used to provide time synchronization with the data system. Signal E was a pulse train with duration and period equal to the burst duration and period, so that the envelope generator output was exactly the desired burst envelope. (Thus, burst duration was measured from the beginning of the rising phase to the beginning of the falling phase.) Signal W turned on the Wave-Tek sine wave

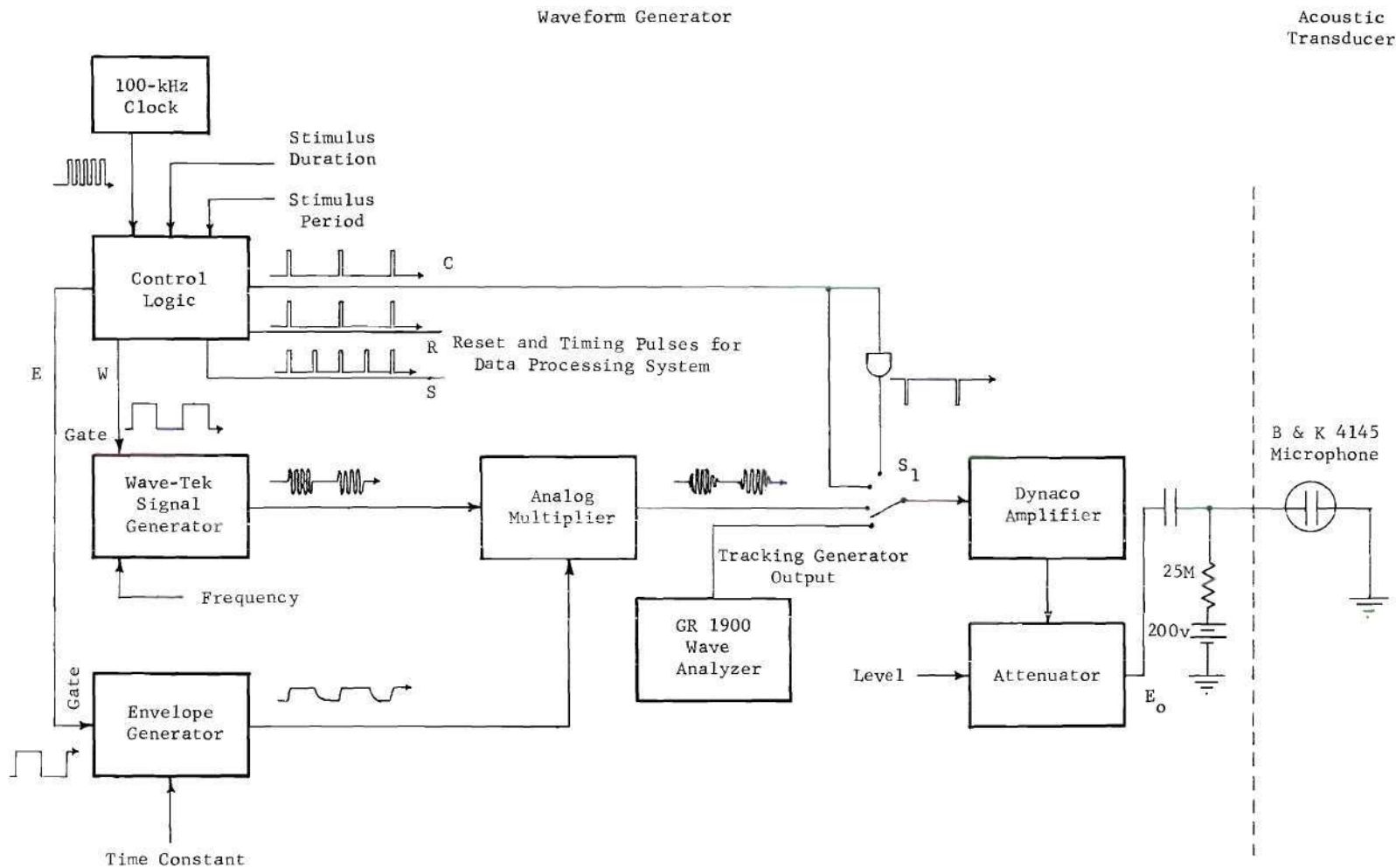


Figure 6. Block Diagram of Waveform Generator and Acoustic Transducer

generator (each time with the same phase angle) at the beginning of stimulus periods and turned it off within five time constants of the falling phase of the envelope. Wave-Tek and envelope outputs were multiplied with a Burr-Brown Model 4096/15 analog multiplier, the output of which was amplified with a Dynaco Mark III amplifier. Output level control was accomplished with a Hewlett-Packard Model 350D attenuator, which provided 110 dB of attenuation in 1-dB steps. Multiplier gain was set so that an attenuator setting of 0 dB corresponded to a system output of 50 v (p-p) for bursts.

For click waveform generation, 100- μ sec duration pulses were derived from the control logic circuits and fed to the Dynaco amplifier with positive or negative polarities via a selector switch S_1 . Click stimulus period was set with the same control used for burst period; and amplitude was adjusted so that 0 dB on the attenuator gave an output pulse height of 36 v.

Pure tones were produced on the burst generator by setting in a burst duration longer than stimulus period. Tones were also available from the tracking generator of a General Radio 1900 recording wave analyzer for use in automatic recording of the cochlear microphonic frequency response.

Acoustic Transducer

Attenuator electrical output was converted into sound stimuli by a Bruel and Kjaer 4145 capacitor microphone, which required a 200-v polarization level for earphone use (see Figure 6). The earphone was supported in the head-holding apparatus and equipped with a specially

made low volume acoustic coupler for direct connection with the external ear. A cross-section of the earphone, acoustic coupler, and mounting hardware is shown in Figure 7.

Earphone Calibration. To relate the results obtained in this research to other studies, it was necessary to ascertain the sound levels delivered to an ear by the earphone system. In bio-acoustics work, the strength of a sound stimulus is taken to be the pressure, in dynes/cm², exerted by the sound pressure wave. Figures are usually given in dB referenced to 0.0002 dynes/cm², which is the average threshold for detection of 1-kHz tones by male human subjects.

Absolute sound pressure level (SPL) measurements were made at the eardrum of an animal under stimulation by the earphone system to obtain the calibration curve of Figure 8, in which is shown SPL (expressed in dB referenced to 0.0002 dynes/cm²) resulting from a peak-to-peak sinusoidal earphone input of 2 v, which is -28 dB referenced to 50 v (p-p). To obtain the data for Figure 8, sound pressure levels were measured with a 1/2-inch calibrated measuring microphone (Bruel and Kjaer 4134) and microphone amplifier (Bruel and Kjaer 2603). The measuring microphone was coupled to the outer ear with a 1-inch by 0.015-inch probe tube inserted into a small hole drilled in the bulla external to the eardrum, and calibrated according to the procedure described by Beranek (30). To determine if the presence of the probe tube altered acoustic conditions at the eardrum, cochlear microphonic frequency response curves were obtained before and after drilling the hole and inserting the tube; the curves were almost identical,

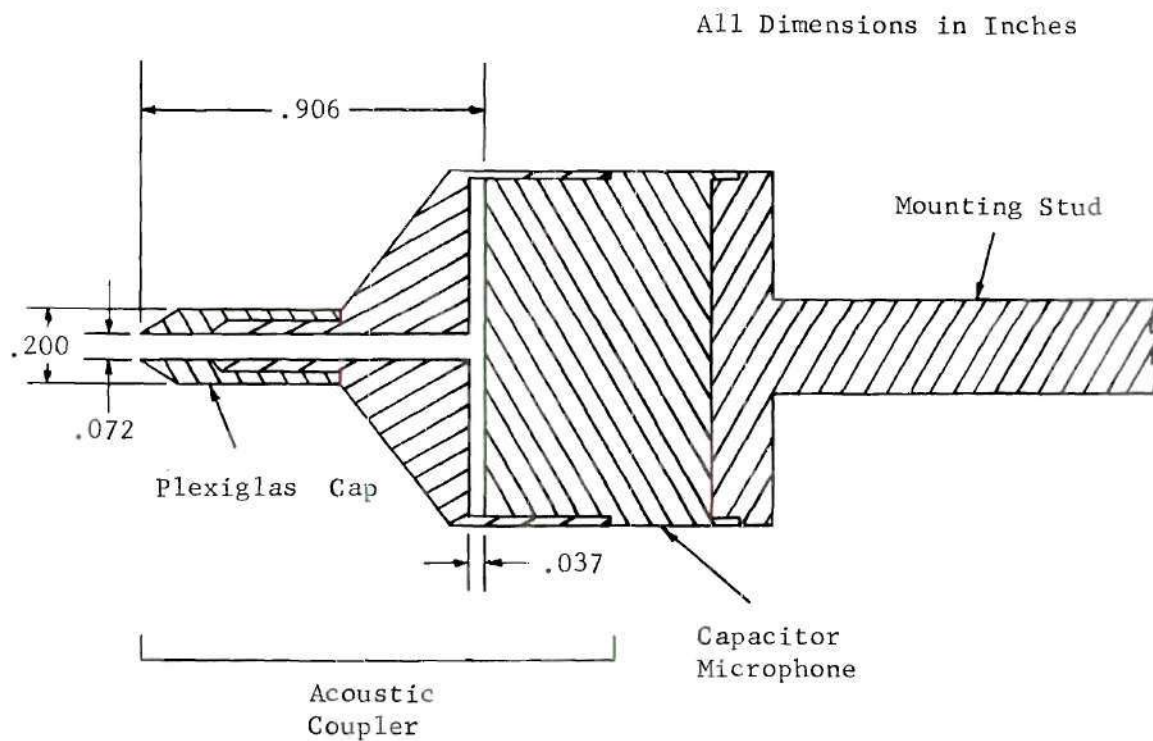


Figure 7. Cross Section of Capacitor Microphone, Acoustic Coupler, and Mounting Hardware

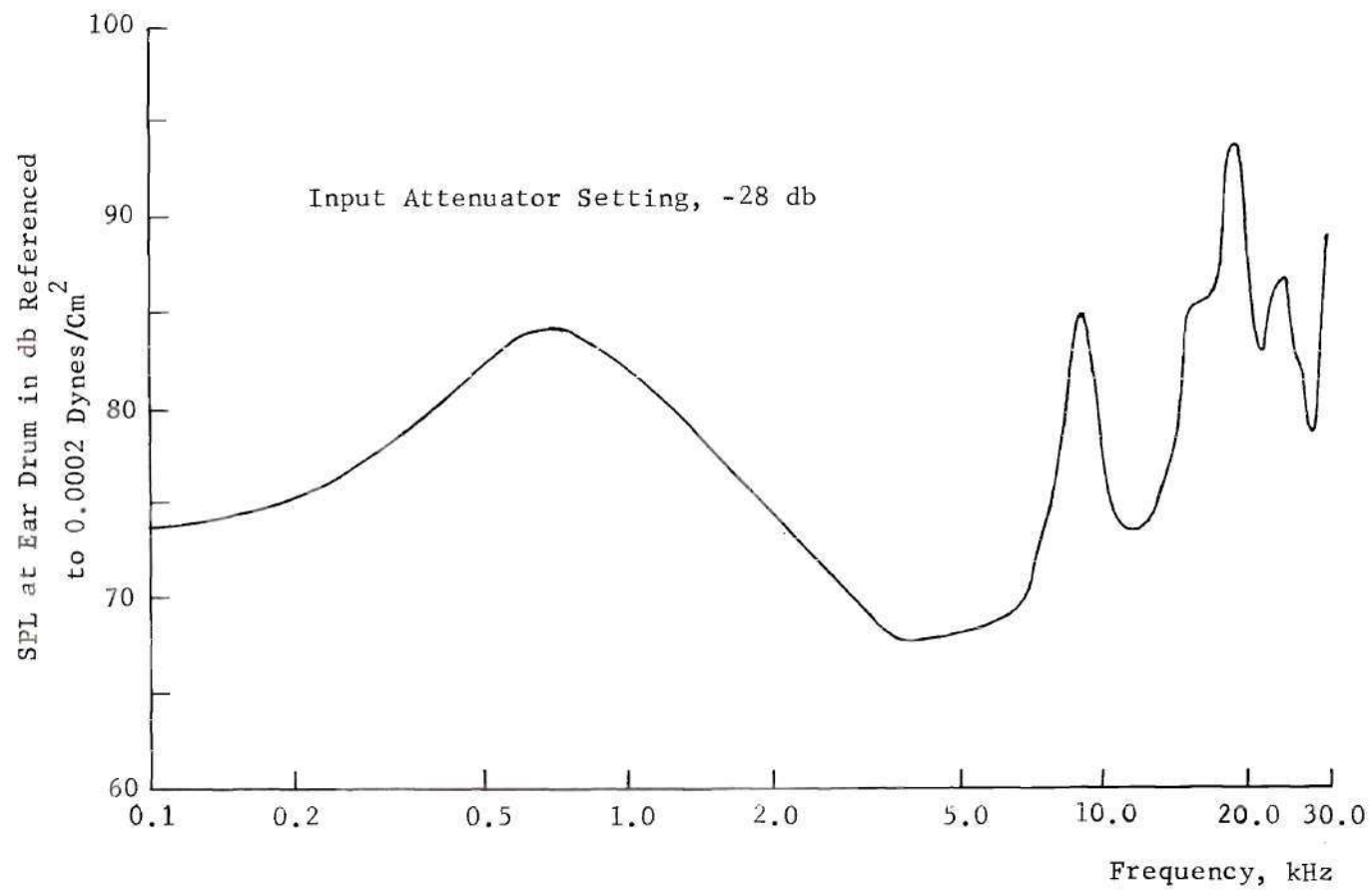


Figure 8. Calibration Curve for Acoustic Transducer

indicating no significant loading of the system by the measuring probe.

In later chapters of this dissertation, stimulus level or intensity, will be specified in terms of voltage input to the Bruel and Kjaer earphone system. For tone bursts of stated frequency, Figure 8 will allow these voltages to be converted into SPL in dB. For click stimuli, however, no attempt was made to obtain a calibration with the probe tube method, since the tube dynamics provided more than 20 dB of attenuation over a significant portion of the frequency spectrum for a 100- μ sec pulse. Nevertheless, an estimate of the click intensity delivered was obtained based on data given by Kiang (18). He indicates that a cochlear microphonic click response peak of about 200 μ v (measured on the round window of a cat) corresponds to a peak SPL of approximately 32 dynes/cm². (His method of calibration is unspecified.) To obtain a similar-sized response from the scala vestibuli of the guinea pig with the equipment described above, required an earphone pulse of 2.9 v, or a setting of -22 dB on the attenuator. Therefore, an order of magnitude estimate of peak instantaneous click SPL is 11 dynes/cm² per volt of earphone click input.

Some comment may be in order concerning the unevenness of the response curve of Figure 8, which is due to a combination of microphone dynamics and the acoustics of the coupling system. Certainly, a flat frequency characteristic would be more desirable, but none of the experiments performed in the prosecution of this research depended heavily on having constant intensity for all frequencies. In general,

it was felt that the imperfections of the system were acceptable, considering the wide dynamic range and small size of the Bruel and Kjaer earphone system.

Data Acquisition

Equipment for securing microphonics and spike data included the room in which procedures were carried out, microelectrodes for electrical contact to single nerve fibers (including devices for electrode production and mechanical manipulation), and amplifiers for nerve spikes and microphonic signals.

Experiment Room

The physical environment for the experiments was an acoustically shielded Faraday room measuring 8 feet by 12 feet. Acoustic shielding was accomplished by interior and exterior walls of 7/16-inch sheetrock with 1/2-inch sound-stop in the outside wall. This structure provided approximately 40 dB of attenuation for externally generated sound.

Sound pressure level measurements made in the room with a capacitance microphone (Bruel and Kjaer 4145) and amplifier (Bruel and Kjaer 2603) indicated high intensities (40-60 dB) of ambient sound of very low frequency (6-20 Hz) arising from vibrations of ventilation equipment in the building. However, since this type of sound is generally regarded as infra-sonic, it is felt that such interference was of no serious consequence. Sound level measurements made using the "A" weighting curve of the Bruel and Kjaer microphone amplifier, which provides considerable low-frequency filtering (40 dB at 30 Hz),

showed an ambient noise level in the room of less than 20 dB.

Microelectrodes

The nerve fiber responses were obtained by electrically contacting single fibers with glass pipette electrodes filled with 3M KCl electrolyte. They were produced by drawing 1-mm i.d. capillary tubing (Fisher 2-668-40) with a Kopf Model 700 C pipette puller. This machine supports the tubing vertically and heats the middle portion with a nichrome heating loop until the glass begins to melt, at which time a solenoid system pulls the glass apart, forming two very finely tapered pipettes. The actual tip geometry is a function of the size of the glass tubing stock, the heater coil current and geometry, and the amount of solenoid current. After some experience with the puller, values for these variables were found which repeatably produced pipettes of the required geometry. Scanning electron microscope pictures of the pipettes (taken at the Georgia Tech Engineering Experiment Station) showed them to have tip diameters of 0.3-0.4 μ , a size known to be sufficiently small for single fiber recording (10).

The filling of the microelectrodes with 3M KCl electrolyte was done by boiling them in the KCl under vacuum (31). It was found that reliable filling depended on having extremely clean glass and fluids; hence, the glass tubing was washed in HCl and detergent baths, and rinsed with distilled water which had been passed through 2- μ pore size filter paper (Gelman GA-8). The electrolyte bath was also passed through the filter before every use. For protection of the tips after filling, they were placed in a buffer bath of warm distilled

water before being placed under the light microscope for inspection of the tip region. Elimination of this procedure usually resulted in tip damage from sudden temperature changes.

Electrical Characteristics of Microelectrodes. Since microelectrodes similar to those described above have been so widely used in the past twenty years for intra- and extra-cellular research, considerable effort has been directed toward theoretical treatments of their operation, much of which has been summarized by Schanne et al. (32). However, from an operational viewpoint, the model of Figure 9 adequately describes the probes used in this study.

e_N = Nerve Potential
 T_P = Tip Potential
 R_{EL} = Electrode Resistance
 C_{EL} = Electrode Capacity
 e_{EL} = Electrode Output

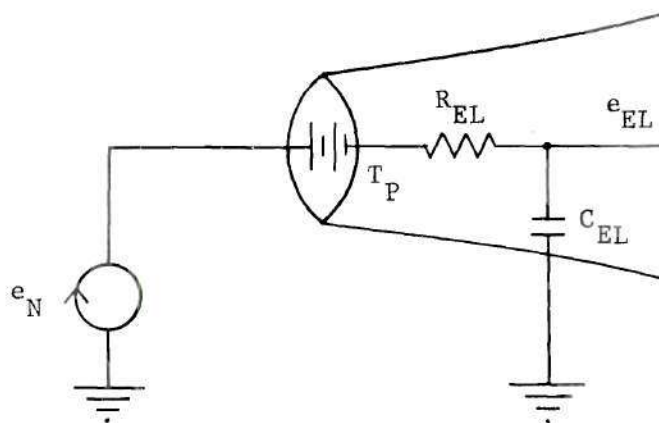


Figure 9. Electrical Model of a Microelectrode

The constant tip potential, T_P (see Figure 9), is a function of the tip size, the type of glass used, and the composition of the fluids inside and outside the probe. Since T_P merely adds a dc component to the output voltage e_{EL} , it may be disregarded for the measurements of this study, which were all taken with RC-coupled

amplification. However, microelectrode resistance, R_{EL} , and capacitance, C_{EL} , determine the probe's capability for making accurate nerve potential measurements, since the unit's bandwidth for measuring the nerve potential e_N is $1/R_{EL}C_{EL}$. The resistance R_{EL} is a function of the same parameters that determine T_P , and measurements of R_{EL} give fairly good indications of tip size, since the resistance varies inversely as tip diameter (32). The distributed capacitance, C_{EL} , between the fluids inside and outside the electrode, separated by the glass dielectric, depends primarily on the depth of immersion of the tip into the fluids surrounding the nerve fibers. Schanne et al. (32) indicate typical values for a $0.5\text{-}\mu$ electrode filled with 3M KCl, immersed 2 mm in a solution of 0.1M KCl as follows: R_{EL} , 10 M Ω ; T_P , 10 mv; C_{EL} , 2 pF. (Therefore, this electrode would have a bandwidth of about 8 kHz.) Impedances for many of the microelectrodes used in the experiments were measured, and without exception those units which later proved successful in isolating single fibers had R_{EL} 's in the 30 to 70 M Ω range, indicating tip diameters of less than $0.5\text{ }\mu$ (18).

Mechanical Driving System for Microelectrodes. One of the consequences of the small size of the individual nerve fibers and the microelectrodes used in recording from them is that relative motion between the electrode tips and the fibers must be held to a minimum. Otherwise, such motion destroys the electrical contact before sufficient data can be obtained for most of the experiments in the study. (A single experiment usually involved taking data in 30- or 60-second runs as stimulus parameters were varied from run to run, so that three

to four minutes was about the least amount of time that a fiber could be held and provide useful information.) Therefore, the animal's head had to be securely fastened to the frame which supported the electrode carrier, and the whole system had to be mounted on a platform that was as free of mechanical vibration as possible.

As mentioned above, the experiment room was subject to high levels of infrasonic vibration (6-20 Hz) arising from the building ventilation system. To provide some degree of isolation from these vibrations, a special table was constructed with a 500-pound concrete top floated on springs with compliances picked so that the resulting system had a natural frequency of about 3 Hz. Accelerometer measurements indicated that this system provided about 20-30 dB of attenuation for the building vibrations.

To maintain mechanical rigidity between the animal and electrode, the subject's head was secured in a David Kopf Model 900 head-holder, which gave support with a mouth-bar and two earbars. Mounted on the head-holder frame was a two-degree-of-freedom electrode carrier, to which was added an additional worm drive, so that three degrees of motion were possible for gross placements of electrodes.

Fine microelectrode placement was accomplished with a David Kopf 1207B hydraulic microdrive attached to the electrode carrier on the head-holder. This apparatus is essentially a cylinder and piston arrangement connected by a water-filled Teflon tube to a remotely located cylinder and piston and calibrated via a micrometer and gear system. It allowed the electrode to be advanced in increments smaller than $1\text{ }\mu$ with good stability. The microdrive was modified by attaching

a synchronous stepping motor with appropriate logic so that from outside the experiment room the electrode could be advanced or retracted in either single steps (0.25μ) or at an adjustable constant rate.

Microelectrode Amplifier

Fiber spike signals from the microelectrodes were initially amplified inside the experiment room with a vacuum tube system using four EF86 pentodes. Tubes were used because of the inherently higher noise levels of semi-conductor amplifiers.

Input requirements for the amplifier arose from the microelectrode parameters as indicated in Figure 9. Since R_{EL} is on the order of 10-20 $M\Omega$, the amplifier input impedance had to be on the order of 100 $M\Omega$ to prevent excessive signal attenuation. Hence, the first stage was a cathode follower, the grid of which was connected directly to the pipette electrolyte with a platinum wire. In order to keep the system bandwidth as large as possible, it was necessary to minimize any amplifier input wiring capacitance (which would effectively increase C_{EL}) by mounting the cathode follower directly on the microdrive. After the follower, two gain stages, all capacitively coupled, provided amplification, and a final cathode follower output stage gave a low impedance source for driving signal processing equipment located outside the experiment room. With a typical microelectrode connected, the amplifier supplied a mid-band gain of 600, with an upper 3-dB limiting frequency of 3.5 kHz.

Cochlear Microphonic Amplifier

Due to the lower impedance levels associated with CM response,

amplifier input requirements were less stringent than for the micro-electrode amplifier. The input stage for the CM amplifier was an FET source follower, shunted by 22-M Ω resistors, and connected to a Burr-Brown 3054/01 operational amplifier. Coupling capacitors and feedback and input resistors were selected to yield a mid-band gain of 1000, and a 3-dB lower cut-off frequency of 1.6 kHz. The CM amplifier output was fed to the GR recording wave analyzer so that frequency response curves for CM could be easily obtained.

Data Processing and Reduction Equipment

Data processing equipment assembled for this research was arranged so that spike information could be handled in either an off- or on-line fashion (or both). Spike trains were converted in real time into binary numbers corresponding to the time of occurrence of each spike. These numbers were then recorded on an incremental tape recorder (Kennedy 1600) for later off-line analysis on the Univac 1108 computer. Data were also processed "on-line" with a GRI 909 computer, which calculated PST histograms for oscilloscope or strip-chart display. As a back-up precaution, spike trains and timing information were often recorded on an analog tape recorder (Uher 7000D) for later play-back into either the GRI or Kennedy systems with some loss in system accuracy.

Off-line Processing

A block diagram of the data processing and reduction system is shown in Figure 10. For off-line work, the basic idea was to record on the digital tape a binary representation of the occurrence time of

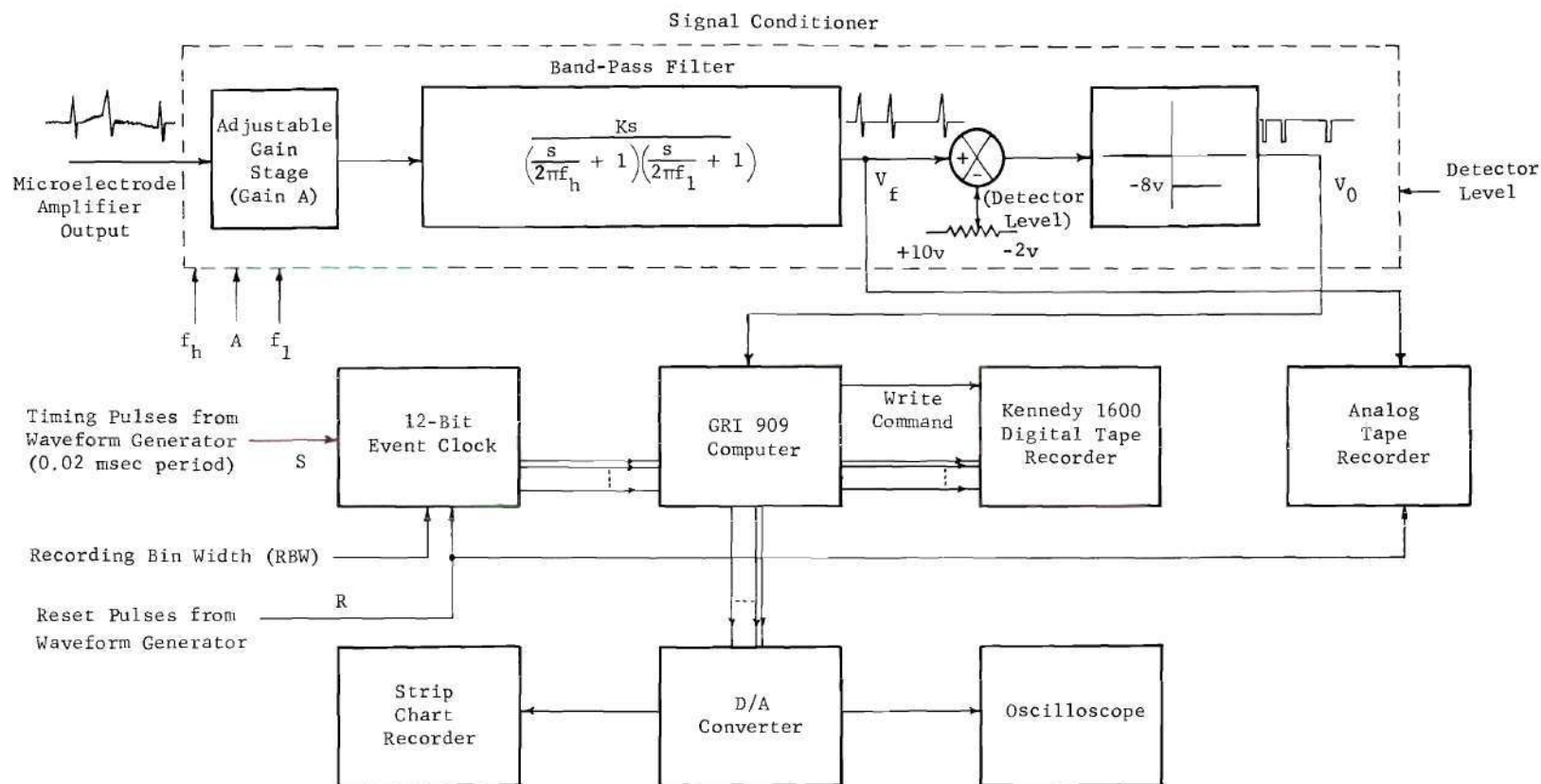


Figure 10. Block Diagram of Data Processing and Reduction System

each spike by causing the recorder to write the contents of an event clock for each fiber response. The event clock was a 12-bit binary counter advanced with 0.02-msec period pulses from the stimulus generator system, which also provided the clock reset at the start of each stimulus period. Clock data could not be placed directly on the tape, because the Kennedy recorder could reliably log spikes only at rates less than about 370/sec. Since actual spike rates can sometimes exceed this limit for a few milliseconds (even though average rates are seldom above 200/sec), it was necessary to use the GRI memory as a data buffer unit, so that regardless of the instantaneous spike rate, the data rate to the recorder was less than 370/sec.

The event clock counter provided timing information with a maximum resolution of 0.02 msec, synchronized with the stimulus period. The maximum amount of time that a 12 bit counter can encode in 0.02 msec steps is $2^{12} \times 0.02 = 91.92$ msec. However, many experiments required longer analysis periods and could be accomplished with resolution times longer than 0.02 msec. Therefore, provision was made to scale the clock input so that each counter state corresponded to selectable intervals of 0.02, 0.05, 0.1, 0.25, 0.5, or 1 msec. Since this scaling effectively changed the width of the time bins into which spike occurrence times were logged by the recorder, this setting was called the "Recording Bin Width" (RBW).

Write commands to the tape recorder were pulses generated by the GRI computer whenever the microelectrode amplifier output exceeded a certain preset detector level. This operation was accomplished by a "Signal Conditioner" (as shown schematically in Figure 10) which

performed three functions: spike amplitude normalization, band-pass filtering, and level detection.

Spike amplitude normalization was necessary since the measured voltage spikes from a nerve fiber normally become smaller over the course of recording (5-20 minutes) as contact with the fiber is gradually lost. However, for level detection of spikes, it is desirable for them to maintain approximately the same amplitude relative to the detection level; hence, the Signal Conditioner was equipped with an adjustable gain stage for gains of from 0.1 to 1000.

Output from the microelectrode amplifier normally contained in addition to action potential spikes, electrophysiological noise of much lower frequency content than the nerve signal and also some high-frequency noise arising from the electrode and amplifier. To minimize degradation of the level detection scheme with these components, simple 6 dB/octave band-pass filtering (with the transfer function indicated in Figure 10) was used. The lower and upper roll-off frequencies, f_l and f_h respectively, were variable but were usually set at 500 Hz for f_l and 10 kHz for f_h .

The final output of the signal conditioner, which caused the computer to trigger the write circuits of the recorder, was a voltage, V_O , which underwent a large positive-negative shift whenever the filter output, V_f , exceeded an adjustable detector level. All sections of the Signal Conditioner were implemented with Burr-Brown 7077C operational amplifiers connected in standard configurations.

On-line Processing

It was often desirable to obtain a preliminary on-line indication

of fiber response patterns. To provide such a capability, the GRI computer was programmed to generate and store PST histograms while simultaneously relaying event clock data to the incremental recorder. Histogram arrays were displayed on an oscilloscope or strip chart recorder after being converted into analog form with a Computer Products Corporation DA635 digital-to-analog converter.

CHAPTER III

PROCEDURES

As indicated in Table 1 of Chapter I, five procedures were involved in obtaining the experimental data for this research. These were as follows: (1) Animal preparation; (2) CM modification; (3) Data acquisition; (4) Stimulus presentation; (5) Data processing and reduction.

Animal Preparation

The most exacting parts of the experiments pertained to the preparation of subjects for data taking. The entire peripheral auditory system of the guinea pigs had to be completely exposed while trying to maintain the animals in a reasonably normal physiological state. Hence, blood loss had to be kept at a minimum, critical blood supplies and respiration uninterrupted, and body temperature had to be controlled. All animals were young, adult guinea pigs, weighing about 250-300 gm.

A qualitative test of the animal's hearing was the first step in preparing for an experiment. This was accomplished by presenting a loud sound (e.g., a hand clap) near the animal, which could not see the sound being made. Normally hearing animals responded with twitching of the pinna (outer ears), but if hearing was impaired, the reflex was absent or noticeably attenuated. Animals passing the test were anesthetized with Dial in urethane (Ciba) administered intraperitoneally.

Initial dosage was 0.7 cc/kg, but often the amount had to be increased to about 1 cc/kg to render the animal quiet enough for surgery.

Subjects anesthetized deeply enough for gross surgery showed at least two forms of physiological deterioration: difficulty in respiring and loss of ability to maintain normal body temperature. To overcome ventilation problems, tracheotomies were performed on all animals and artificial respiration was employed using a Bennet Model PR1 respirator. Body temperature was maintained with a closed-loop system activated by a rectal thermistor probe, the output of which controlled current to an electric blanket supporting the preparation. This system was capable of holding body temperature to within about 1°C of the nominal value, 38° . To provide a check on physiological condition, continuous electrocardiogram (ECG) signals were obtained with all subjects using an ECG amplifier (gain 100) constructed around a Motorola 1741 operational amplifier with FET differential input stages shunted with $1\text{-M}\Omega$ resistors. Signals from this amplifier were boosted with an audio power amplifier and fed to loudspeakers located inside and outside the experiment room, so that the experimenter had a running audible index of the animal's condition.

The surgical approach for exposing the auditory nerve was essentially the same as that originally developed by Tasaki (10). It consisted of exposing the cochlea and drilling a small hole near its base to intersect the nerve bundle. This path to the nerve offers two significant advantages in the guinea pig. First, if the hole does not enter the cerebral cavity, the fibers encountered all lie inside the

internal meatus and may be classified as primary units on this basis alone (10). (All the fibers of the present study meet this criterion.) Secondly, the cochlea is conveniently exposed intact so that electrical measurements may be obtained from it and any desired manipulation performed on it. This situation does not hold in the cat and monkey, since the cochleas of these species are more deeply imbedded in bone and are not so easily accessible.

Since Tasaki's original work in 1953 (10), only one other study utilizing his approach to the auditory nerve has been published (26,27). (The only other report using guinea pigs was Hanna's (20), in which the nerve was approached from the brain.) The reason for this, undoubtedly, is that due to the anatomy of the area at the base of the cochlea, it is very difficult to expose the nerve by drilling without encountering severe hemorrhaging from the transverse sinus vein and its branches. This vein occupies a fissure, which separates the bulla from the bottom portion of the occipital bone, and is situated almost directly in line with the point at the base of the cochlea where the drill hole must be started if the hole is to avoid the scala tympani of the cochlea. It was usually possible to overcome this difficulty by very carefully forcing the transverse sinus to one side after a slight amount of drilling on the occipital bone.

The actual steps in the surgical procedure usually proceeded as follows. First, the tragus cartilage was removed from the external ear so that the ear bar and earphone coupler mounted in the head-holder could later be easily inserted for positive mechanical support. Next, the trachea was exposed by removing an area of skin and muscle from the

neck, and a small hole was cut in the trachea, into which was inserted a Teflon cannula for connection with the respirator. At this point, the animal was firmly secured in the head-holder, ventral side up. In the following discussion, any directions will be referenced to the animal in this position. For example, with an animal in the head-holder, the brain lies "below" the neck.

Since the bulla lies partially below the mandible (jawbone) and its muscle, the masseter, the posterior portions of those two structures above the cochlea to be instrumented were next removed. Bleeding was minimized by ligating the external jugular vein and some of its branches and by firmly tying heavy suture through the mid-portion of the masseter muscle. Next, removal of the stylohyoid, the posterior belly of the digastric, and the stylopharyngeal muscles left the bulla completely exposed. Due to the small size of the guinea pig auditory system, all succeeding procedures were accomplished under 10X magnification from a Zeiss operating microscope.

The next step was to sever the mastoid process at its base and then remove a portion of the bulla with a Kerr high-speed drill. The resulting opening was shaped with the drill so that the peripheral auditory system was exposed from the edge of the ear drum to the base of the cochlea. After this, a small hole ($\approx 35 \mu$) was drilled in the scala vestibuli for cochlear microphonics measurements. Contact with the cochlear fluid was made with 25- μ , enamel-insulated wire, which was secured to the upper side of the bulla with dental cement.

At this point, the animal's hearing was tested by running a response curve for the CM with the recording wave analyzer, the stimulus

being a 0.2 v (p-p) continuously swept sine wave driving the capacitor earphone. After taking these curves from many preparations, it became possible to judge the general condition of the subject's auditory system from them. Additional curves were taken routinely throughout the course of a day's experimentation to monitor any deterioration of the auditory system.

The bulla having been opened and a microphonics curve having shown the animal to have normal hearing, the exposure of the auditory nerve was begun. This was done by drilling a 1-mm hole at the base of the cochlea, directed underneath the scala tympani of the basal turn to approach the nerve in the internal auditory meatus just below the point where it leaves the modiolus at about a 45° angle. The starting point for the hole was near the edge of the bulla and the angle of the hole was such that, as pointed out above, the transverse sinus vein would normally be intersected. Therefore, a small portion of the occipital bone beneath the sinus was drilled away so that the vein could be displaced slightly. This procedure was greatly facilitated by the use of a diamond cutting bit, which removed bone easily but caused minimum trauma to tissue. These operations usually gave sufficient access for drilling at the desired point.

On some occasions there was communication with the scala tympani before reaching the nerve, but usually the only difficulty caused by this was the accumulation of small amounts of perilymph (cochlear fluid) in the drill hole (which was removed by suction). In these cases, CM response curves were run to see that hearing was not grossly impaired. In a few other instances, however, (especially if drilling

of the hole produced bleeding near or in the nerve), the CM frequency response was attenuated 20 or 30 dB for all frequencies above a few kHz. These preparations were discarded.

The auditory nerve bundle was usually encountered at a depth of about 2 mm. A tough membrane (the invagination of the dura mater) covers the bundle, so that light drilling on the surface was sometimes necessary to render the fibers accessible. At this point (unless CM modification was desired), a microelectrode was secured on the electrode microdrive, placed in the nerve bundle by visual control, and advanced by remote control to begin the data acquisition procedures.

Cochlear Microphonic Modification

If an experiment called for CM modification, additional procedures were performed. As indicated in Chapter I, two methods were used for controlling CM levels independently of sound input. The most extensively employed procedure consisted of imposing electric current across the cochlear partition, but results were also obtained for cochlear temperature modification by the application of heat. Both these methods were used in conjunction with continuous tones or tone burst stimuli.

Microphonic Modification by Electric Currents

The procedures used in this study for placing electric current across the basilar membrane were patterned after those given by Dallas et al. (33). Two small holes ($\approx 60 \mu$) were drilled in the basal turn, one in the scala vestibuli, and the other directly across the cochlear partition in the scala tympani. Then, two pipette electrodes (tip

diameter $\approx 50 \mu$), filled with Ringer's solution as an electrolyte, were placed in the holes and secured to the edge of the bulla with dental cement. Connection between the electrodes and the current source was made with silver wires coated with silver chloride (34). This Ag-AgCl electrode system prevented formation of gas bubbles at the electrode-electrolyte interface during current passage.

By changing current sources, three modes of current application were available. First, prolonged direct currents were obtained from a 180-v battery pack. Source polarity was reversible, and a 10-M Ω potentiometer was placed in series so that currents of controllable size could be forced across the cochlea in either direction. To keep the polarization current from taking a path other than directly across the partition, the battery was electrically isolated from animal ground.

In some experiments, it was desired to pulse the polarization current so that it was present only during a 40-msec portion of the tone burst stimulus period. This second mode was accomplished by switching the battery source with a relay activated by signals from the stimulus waveform generator. To reduce the resulting switching artifact, the current electrodes were wrapped with foil shielding and a 0.005-mfd capacitor was connected between the relay output and battery common. Due to the capacitor, the pulse current delivered to the cochlea exhibited a rise time of about 2.5 msec.

The third current mode involved the introduction of alternating currents in an attempt to stimulate fibers with an "artificial microphonic." In this case, the current was derived from the stimulus

waveform generator tone bursts. To gain electrical isolation from animal ground, the stimulus signal was floated with a battery-powered operational amplifier-transformer circuit, as indicated in Figure 11. To determine the resulting current, i_a , without an animal ground connection, voltage across the resistor R was measured with a second operational amplifier-transformer circuit to produce signal V_1 , which was proportional to i_a .

Microphonic Modification by Cochlear Heating

The other method for non-acoustic alteration of CM was by the application of heat directly to the cochlea. This was accomplished by focusing infra-red radiation from a nichrome heating coil with a spherical reflector. Heating coil current was supplied from storage batteries and was adjusted with a potentiometer. This arrangement allowed heat to be concentrated in about a 6-mm circular area, which covered the entire cochlea. Care was taken in positioning the coil and reflector so that the edge of the bulla shielded the eardrum and ossicles from direct radiation.

Data Acquisition

After an animal was prepared, fiber spike data acquisition commenced with slowly advancing a microelectrode into the nerve bundle and searching for fibers responding to sound stimuli. This process was greatly facilitated by listening to the nerve spike amplifier output over a loudspeaker while simultaneously presenting loud tone bursts to the animal at a rate of 10/sec. Since all primary auditory fibers exhibit spontaneous activity, an alternative procedure was to look for

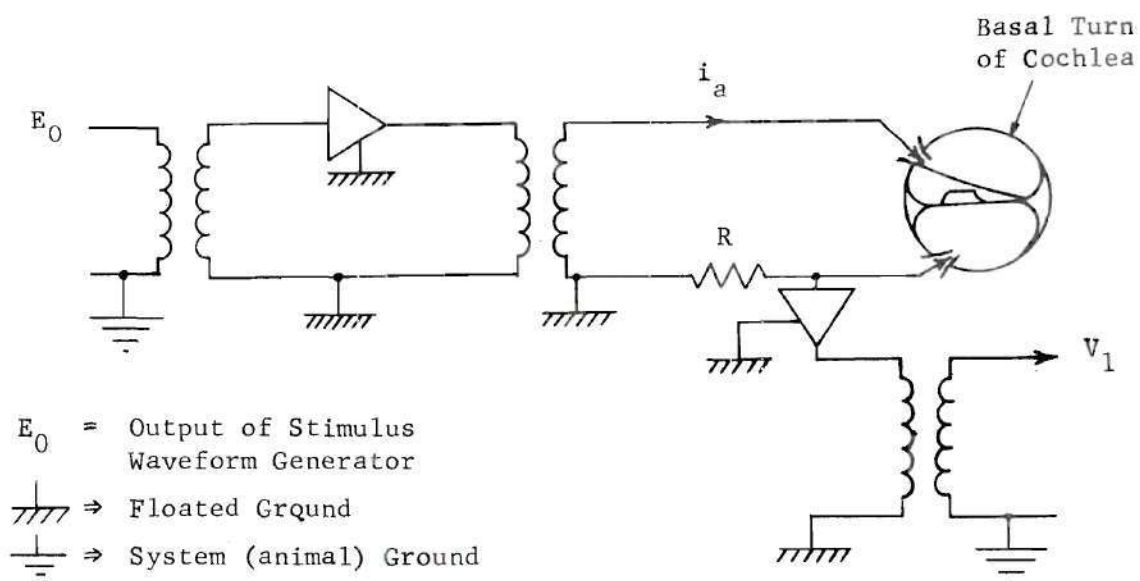


Figure 11. Schematic Diagram of Alternating Current Stimulating System

nerves firing in the absence of sound and then present bursts. In either case, auditory fibers responded noticeably with periods of increased firing rates during stimulation. A portion of a spike train showing the response of a fiber to tone bursts is shown in Figure 12. This unit was obviously responding to the acoustic stimulation, and spontaneous activity was evident between stimuli. The shape of the spike wave form in the figure is typical of all those encountered in the study.

In addition to the fiber responses typified in Figure 12, two other types of neural behavior were encountered in the nerve bundle, both of which are noted by Kiang in the cat (18). First, many fibers were contacted which showed spike behavior which could not be modified by sound stimuli. These fibers presumably belonged to the vestibular branch of the auditory nerve, which originates in the semi-circular canals. The other type of behavior was characterized by very high initial spike rates (as great as 200/sec), which dropped to zero over a period of less than a minute, during which time the fiber was not responsive to sound. This type of behavior probably resulted from injury of a cell body by the electrode. For all the fibers used in this study, it is believed that the electrode had no damaging effects, since general characteristics of behavior (e.g., rate of spontaneous activity) remained essentially unchanged from the time a fiber was contacted until it was lost.

Immediately after a fiber was contacted, its characteristic frequency (CF) was determined by presenting 50-msec tone bursts at a rate of 10/sec and searching for the burst frequency which resulted

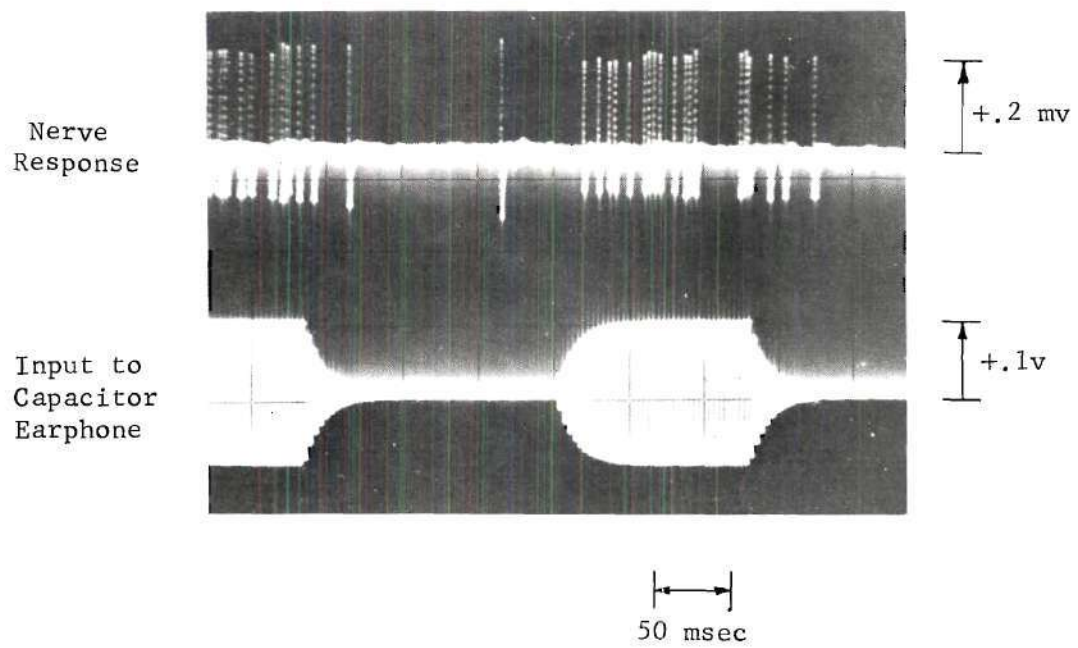


Figure 12. Spike Response of a Single Fiber to Tone Bursts

in alterations in spontaneous activity for minimal sound level. That level was then taken to be the fiber's tone burst threshold (TBT). With the unit thus characterized, automatic stimulus presentation procedures were initiated.

Stimulus Presentation

To obtain histogram response patterns, tone burst or click stimuli were presented for periods of 30 or 60 seconds, during which time the same stimulus was repeated with a constant period between the beginnings of consecutive stimuli. A complete experiment, then, consisted of a series of 30 or 60-second runs, with either a stimulus parameter (e.g., level, or burst duration) or CM modification being altered between runs.

Data Processing and Reduction

Procedures for generating PST and ISI histograms involved straightforward programming both for the Univac 1108 computer (off-line analysis) and for the GRI 909 on-line computer.

Off-line Analysis

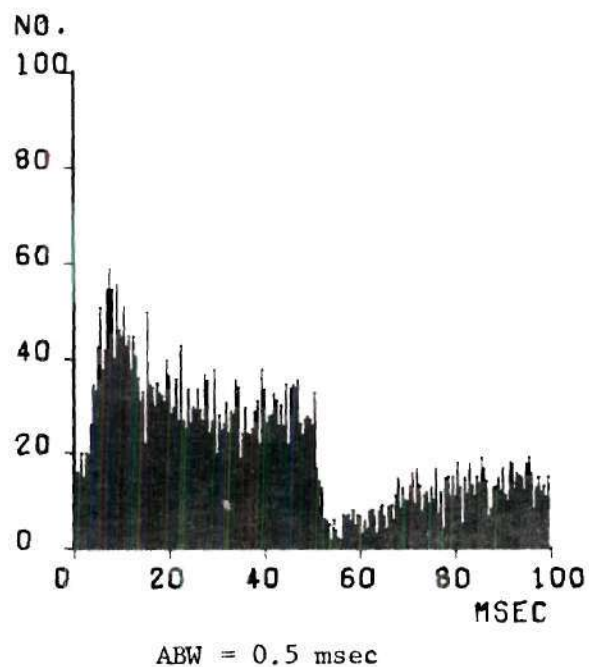
For off-line data reduction a program was written to enable the 1108 computer to read spike occurrence times from the digital tape of the Kennedy recorder and to compute PST and ISI histograms. In most cases data were originally taken with a recording bin width (RBW) considerably smaller than the actual bin width (ABW) desired in the final histograms. Therefore, ABW (necessarily an integral multiple of RBW) was made a program parameter, and it could be adjusted in the processing for each experiment run. The resulting histograms were

printed out in one-dimensional arrays and were also plotted with a Calcomp plotter.

A typical Calcomp-produced histogram is shown in Figure 13. Stimuli in this example were tone bursts of 50-msec duration, stimulus period 100 msec, and -35 dB level; RBW was 0.1 msec. ABW in this plot was 0.5 msec, so that the height of the k^{th} bar represents the number of spikes occurring between $0.5k$ and $0.5(k + 1)$ msec.

On-line Analysis

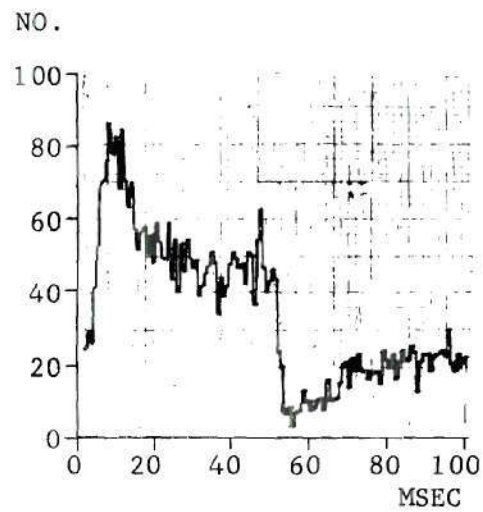
The programming for the GRI 909 computer for use in on-line processing accomplished the same results as that for off-line analysis. Differences were due mainly to the limitation of GRI memory size (4096, sixteen-bit words) and the fact that a strip chart recorder or oscilloscope was used to display the histograms. One processing constraint was that ABW's for the GRI computations were binary multiples of the RBW instead of the arbitrary integral multiples available from off-line analysis. Also, plots from the oscilloscope or strip chart showed only the tops of the histogram bars, so that the graphs were more difficult to assess visually than their Calcomp counterparts. A strip chart histogram for the same data used in Figure 13 is shown in Figure 14. Note that the shape is the same, but heights of the points are larger than the bar heights of Figure 13 because ABW in this display is 0.8 msec (2^3RBW) as opposed to 0.5 msec (5RBW) for the Calcomp plot.



Stimuli: Tone Bursts; Duration = 50 msec; Rise-Fall Time = 2.5 msec;
Stimulus Period = 100 msec; Frequency = 19 kHz (CF)
Level = -35 db

Histogram was computed from a 30-sec data sample.

Figure 13. PST Histogram Drawn by the Calcomp Plotter



ABW = 0.8 msec

Figure 14. PST Histogram for Data of Fig. 13 Drawn with Strip Chart Recorder

CHAPTER IV

RESULTS

The results of this research are twofold. First, response characterizations for individual primary auditory nerve fibers in the guinea pig were obtained as selected stimulus parameters were varied. This was accomplished with a data acquisition and reduction system which greatly facilitated the analysis of such data. The response characteristics turned out to be essentially the same as those that have been previously shown from cat and monkey data. Secondly, response patterns were generated as the cochlear microphonic voltage of the inner ear was modified by non-acoustic means. These experiments showed that fiber activity changes can be related to changes in the CM, a result which may be interpreted as strengthening the microphonic trigger hypothesis.

During the execution of the research, approximately 180 guinea pigs were operated on. The first hundred or so were devoted to developing the surgical techniques necessary to expose the auditory nerve. Fiber responses to acoustic stimuli were obtained in about 50 per cent of the remainder, and from those preparations, over 250 nerve fibers were contacted long enough to measure at least the CF.

The results are presented in two parts. Part I deals with response characterization, and Part II pertains to the effects of CM modification.

Part I - The Characterization of Response Patterns

The first research objective was to characterize individual auditory nerve fiber responses to selected sound stimuli and to correlate those response patterns with data obtained from cats and monkeys.

To satisfy this objective, fiber responses were studied for stimulation by tone bursts and clicks of varying parameters. These easily produced and controlled stimuli have traditionally been widely used in many types of auditory research. Their utility is obvious in view of the apparent linearity of the middle ear-basilar membrane system. Short acoustic clicks, precisely defined in time, yield data related to impulse response. Continuous tones give frequency information, but with little or no indication as to the overall time structure responses. Tone bursts, however, provide a compromise between clicks and continuous tone stimulation, since they possess precise on and off times and still exhibit definite frequency content.

Response to Tone Burst Stimuli of Changing Parameters

PST and ISI histograms were obtained with tone bursts of varying duration, level, stimulus period, and frequency -- parameters defined by Figure 15 in terms of the electrical signal delivered to the earbar transducer. Note that leading and trailing edges of the burst envelopes were exponential to minimize spread of energy to frequencies other than the burst frequency. The time constant of the envelope, or rise-fall time T_e , was maintained at 2.5 msec for all burst experiments in this research. In the discussions and figures to follow, parameters will be referenced by the symbols indicated in the figure, and L , burst amplitude, will be specified in dB referenced to 50 v. One other parameter,

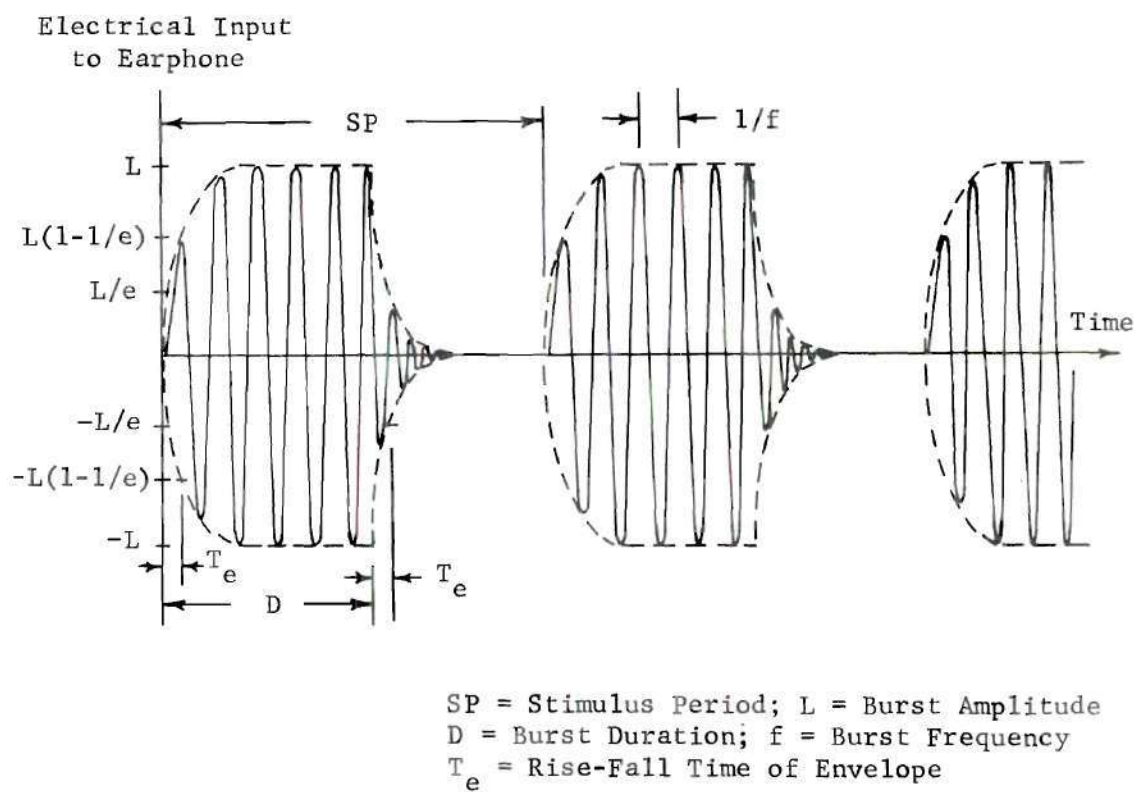


Figure 15. Definition of Tone Burst Parameters

the phase of the tone relative to onset time, would be necessary to specify the waveform exactly. That quantity was, of course, constrained to be constant for each burst in an experiment run, but as a consequence of the waveform generation system, it varied with frequency and was not specified.

Effects of Changing Burst Duration. To examine the manner in which primary fibers react to short tones of varying duration, a series of experiments was run in which burst duration, D , was systematically varied while the other parameters were held as follows: $SP = 100$ msec (burst rate of 10/sec); $T_e = 2.5$ msec; $f =$ characteristic frequency (CF); $L = 10$ -20 dB above threshold (as defined in Chapter III).

The results from a typical experiment with a low-CF (1 kHz) unit are given in Figure 16, in which many characteristics of burst response are apparent. (High-CF units show the same general characteristics also.) In this and all succeeding histogram figures, T indicates the length of the samples used in computing the graphs. In general, the PST burst response envelopes show a sharp peak at the beginning of the stimulus, followed by a decline to a fairly constant discharge rate, which holds until the end of the burst, after which activity almost disappears and then slowly builds up to spontaneous level. The ISI histograms show two peaks which approach each other and merge as duration becomes long, the second peak representing occasions on which no spontaneous spikes occurred between bursts.

The initial peaks of the PST histograms in Figure 16 show clearly that the probability of a spike occurrence is greatest at the beginning of a burst and then falls to a fairly stable value within

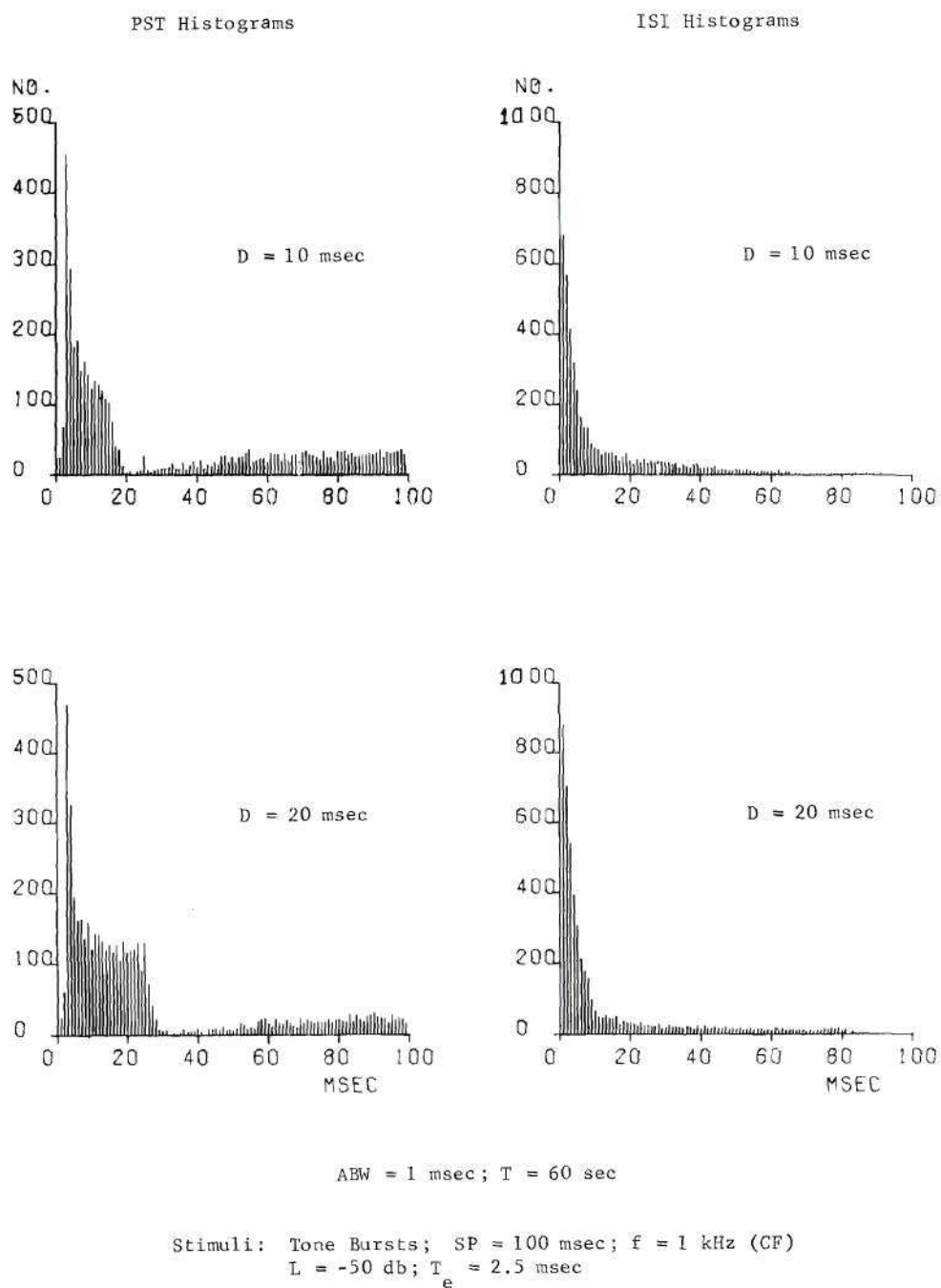


Figure 16. PST and ISI Histograms for Unit 115-6
as Burst Duration is Increased

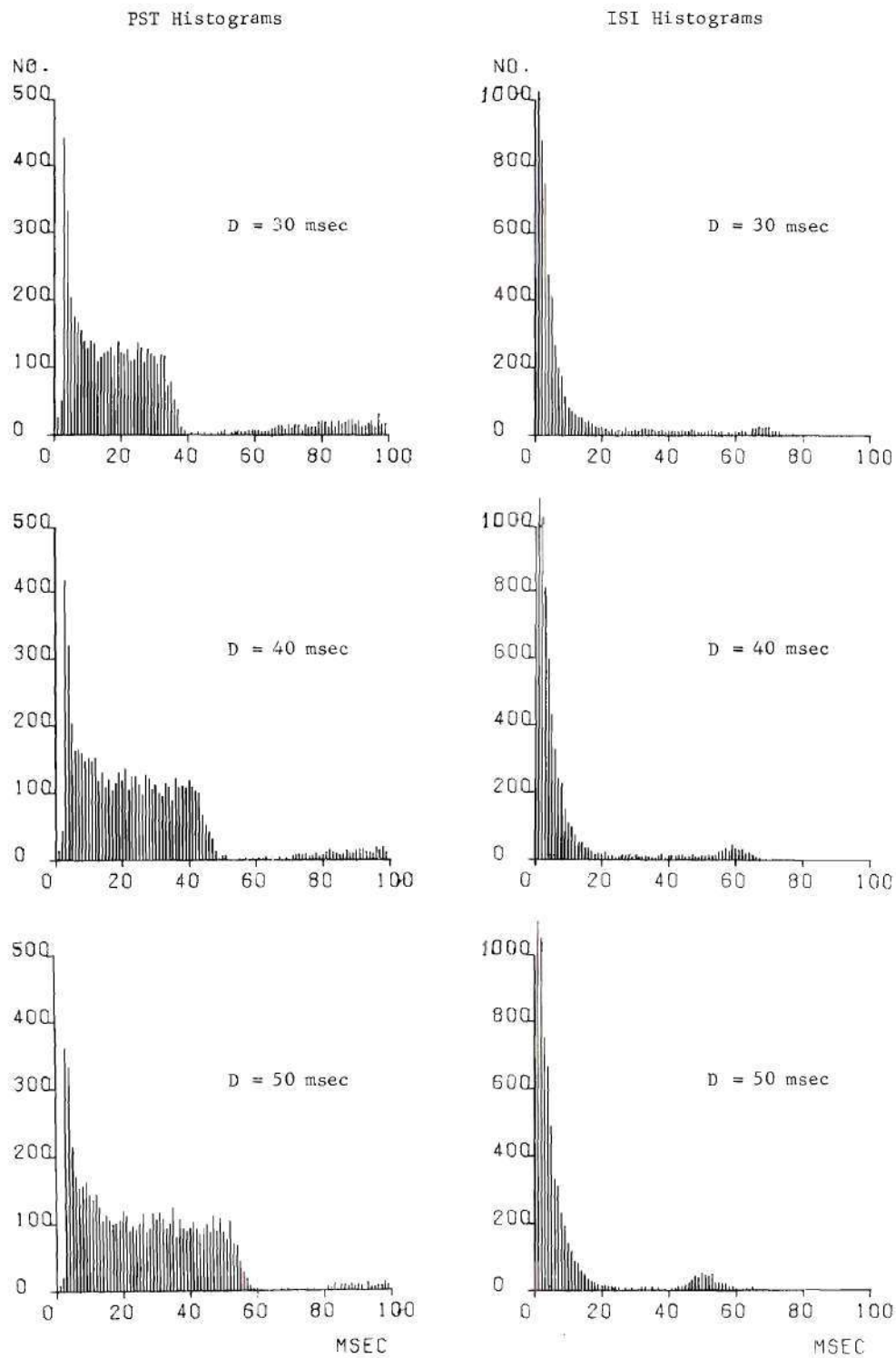


Figure 16. (Continued)

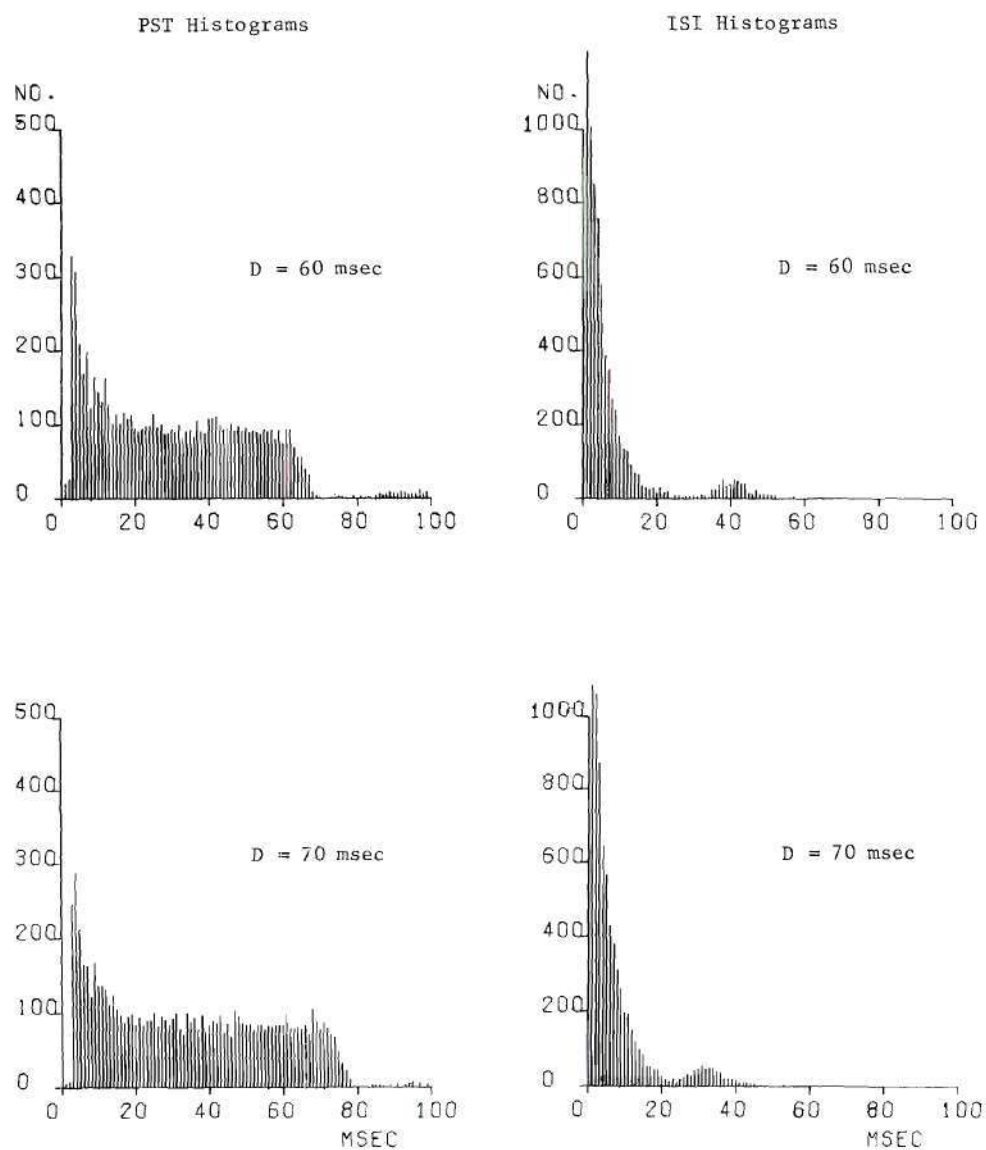
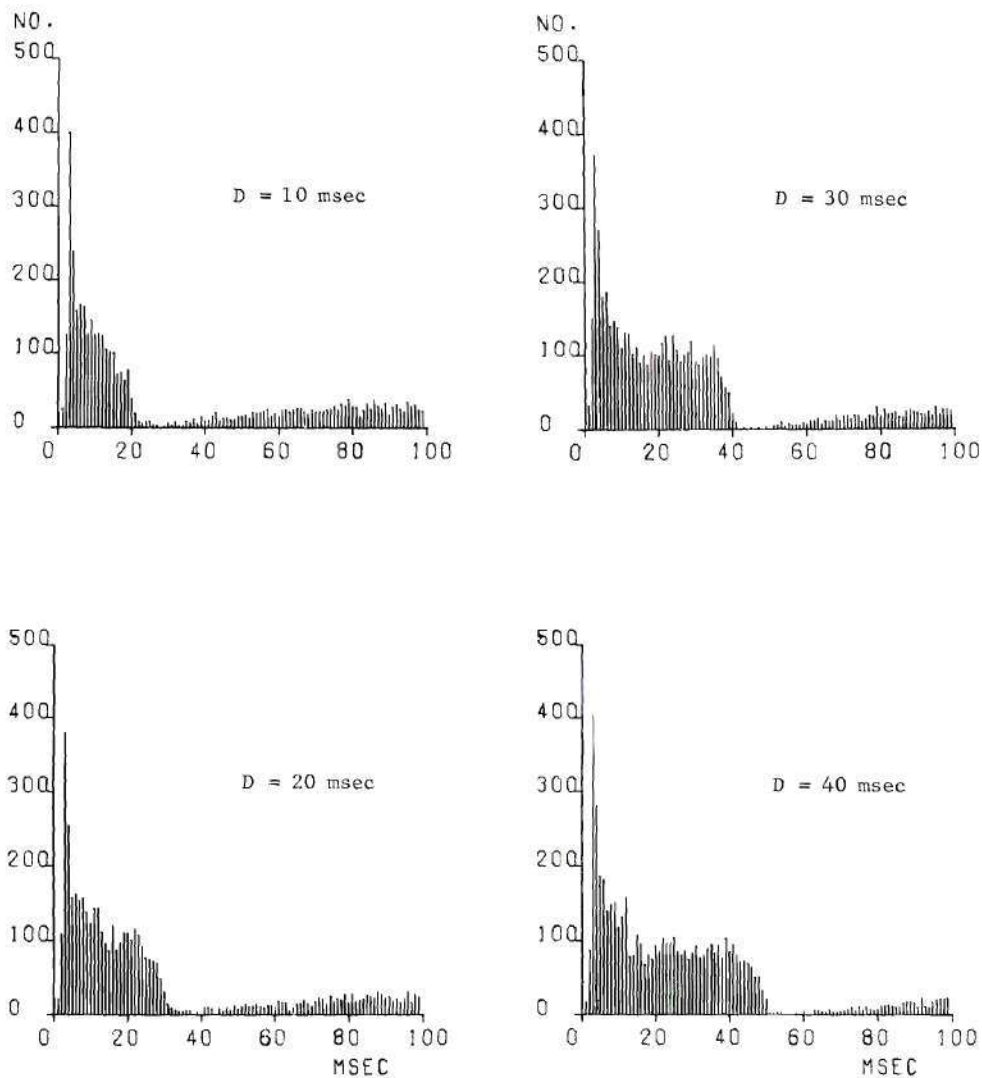


Figure 16. (Continued)

about 20 msec. This phenomenon of "adaptation" is well known in many parts of the nervous system, and was originally thought to derive exclusively from the refractory characteristics of neurons (18). (For a time interval immediately after a nerve firing, called the absolute refractory period, a fiber may not be excited regardless of stimulus magnitude. After that interval, the unit's excitability gradually increases to a steady-state value, after which it is said to be "recovered." For mammalian fibers this absolute refractory period is approximately one millisecond long, so that an upper limit on firing rates is about 1000/sec.) However, Gray (19), and Rose et al. (16) using cats and monkeys respectively showed that after the recovery period of an auditory fiber, the probability of a response to a cycle of a tonal stimulus becomes independent of time, implying that some mechanism other than refractory effects, presumably peripheral to the fiber ending, has direct influence on unit temporal response.

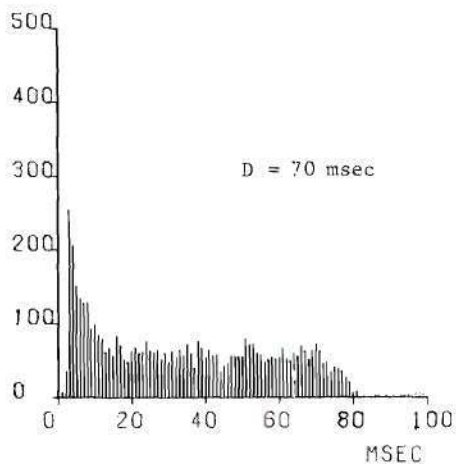
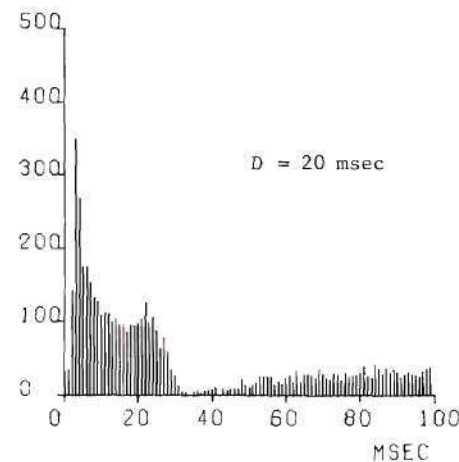
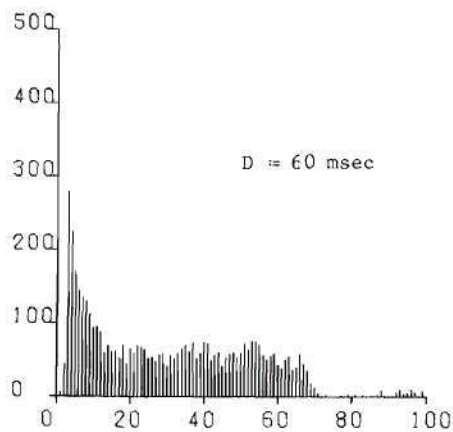
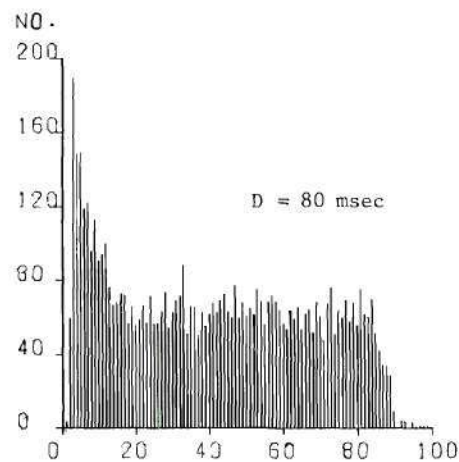
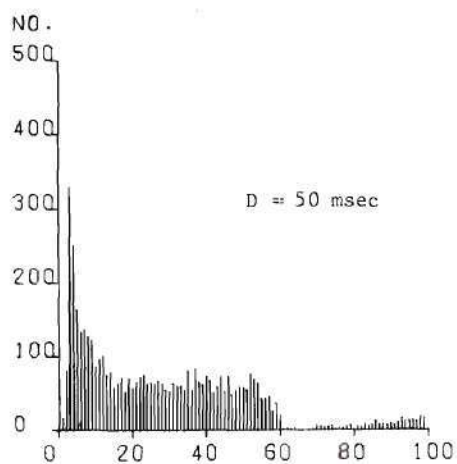
Note that in the series of Figure 16 the shape of the initial portion of the PST envelope remains fairly uniform as burst duration increases. Also, the "steady-state" level appears to be independent of duration, at least up to 70 msec. This situation was by no means universal in the fifteen fibers from eight animals for which duration series were run. Figure 17 shows an example from the same animal of Figure 16, in which the initial peak shape is well preserved as duration extends to 80 msec, but steady-state level declines about 20 per cent from the height at 20 msec duration. It is reasonably certain that this series represents a stable response since two widely separated runs were made for 20 msec duration and both appear essentially



ABW = 1.0 msec; T = 60 sec

Stimuli: Tone Bursts; SP \approx 100 msec; $f = 1 \text{ kHz}$ (CF);
 L = -50 db; $T_e = 2.5 \text{ msec}$

Figure 17. PST Histograms for Unit 115-5 as Burst Duration Is Increased



Second histogram at D = 20 msec shows fiber response remained stable in the interval between the two runs, during which time five other histograms were obtained.

Figure 17. (Continued)

identical. Finally, Figure 18 depicts a fiber for which the initial envelope peak becomes much less pronounced as duration exceeds 40 msec. In fact, the total number of spikes actually decreases by about 8 per cent as duration increases from 50 to 60 msec. (Such decreases in total spike response with an increase in total stimulus energy were not uncommon and usually could not be attributed to measured spike amplitudes falling below detector level.)

These results (and others not presented) indicate that the precise manner in which a unit will change its behavior as burst duration is increased is somewhat variable. The probability of a spike occurrence is greater during the burst duration than during the silent period, and some steady-state discharge rate is usually developed, but the exact histogram envelope in general probably depends on factors, such as mode of innervation, that vary from fiber to fiber. Perhaps these factors could be elucidated from a correlation with CF, threshold, or spontaneous rate, but the number of units tested for duration effects in these experiments was too small for such relationships to be statistically significant.

The burst response histograms obtained by Kiang (18) from cat data are in general agreement with the above comments regarding the existence of initial envelope peaks, steady-state levels, and post-burst suppression of spontaneous activity. However, he does state that initial peaks always decrease with burst duration, and shows only one histogram series, which is quite similar to Figure 18. This is the only example in which data of the present study do not agree completely with response patterns from cats or monkeys.

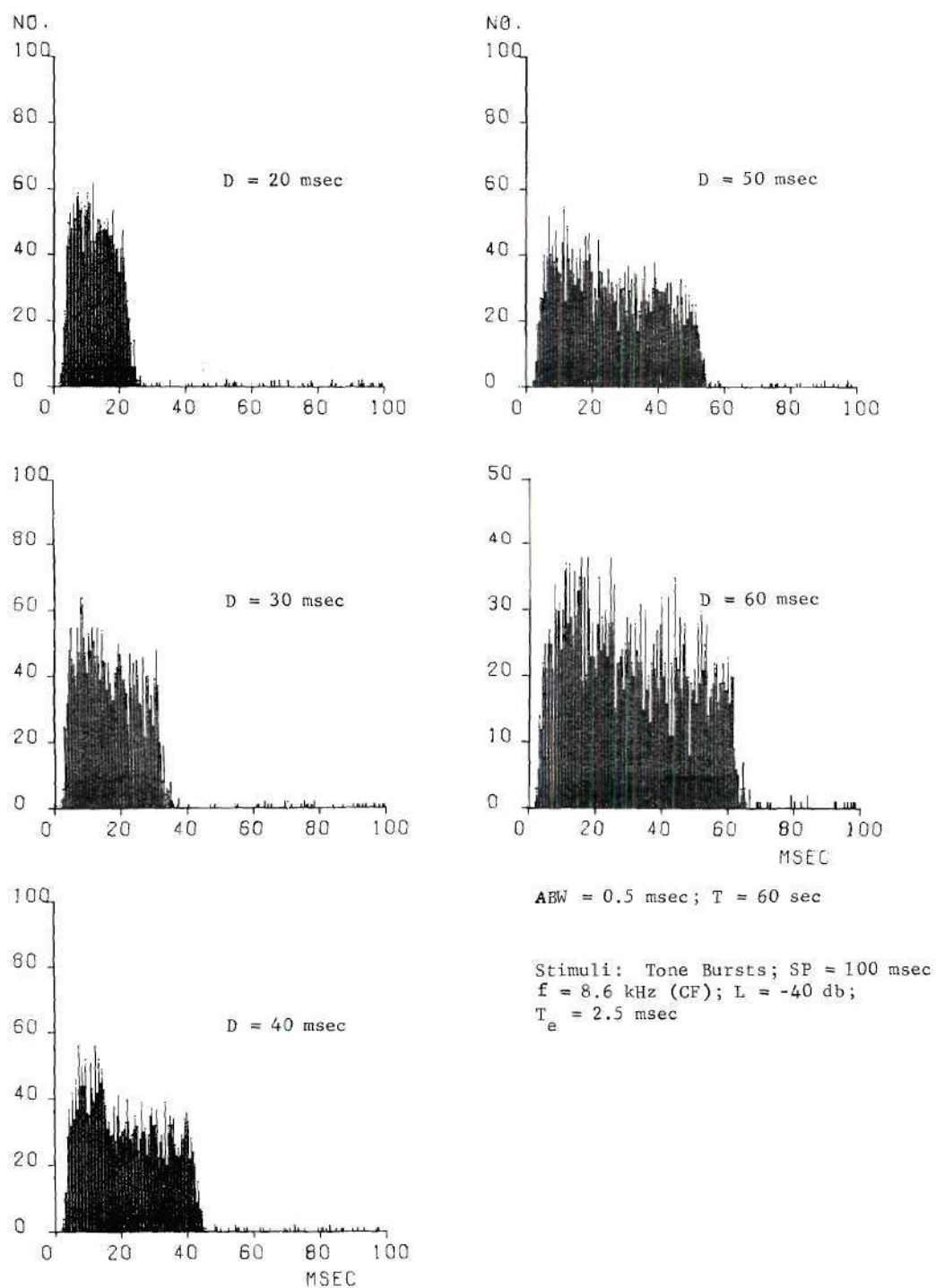
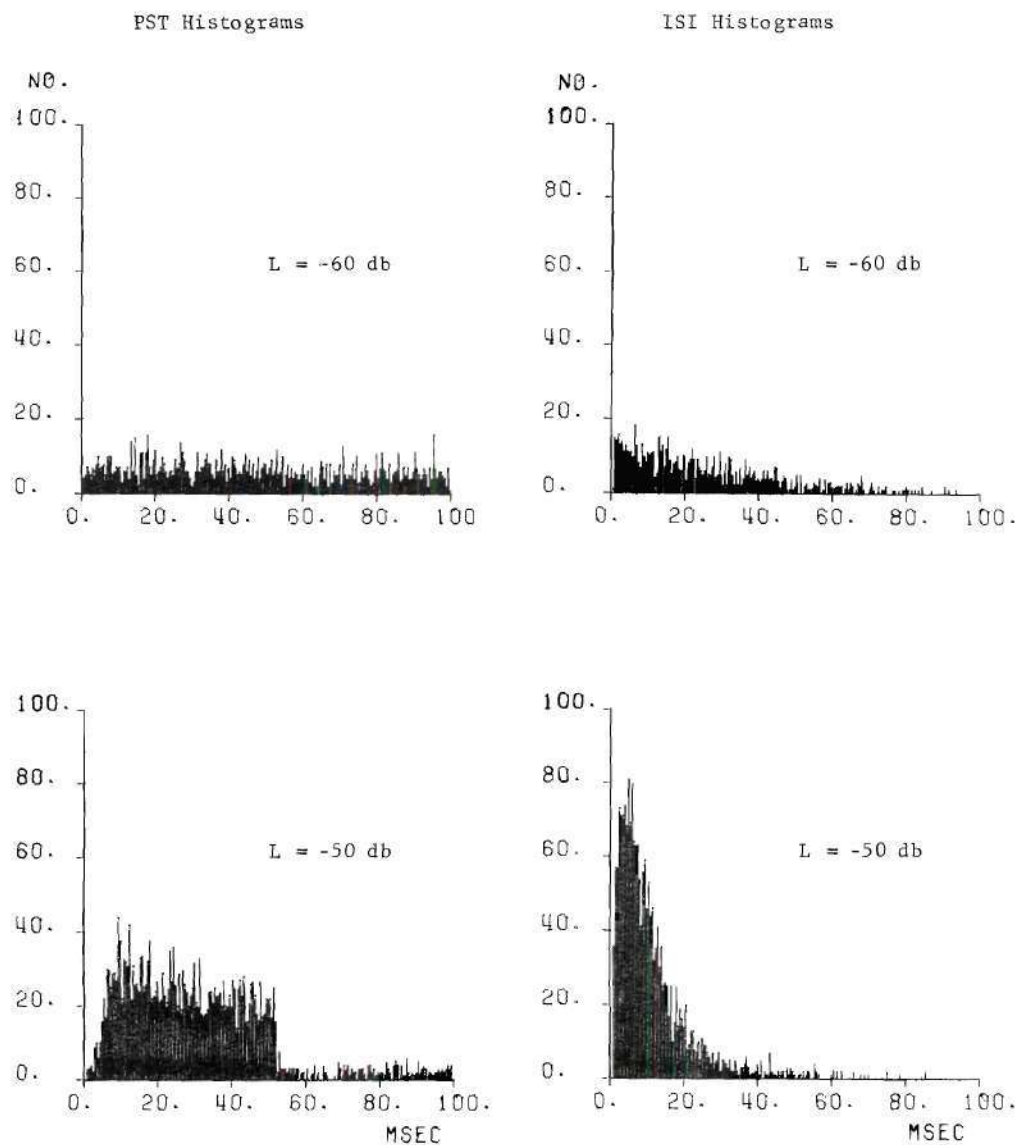


Figure 18. PST Histograms for Unit 122-2 as Burst Duration is Increased

Effects of Changing Burst Intensity. Subjective determination of the loudness of a given sound must develop from the relationship between sound intensity and single fiber responses. This relationship was investigated by determining response patterns as burst level was increased. In contrast to the variable nature of nerve responses as duration was increased, the results from burst intensity tests are all quite similar, and agree exactly with Kiang's data (18). Figure 19, which shows PST histograms for a unit as burst level is increased in 10-dB increments ($SP = 100$ msec; $D = 50$ msec; $f = CF$), illustrates the pattern. Essential features are that as intensity is increased, the initial peaks in the PST envelopes become more prominent, as does the suppression of spontaneous activity following the burst. Also, the steady-state level reaches a plateau (about 60 responses per bin, or 200/sec, at about -30 dB in this example), which is not exceeded for further SPL increases. All fibers examined exhibited such steady-state saturation effects appearing at 20 to 40 dB above threshold, which itself could vary by as much as 30 dB for fibers of the same CF. Similar effects have been reported commonly for auditory fibers in cats and monkeys (11,15,18).

In general terms, then, as a fiber is excited from near threshold by increasingly intense tone bursts, spontaneous activity becomes suppressed, and the steady-state response level increases with SPL over about a 20-40 dB range. More intense stimulation is incapable of elevating the steady-state level further, but it can continue to affect the initial envelope peak. Various interpretations have been put forth as to how such patterns reflect the method of transmitting



ABW = 0.5 msec; T = 60 sec

Stimuli: Tone Bursts; SP = 100 msec; $f = 7$ kHz (CF)
 D = 50 msec; $T_e = 2.5$ msec

Figure 19. PST and ISI Histograms for Unit 104-5
 as Burst Intensity is Increased

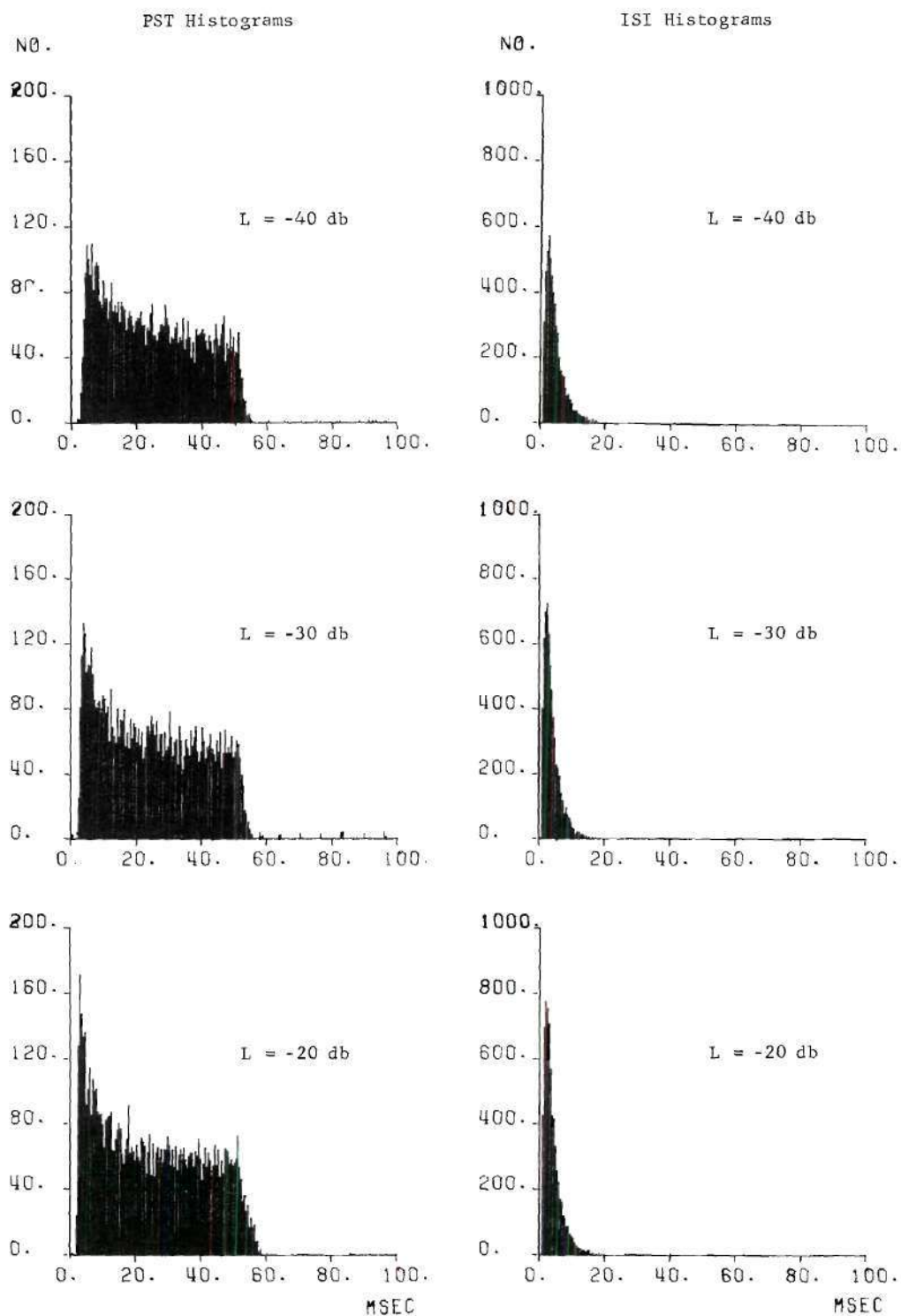


Figure 19. (Continued)

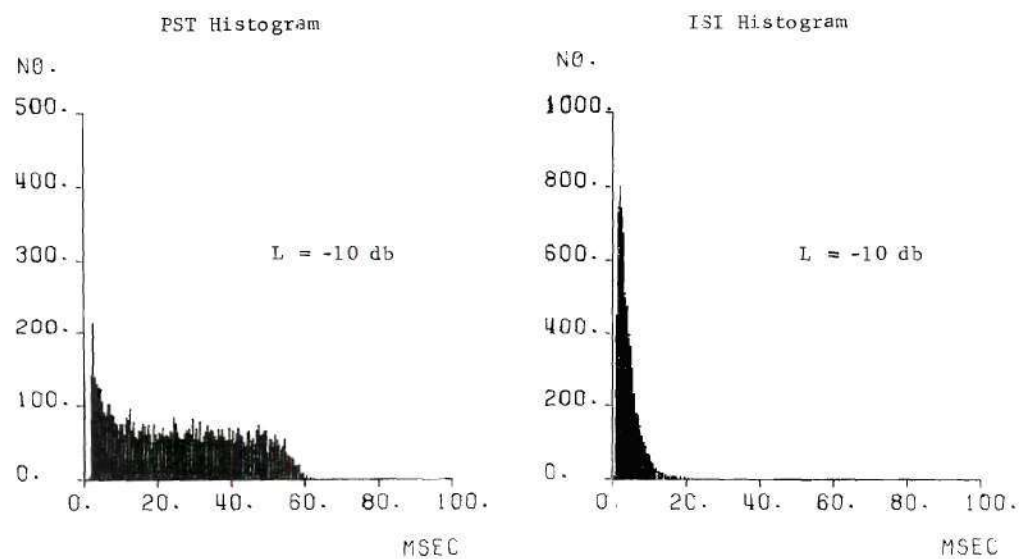
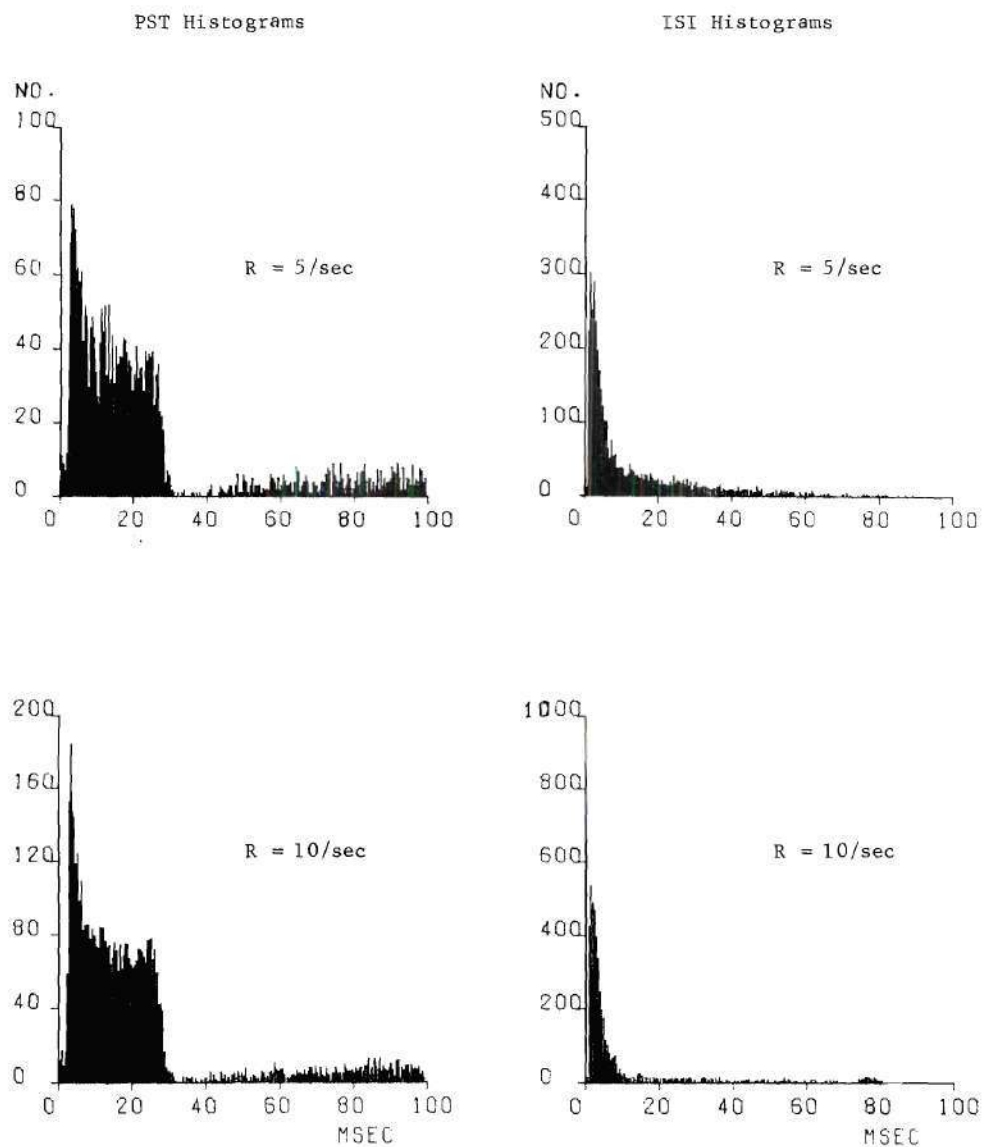


Figure 19. (Continued)

intensity information to higher brain centers (16,18). While increasing single unit discharge rate is likely an important cue, the fact that subjective loudness discriminations may be made over ranges greater than 100 dB (35) suggests a complex intensity code, which probably utilizes the differing thresholds of various fibers.

Effects of Changing Burst Period. From the histogram results shown with regard to stimulus duration, it is apparent that the length of time from the termination of one burst until the beginning of the next may have a considerable influence on PST envelopes. For bursts of constant duration, this effect was studied by generating response patterns for 25-msec bursts ($L = 5-10$ dB above threshold; $f = CF$) presented as stimulus period, SP, was reduced. Figure 20 shows typical PST and ISI responses in terms of the burst repetition rate, $R = 1/SP$. As R is increased, the envelope heights rise and the initial peaks become less pronounced, indicating incomplete recovery of the fiber between bursts. The ISI plots, as seen earlier, show two peaks which move together and merge as inter-burst time decreases. It is noteworthy that the only effect of changing from $SP = 200$ msec to $SP = 100$ msec is to produce twice the responses, but with the same relative time behavior. This implies that the stimulus presentation rates of 10/sec used in most other experiments of this research were slow enough that inter-burst effects are probably not major factors in response pattern changes, except, perhaps, with long duration bursts.

Although the envelopes of Figure 20 do rise with increasing burst rate, the ability of an individual burst to elicit responses is actually declining, since each histogram is based on a larger number



ABW = 0.5 msec; T = 60 sec

R = Burst Repetition Rate (1/SP)

Stimuli: Tone Bursts; D = 25 msec; f = 7.5 kHz (CF)
L = -45 db; $T_e = 2.5$ msec

Figure 20. PST and ISI Histograms for Unit 122-3
as Burst Repetition Rate is Increased

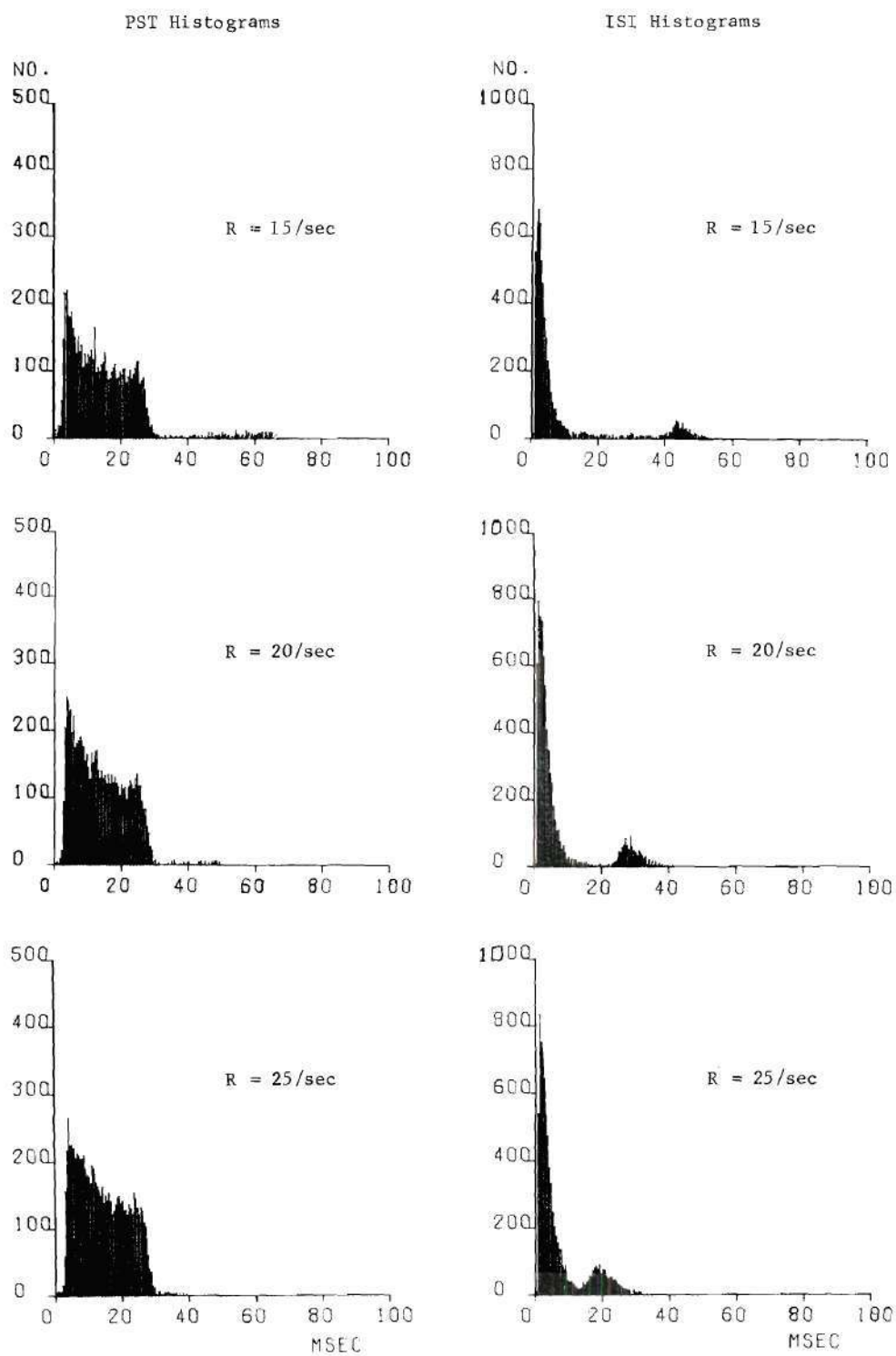


Figure 20. (Continued)

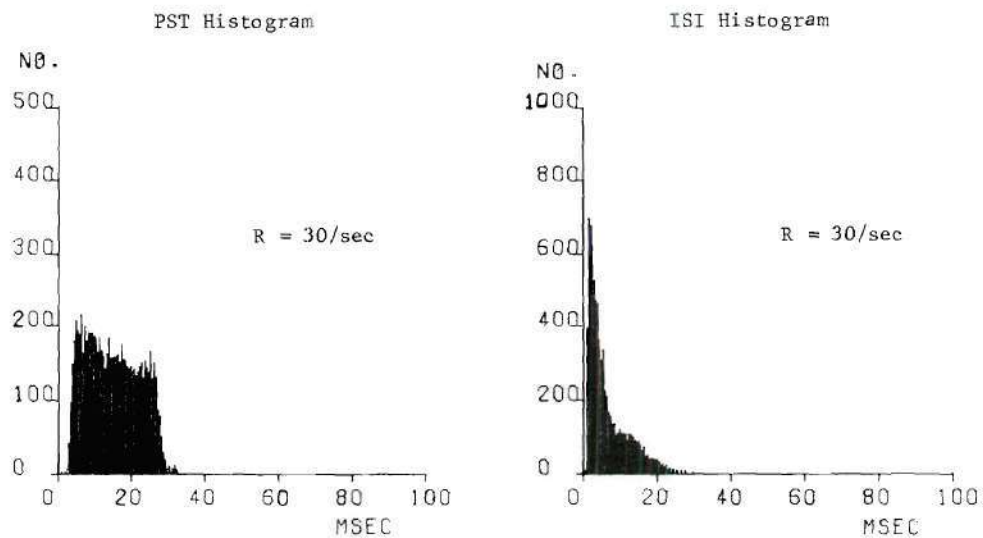


Figure 20. (Continued)

of stimuli. This is shown in Figure 21, which plots average spike rates during the "burst-on" times as a function of burst rate for the data of Figure 20.

In general, increasing the burst rate (decreasing the burst period) does increase total neural activity, but the average rates during those bursts decrease if the rate is raised above, say, 20/sec. This is accompanied by a reduction in prominence of the initial envelope peaks. Both observations are consistent with conclusions reached by Kiang (18) in cat studies.

Phase-Locking of Low-Frequency Responses. Phase-locking in auditory neurons refers to the tendency of a unit to discharge, under sinusoidal stimulation, at intervals equal to integral multiples of the reciprocal of the stimulus frequency. The phenomenon has been reported by several investigators, including Rose et al. (16) and Kiang (18), in the cat and monkey, respectively. Tasaki (10) noted it in the guinea pig, but did not show histogram representations. Implications of phase-locking (which is usually said to be observable for frequencies up to about 4 kHz if the fiber responds in that range) are, first, that displacement of the basilar membrane in only one direction results in increased nerve excitation, and, secondly, that for low frequencies at least, the spacing of discharges on single fibers provides frequency information.

During the execution of the present research it was always found that fibers responsive to low frequencies (say, less than 2 kHz) exhibited phase-locked behavior linked directly to the stimulus frequency. Locking in the low-CF units of the histograms presented above is not apparent from them because the ABW's of the figures are too large. The phenomenon is, however, clearly shown in Figure 22, which

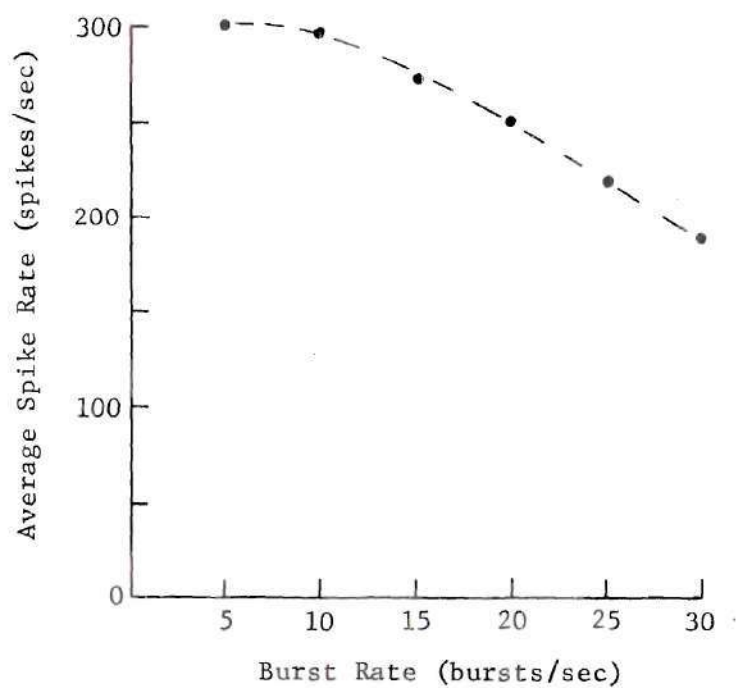
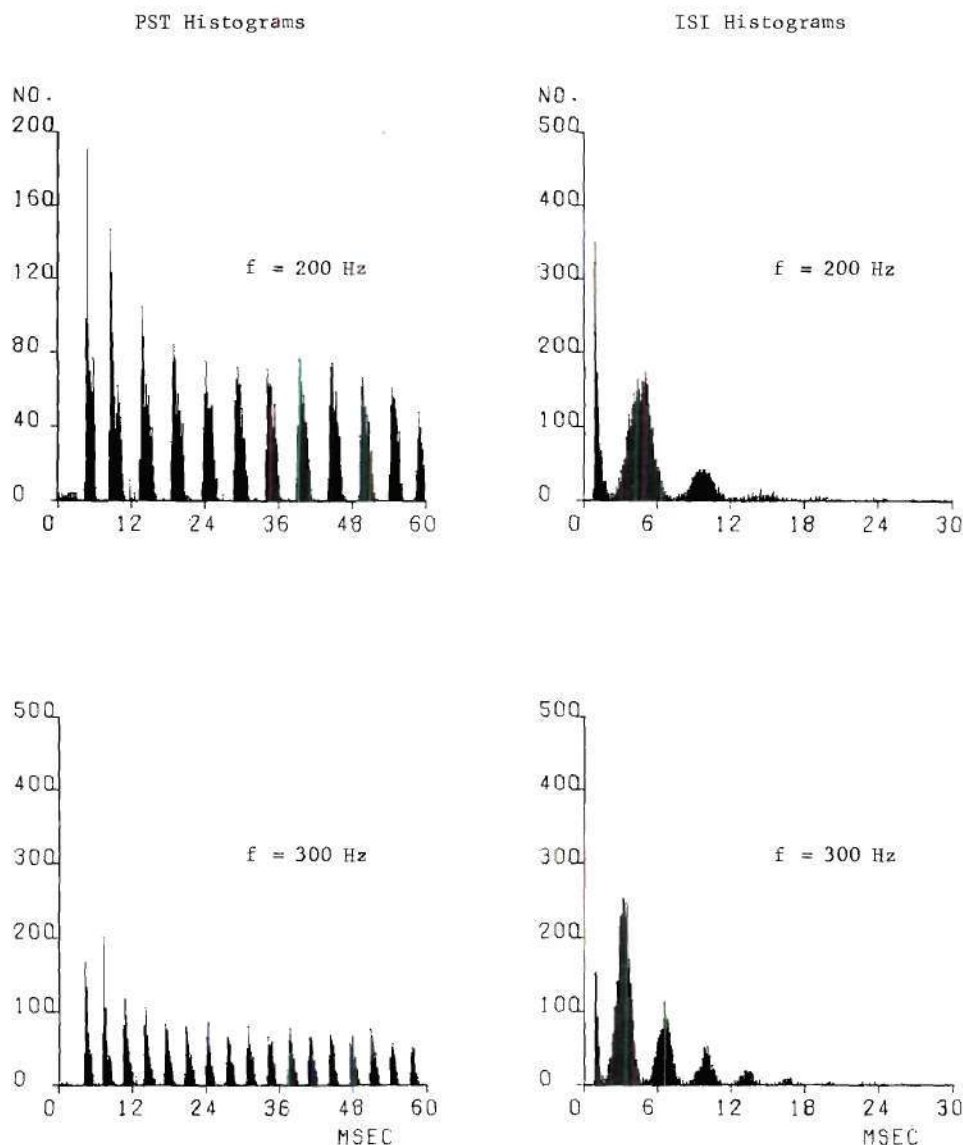


Figure 21. Average Spike Rates During "Burst On" Periods for Data of Fig. 20 Plotted Against Burst Rate



PST ABW = 0.2 msec; ISI ABW = 0.1 msec; T = 60 sec

Unit 121-2

CF = 300 Hz

Stimuli: Tone Bursts; SP = 100 msec; L = -40 db
D = 50 msec; $T_e = 2.5$ msec

Figure 22. PST and ISI Histograms Showing Phase-Locking of a Low-CF Unit

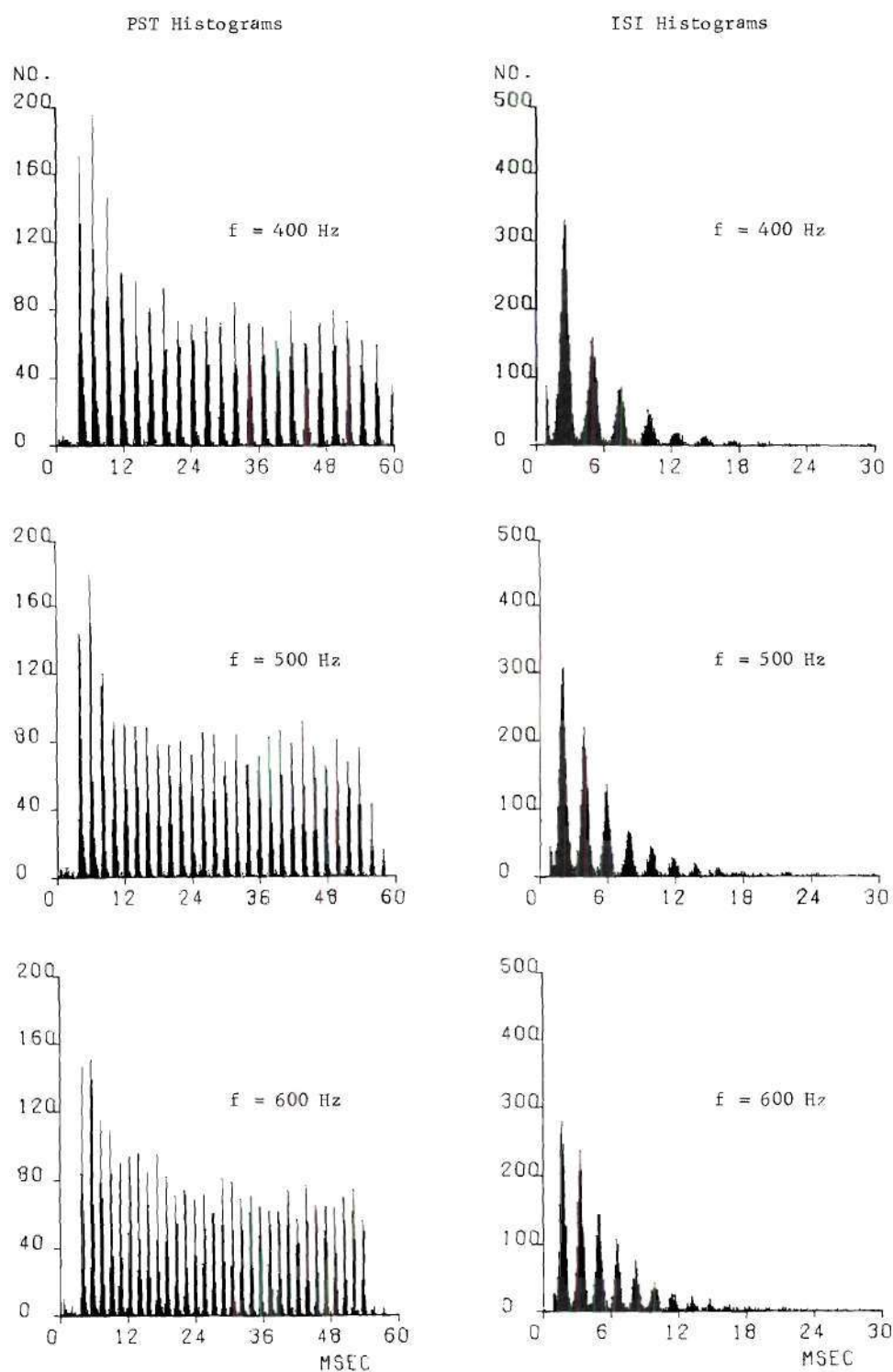


Figure 22. (Continued)

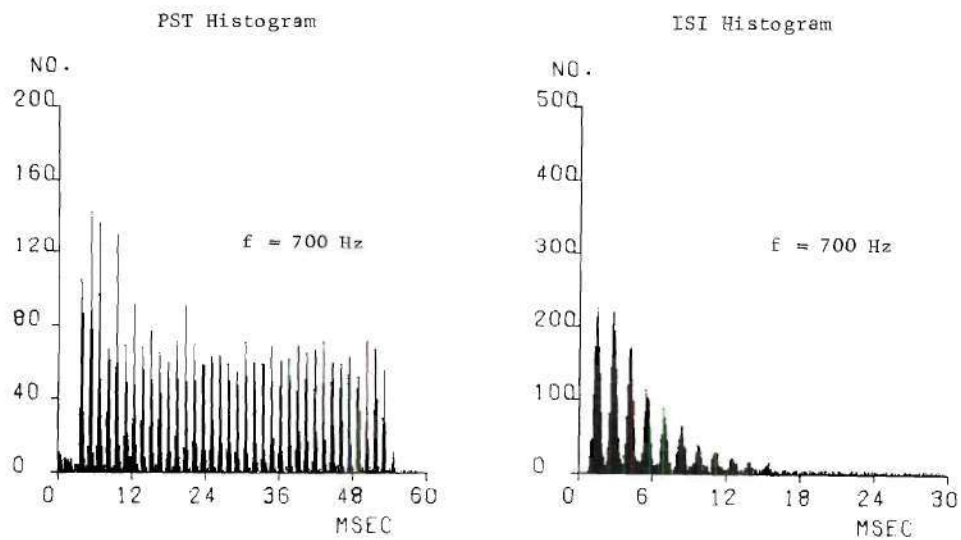


Figure 22. (Continued)

gives high resolution PST and ISI representations of a low-CF (300 Hz) fiber excited by bursts of varying frequency (SP = 100 msec; D = 50 msec; L = -40 dB). The PST peaks occur exactly at intervals corresponding to the period of the burst frequency, the initial cycles of the stimulus being more effective in producing responses than later cycles, which exhibit the expected steady-state levels associated with burst response.

Two features of the ISI series in Figure 22 are of interest. First, especially at low frequencies, sharp, highly-skewed peaks are present, indicating a number of spike intervals of about 1 msec, independent of stimulus frequency. These peaks represent so-called "second firings," or the tendency of a unit to discharge a second time within a constant short period following sound-induced response. In this study, many (but not all) units showed this behavior, which has been demonstrated by Kiang (18) and Gray (19) in the cat, and by Rose et al. (16) in the monkey. As will be seen in later discussions of click response, the effect was present also with high-CF units. It is probably doubtful that second firings are a significant factor in neural coding since they appear in relatively small numbers compared to the total neural output, and since they do occur within a constant interval (about 0.75-1.25 msec) of the original response for fibers of widely differing CF's.

The ISI histograms of Figure 22 also verify the phase-locking of the fiber response, since peaks (other than those from second firings) are seen to occur at inter-spike interval times exactly equal to the period of the stimulus, or to multiples of that period. Note,

however, that the tendency to fire at multiple periods becomes more marked as frequency is increased, indicating that the unit's ability to respond to consecutive stimulus cycles decreases with frequency. Furthermore, this decrease is such that the total number of responses represented in each histogram remains constant within 5 per cent even though the total number of stimulus cycles increases by a factor of 3.5 (200 Hz to 700 Hz). Hence, for this unit, the total number of low-frequency stimulus cycles does not appreciably affect the average response rate, a fact which would appear to be a verification of the results of Gray (19) and Rose et al. (16) cited earlier in the discussion of "burst duration," and which indicate that factors (other than the stimulus alone) peripheral to the fiber endings have significant control over single unit response.

In summary, phase-locking was observed for all units excitable by low frequencies, with the frequency of stimulation, not the CF, determining the cadence of discharges. The effect was easily seen for frequencies up to 2 kHz; however, no attempt was made to determine the highest frequencies for which phase-locking could be shown. All these results are completely compatible with available data from cats and monkeys.

Tuning Curves. The last example of response characterization for tone burst stimuli is the determination of tuning curves.

Tuning curves are simply plots of tone burst threshold (the minimal level of a tone burst stimulus which causes a "detectable" change in fiber response) versus the stimulating frequency. Such

graphs yield information as to how the basilar membrane responds in the region innervated by the instrumented fiber. Many curves have been reported based on units in cats and monkeys (13,18), but almost no comparable curves are available from the guinea pig. Hence, in this research a small number of tuning curves were generated to verify that they do show the same general characteristics as those from the other species.

The procedure used was as follows: Fifty-msec tone bursts at a rate of 10/sec were presented at a given intensity, and the frequency ranges were determined for which stimulus-produced responses were heard from the microelectrode-audio amplifier system described in Chapter III. This procedure was then repeated for other levels to define all combinations of frequency and level producing fiber response.

The resulting curves, some of which are shown in Figure 23, typically show an unsymmetrical, V-shaped pattern, with a minimum at the CF. Even accounting for the logarithmic scale of the plots, the curves have much steeper slopes for frequencies above the CF than for those below, in complete agreement with results from cats and monkeys. These profiles reflect statements made in Chapter I that fibers may be stimulated by all frequencies lower than their CF's provided stimulation is intense enough, but that only a small range of frequencies above the CF is excitatory, regardless of intensity. Similar observations from cat data, combined with the fact that high-CF units innervate the basal turn of the cochlea and low-CF units the upper turns, have been interpreted (18) as confirmation of Tasaki's findings concerning the space-time pattern of basilar membrane excitation (24). He

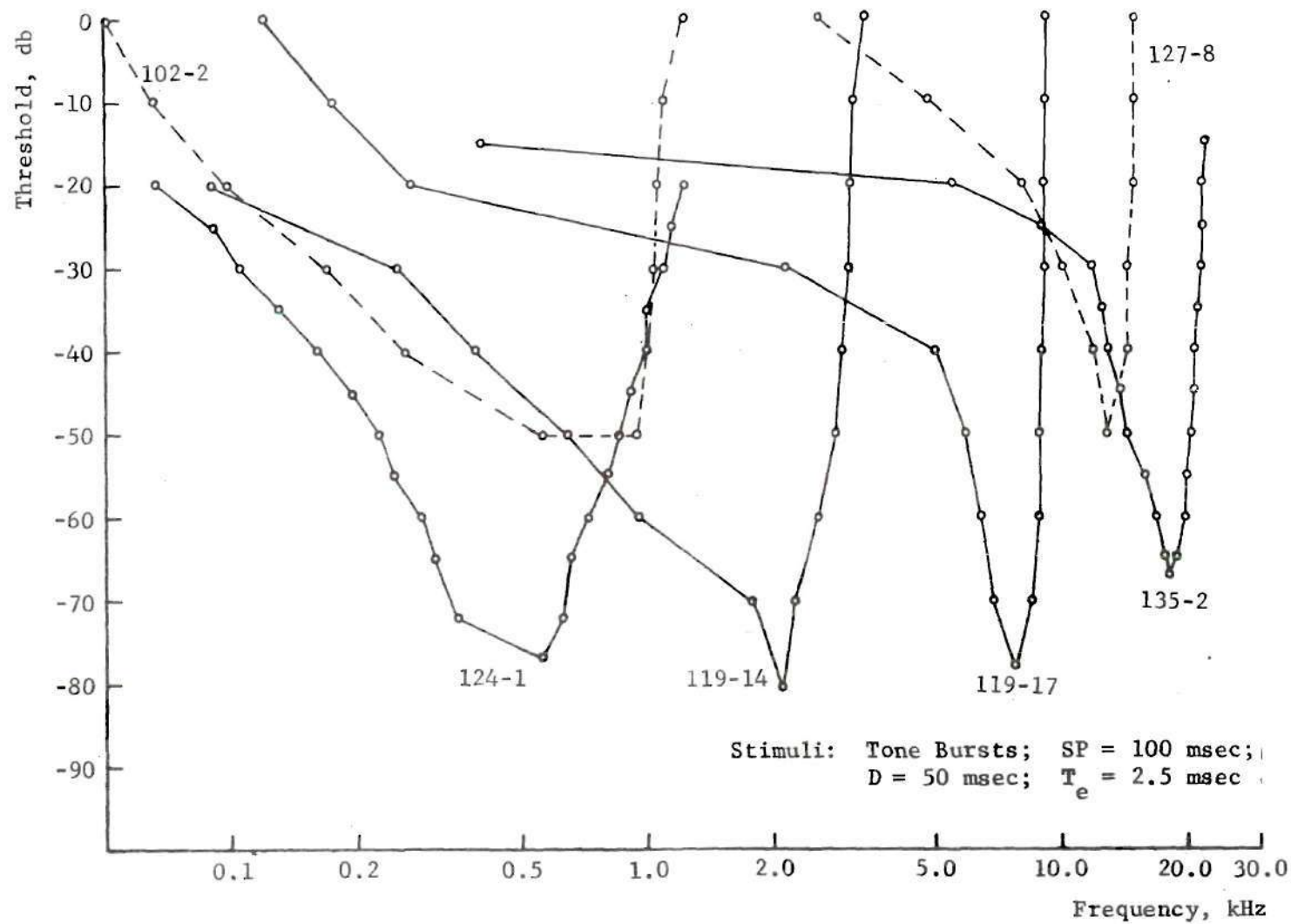


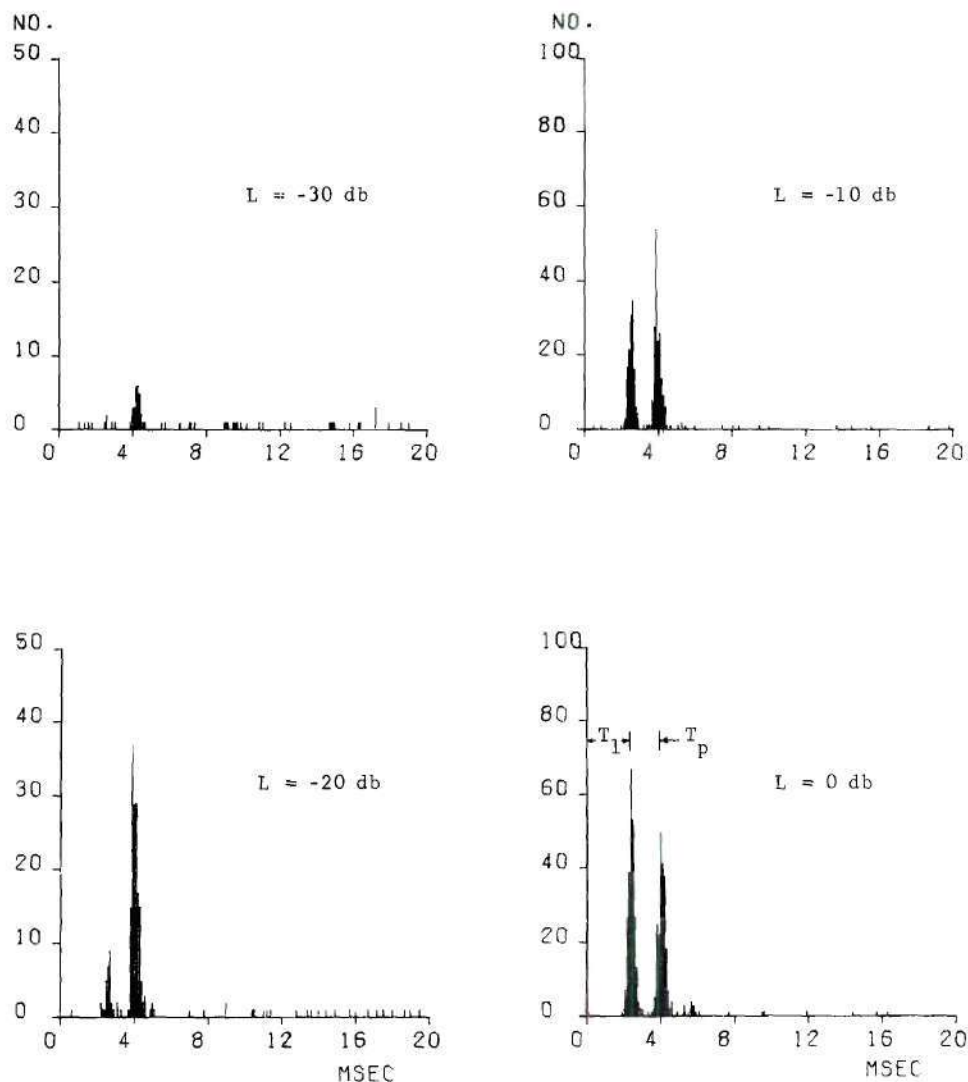
Figure 23. Tuning Curves for 6 Units from 5 Animals

concluded that low frequencies stimulate the whole cochlea to some extent, but that as frequency is increased, the stimulated portion of basilar membrane, extending from the stapes, becomes shorter.

Response to Click Stimuli

To determine nerve fiber responses to impulse-like excitation, histograms were computed for 100- μ sec click stimuli of varying level and polarity. In the following discussion, click polarity will be designated as either rarefaction (i.e., clicks resulting in an initial outward motion of the eardrum) or condensation (initial inward eardrum movement). The results obtained verify many of the conclusions reached from cat data by Kiang (18) and Gray (19).

Response to Click Level Changes. In general, the response of a fiber to increasing click intensities depends greatly upon its CF. PST histograms for units with CF below 4-5 kHz always show multiple response peaks, whereas those for higher-CF units exhibit single peaks. PST plots for a typical low-CF click series are shown in Figure 24. Stimuli were rarefaction clicks delivered at the rate of 10/sec with increasing levels, given in dB referenced to 36 v into the earphone. At -30 dB, there is an unmistakable response to the clicks at about 4 msec. When the click level, L, is increased by 10 dB, an earlier response appears at 2.8 msec. With further increasing level, this early response becomes larger relative to the second, finally surpassing it at 0 dB. Also, the latency of the initial peak, T_1 , (as defined in the 0-dB graph of Figure 24) decreases slightly as level goes up; and, at the most intense level, a third peak is evident at 5.5 msec. This same pattern was seen for all low-CF units; i.e.,



ABW = 0.1 msec; T = 30 sec

CF = 650 Hz

Stimuli: 10/sec Rarefaction Clicks

T_1 is the latency of the first response peak,
and T_p is the inter-peak interval.

Figure 24. PST Histograms for a Low-CF Unit (163-3)
as Click Level is Increased

multiple peaks were evident, the initial peaks usually starting out smaller than the others and then overtaking them in amplitude at higher click levels with small latency decreases.

The usual high-CF click response is seen in Figure 25. It consists of a single peak which grows monotonically with level, except that for 0 dB clicks in this case, a second much smaller peak occurs about 1 msec after the main response. This latter peak results from the "second-firing" phenomenon mentioned earlier, and was often (but by no means always) seen in both low- and high-CF fibers.

Kiang observed parallel intensity relations in cat fibers (18) and related the timing of the click response peaks to mechanical events in the cochlea by showing that the time between adjacent low-CF peaks, T_p , (again defined in Figure 24) and T_1 are systematically related to the CF. His results were that T_1 generally decreases with CF and that T_p is approximately equal to $1/CF$. It should be noted, however, that close examination of some of his graphs shows that T_p may vary from peak to peak, so that one value may not be sufficient to characterize completely the timing of low-CF, PST peaks. This same effect may also be observed in a few of the histograms given by Gray (19).

Kiang (18) interpreted the decrease in latency with increasing CF as a verification of the fact that high-CF fiber endings populate the basal portion of the cochlea, and that as one moves toward the apex, the CF's decrease. His argument was that T_1 should increase (and CF should therefore decrease) with the distance from the stapes of the region innervated by a fiber for two reasons. First, the more apically located the fiber endings, the greater the time needed for disturbances

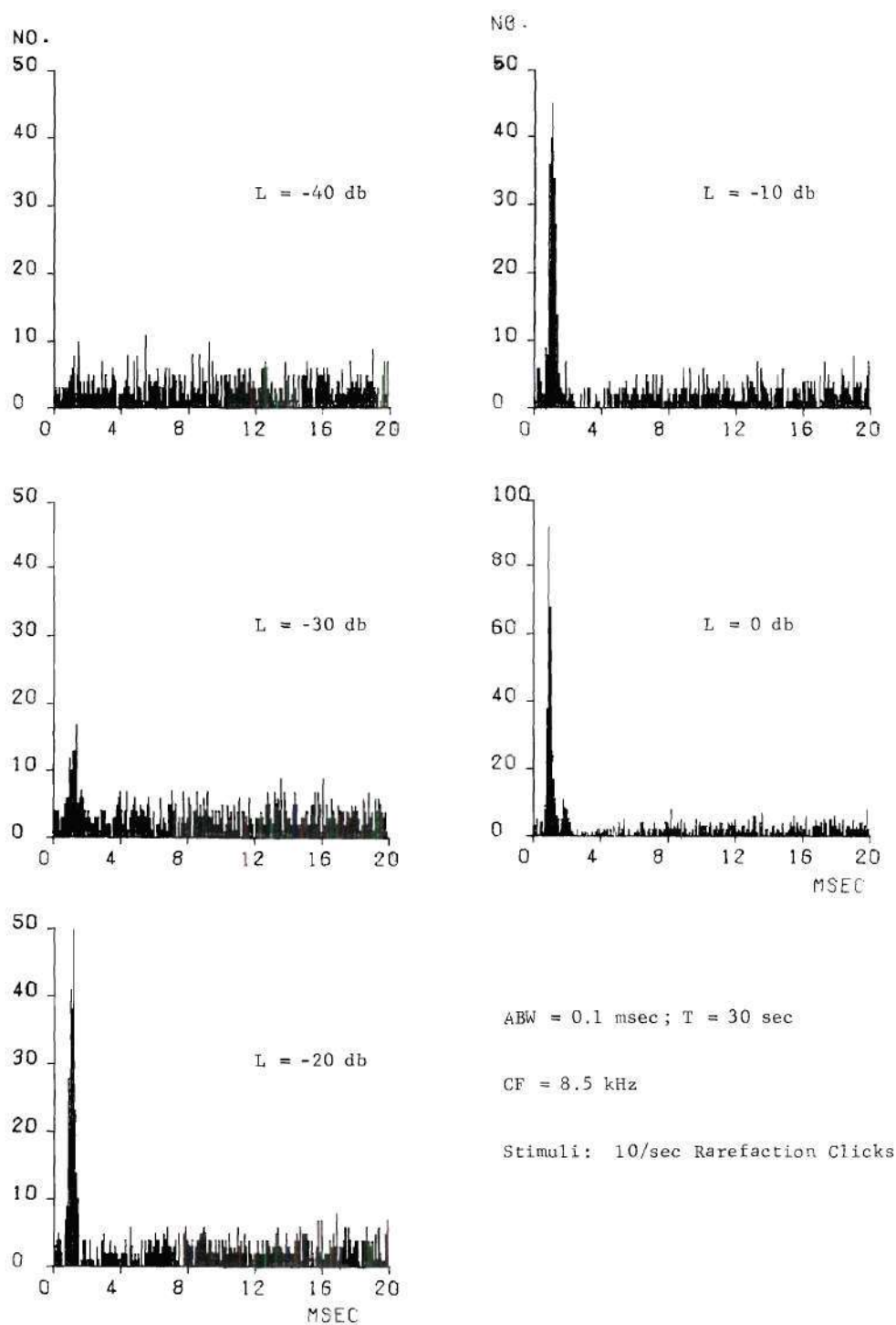


Figure 25. PST Histograms for a High-CF Unit (163-3) as Click Level is Increased

to propagate (in traveling wave fashion) along the membrane and stimulate the fiber. Secondly, the length of the neural path from fiber ending to recording site in the internal meatus increases as endings originate further from the stapes. Since action potential spike propagation speed is only about 10 m/sec (10), the conduction time of the nerve impulse is significantly longer for more apical units.

Kiang (18) also explained the close identification of T_p with $1/CF$ as a neural correlate of the ringing of the basilar membrane with a frequency corresponding to the maximum of the membrane transfer function associated with the region innervated by the fiber. That is, the responses are "phase-locked" to individual cycles of the underdamped membrane impulse response. This is a further indication that displacements of the membrane in only one direction tend to give rise to fiber responses. (If both displacement polarities were excitatory, T_p should be $1/2CF$.)

In the present research the above relation between CF and latency was verified and is seen in Figure 26, which plots CF against T_1 for all the units from which rarefaction click data were taken. (In this figure, T_1 is measured from the histogram corresponding to the most intense click stimulus of a given series.) Even though the scatter of points in the figure is great, and the number small, the general trend of latency decrease with CF is fairly apparent, and the T_1 values correspond well with Kiang's data (18).

With regard to the connection between T_p and $1/CF$, most of the units encountered in this study showed good agreement; i.e., low-CF units responded to clicks with regularly spaced peaks separated by

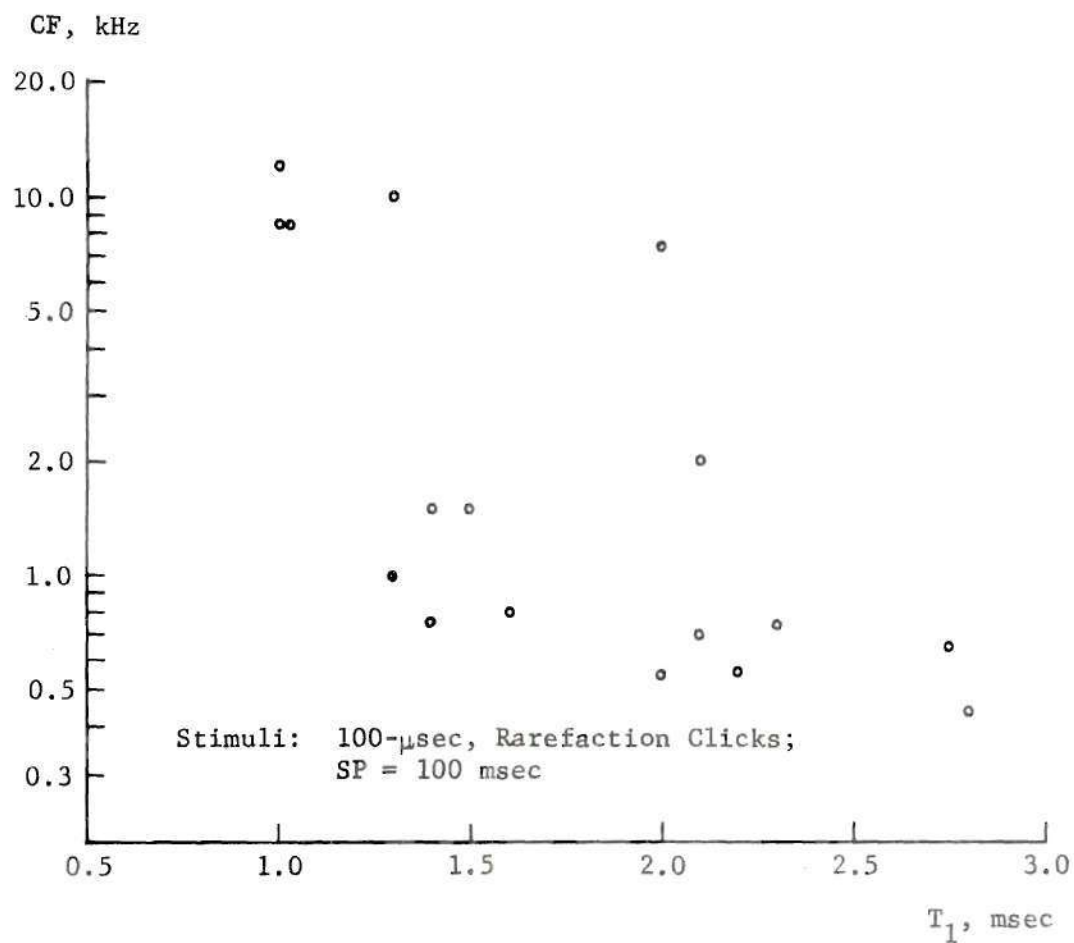
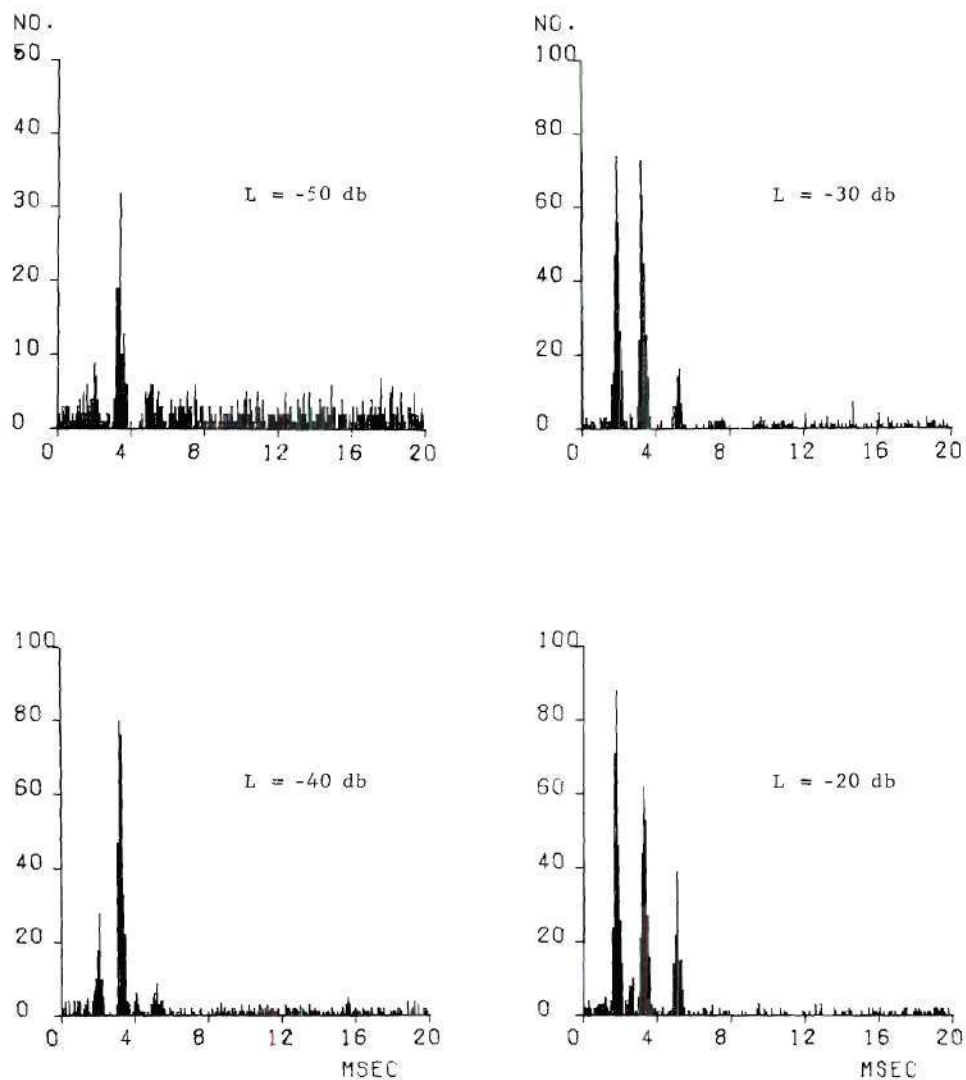


Figure 26. CF for 17 Units Plotted Against T_1

1/CF. For example, CF for the fiber of Figure 24 is 1.54 msec and T_p is about 1.6 msec. Also, in agreement with Kiang (18) and Gray (19), several units were seen in which the inter-peak interval, T_p , did not remain constant, but changed from the initial to the final peaks. An example of this phenomenon is shown in the PST histograms of Figure 27. Note that small "second firing" peaks occurring at about 2.3 msec or 4 msec may be ignored when discussing the "ordinary" firings represented by the other peaks. At -50 dB there are three peaks which grow with level, with a fourth appearing as level reaches -10 dB; and at 0 dB, six peaks are clearly present, the last three being more closely spaced than the others. The spacing of the "ordinary" peaks is indicated in Figure 28, which plots the latencies of the response peaks versus click level. From this figure it is clear that T_p for latter peaks at 0 dB is considerably less than the inter-peak intervals for the initial three peaks. No interpretation of this behavior is offered, other than the observation that it does not appear to reflect non-linear behavior of the basilar membrane response, since the latencies of the second and third peaks remain essentially constant as input is increased by 50 dB. (The latency decrease of the initial peak is normal, as was noted earlier.) It is also noted that the last three inter-peak intervals (1.3, 1.2, and 1.1 msec) are closer to 1/CF (1.25 msec) than is the interval between the second and third peaks (1.8 msec).

Response to Click Polarity Changes. The preceding remarks concerning the correspondence between T_p and 1/CF, coupled with the phase-locking phenomenon are strong indications that nerve fibers in the



ABW = 0.1 msec; T = 30 sec

CF = 800 Hz

Stimuli: 10/sec Rarefaction Clicks

Figure 27. PST Histograms, Unit 153-4 for Which Inter-Peak Intervals are not Constant

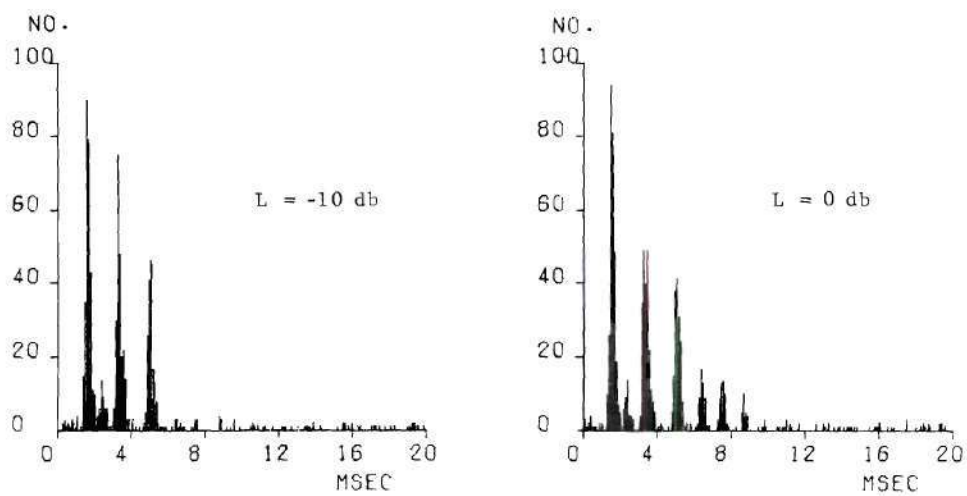


Figure 27. (Continued)

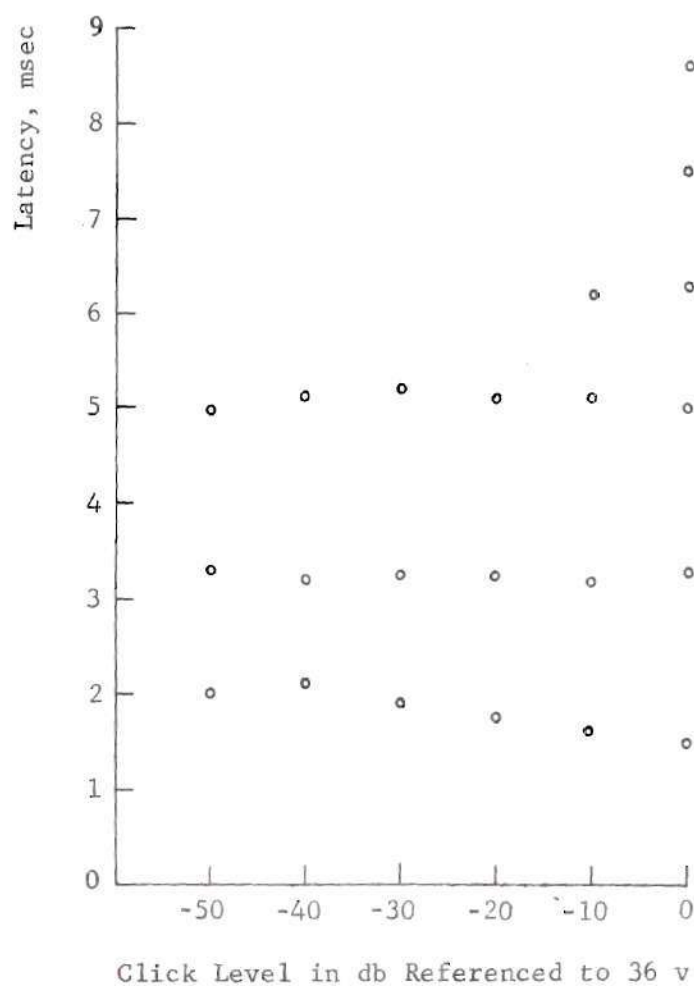


Figure 28. Latencies of the Histogram Peaks of Fig. 27 Plotted Against Click Level

organ of Corti are excited when the basilar membrane is displaced in one particular direction. This fact is further demonstrated by comparing PST responses to clicks of opposite polarity. An example is shown in Figure 29, which gives histograms from condensation and rarefaction clicks of increasing level. Note that peaks for either polarity (indicating periods of increased neural activity) occur during the response valleys of the other. This "180-degree phase shift" happens because the basilar membrane rings with a linear response to an impulsive stimulus. When stimulus polarity is reversed, the ringing is also inverted so that time periods corresponding to non-excitatory membrane movements in the original response correspond to excitatory movements for the reversed stimulus.

Figure 29 also shows that the rarefaction phase of basilar membrane movement, corresponding to stapes motion out of the oval window, is the excitatory polarity. This is because at higher intensities, the earliest peaks always occur for rarefaction clicks.

In addition, the data from this research support the notion that the condensation phase of basilar membrane movement actually inhibits fiber activity, resulting in a decrease of baseline, or spontaneous, levels. This implication is drawn by comparing PST click responses for both click polarities for units with relatively high spontaneous firing rates, a comparison typified in Figure 30. Note that for rarefaction clicks the first deviation from baseline activity is a small peak at 2 msec; whereas for the other polarity, the first deviation is a depression in spontaneous activity, again at 2 msec. Clearly, then, motion

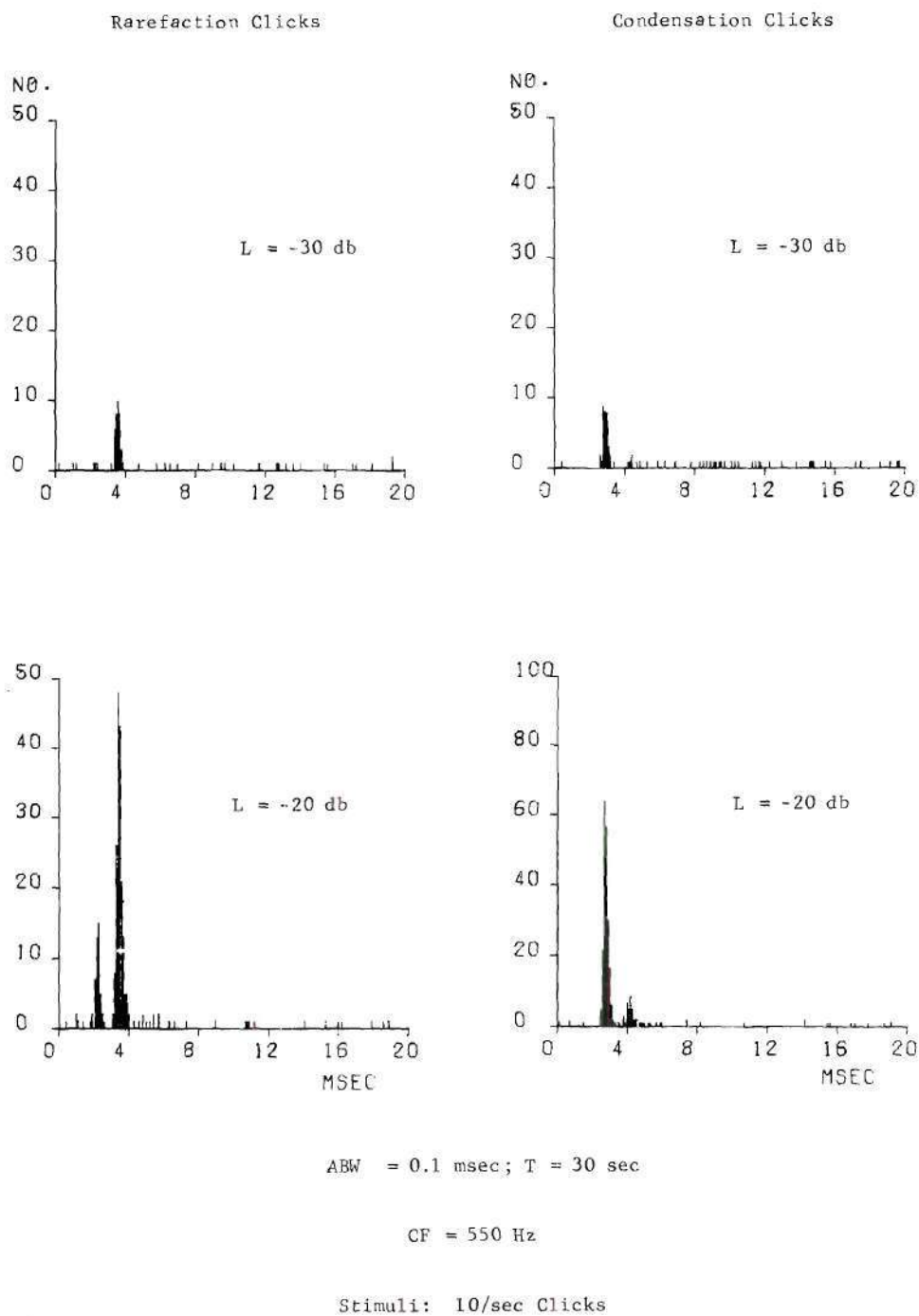


Figure 29. PST Histograms, Unit 161-7, for Rarefaction and Condensation Clicks as Functions of Click Level

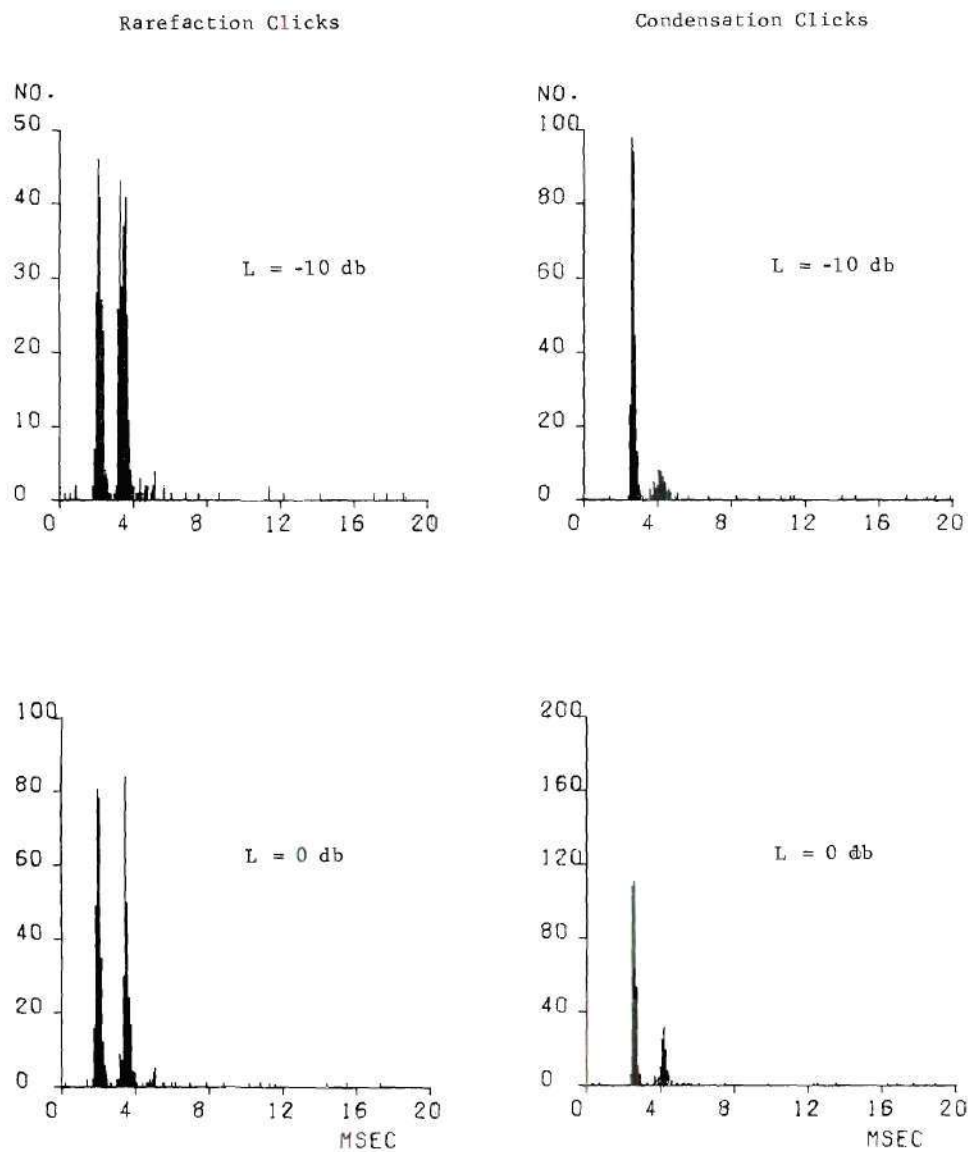
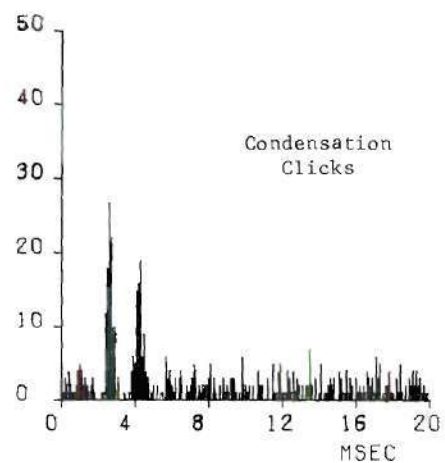
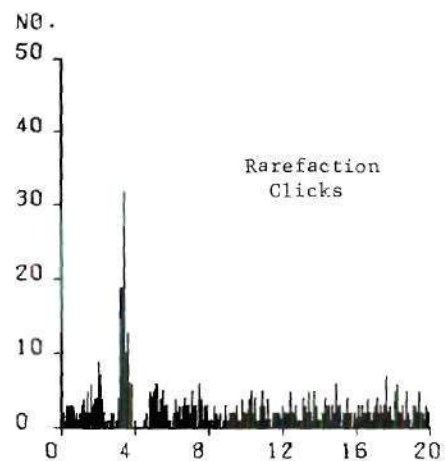


Figure 29. (Continued)



ABW = 0.1 msec ; T = 60 sec

CF = 800 Hz

Stimuli: 10/sec Clicks; L = -50 db

Figure 30. PST Histograms Unit 153-4, for Low-Level
Rarefaction and Condensation Clicks

of cochlear structures corresponding to rarefaction stimuli leads to increased firing probabilities and the opposite motion tends to depress neural response. These conclusions are identical with those reached by Kiang (18) from a similar analysis of cat data.

Part II -- Effects of Microphonic Modification

This section presents results relevant to the second research objective. It was desired to obtain an experimental verification of the cochlear microphonic trigger hypothesis for nerve spike initiation. This hypothesis holds that auditory nerve fibers receive their excitation through the action of CM, either directly or via a chemical mediator which is released by microphonic current activity. To test the theory, CM was modified by non-acoustic means and fiber response changes were assessed. If the theory is correct, then fiber responses to acoustic stimulation should increase when CM is elevated, and they should decrease when CM is depressed.

The two methods used for CM modification were the forcing of currents across the cochlear partition and the application of heat directly to the cochlea. By the current passage procedures, it was possible to raise and lower microphonic levels and show that fiber activity is generally enhanced with CM increase and lessened with CM decrease. Heat application, however, caused only microphonic decrease, which was accompanied by a reduction in fiber activity if the decrease was great enough.

The organ of Corti is a highly complicated structure. Therefore, in the analysis and interpretations to follow, no attempts are made to

assign current or temperature effects to specific locations internal to the organ or to relate such effects to electrophysiological events in hair cells, fiber endings, or fibers. Hence, the discussion will be directed primarily toward identifying concomitance between fiber response changes and CM modification and toward indicating whether or not response changes associated with CM increase (or decrease) are similar to those resulting from sound level increase (or decrease).

Effects of Electric Currents in the Cochlea

It will be recalled from Chapter I that forcing a direct current across the cochlear partition in the direction scala vestibuli-scala tympani results in an increase of microphonic response and that an opposite current decreases CM in the region near the current electrodes. The effects of such current-produced CM changes on nerve fiber activity were studied by obtaining response histograms for various combinations of current and tone burst stimulation. In the following discussions, vestibuli-tympani currents will be considered positive and tympani-vestibuli currents negative.

Three modes of current passage were utilized in these studies. The first was the simple application of prolonged direct current of controllable magnitude and polarity; currents of this type are designated I_c . The second mode, designated I_p , was application of current pulses synchronized with 80-msec tone bursts. Pulses began 20 msec after the beginning of each tone burst and ended 40 msec later. The last type of current stimulation was the use of audio-frequency alternating currents derived from the tone burst waveform generator.

Toward the completion of the present research, Konishi, Teas, and Wernick (26) and Teas, Konishi, and Wernick (27) published results also dealing with current effects on fiber response. Those findings overlap to some extent with the present studies primarily with regard to prolonged direct current effects. Their other experiments showed the effects of either 5-sec current pulses or of very low-frequency (5 Hz) alternating current application. Because of artifacts in the case of pulses, they excluded from analysis any responses occurring for one second after current make or break. Thus, their results derive mainly from static or slowly varying current conditions. In the present study, however, the use of the second current mode (40-msec pulses occurring during a tone burst) permitted the transient effects of current passage to be examined.

To facilitate discussion of the present results it is convenient to define the average fiber response rate associated with a selected time interval within a PST histogram. If the desired interval begins with the histogram bar for m milliseconds and extends up to (but does not include) the n -millisecond bar, then $Q(m:n)$ will be called the average spike rate for the interval. It is computed according to the formula

$$Q(m:n) = \frac{N}{0.001(n-m)z}$$

where N is the total number of spikes associated with histogram bars of the interval; and z is the total number of tone bursts represented in the histogram.

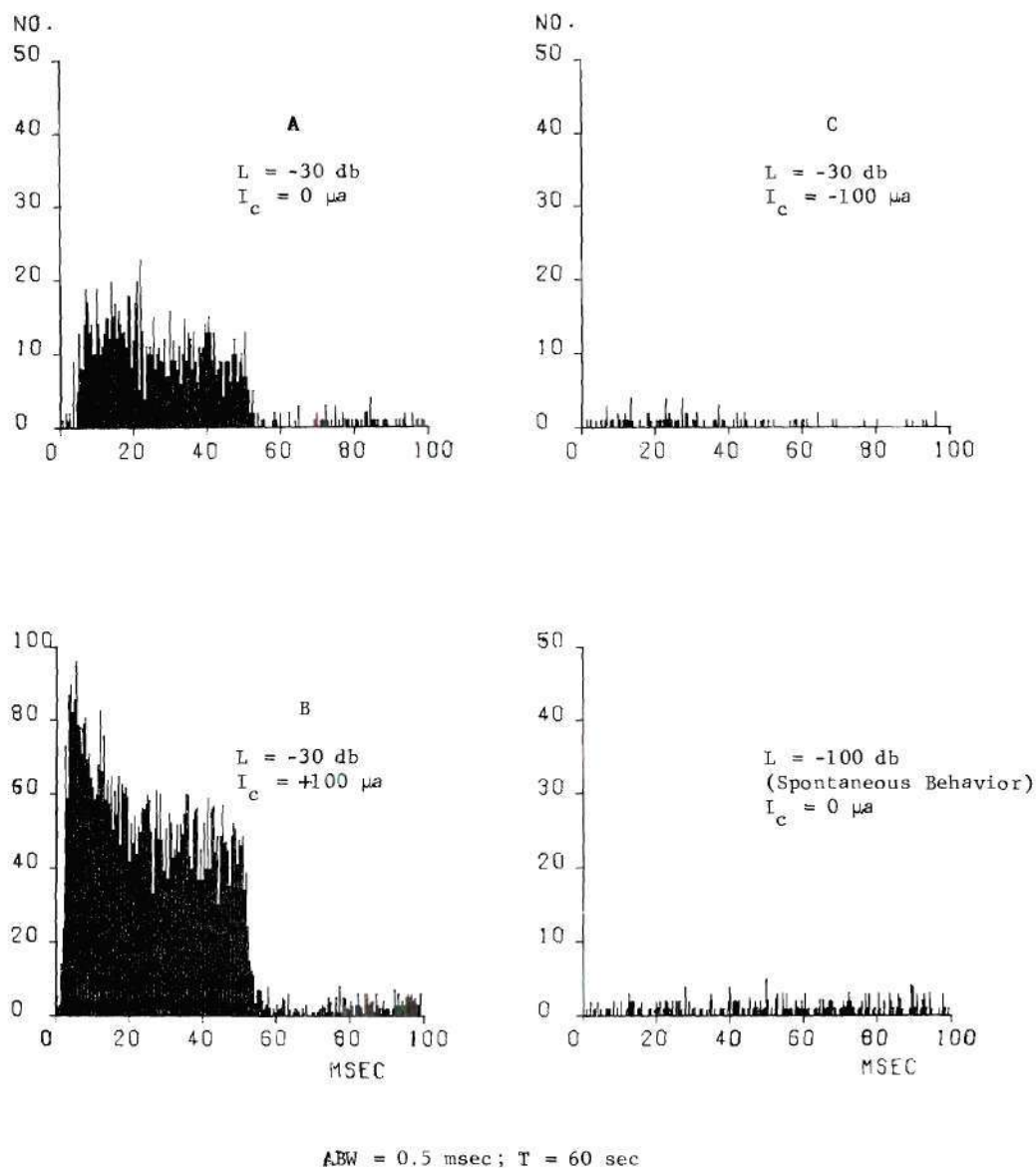
Effects of Prolonged Direct Currents. The effects of long term

direct current passage across the cochlear partition were studied in fibers obtained from seven animals. Since the polarizing current was applied in the basal turn, the search for affected fibers was generally limited to high-CF (7 kHz or greater) units. Responses from almost all such fibers could be altered by current passage. A few units with CF less than 1 kHz were examined, but these showed no current effects.

PST histograms from a typical experiment are given in Figure 31, which shows response patterns for several combinations of I_c and tone burst stimulus level ($f = CF$; $SP = 100$ msec). These patterns show that the presence of the current I_c has a very striking effect on the unit response to sound. Consider Panels A, B, and C, for which L was maintained at -30 dB. With $I_c = 0$, Panel A shows the unit to be responding to the burst, but the lack of a well-defined initial envelope peak indicates that stimulation is near threshold. For $I_c = +100 \mu a$, Panel B, however, shows a much greater response, with a marked initial envelope peak. Panel C indicates that an I_c of -100 μa suppresses the fiber sound response almost completely. The remaining panels show corresponding effects with L increased to -20 dB and I_c 's of $\pm 100 \mu a$ and $\pm 50 \mu a$.

The data of Figure 31 are more conveniently compared in terms of the average spike rates $Q(6:16)$, $Q(20:30)$, and $Q(40:50)$, which are plotted in Figure 32. $Q(6:16)$ gives information about the average response during the initial histogram peaks, and the other rates reflect the later time structure of the response envelope.

Figure 32 shows that for constant L , positive I_c increases all three rates, and negative I_c decreases them. Also, the effectiveness



Stimuli: Tone Bursts; D = 50 msec; $f = 15$ kHz (CF)
 SP = 100 msec; $T_e = 2.5$ msec

Figure 31. PST Histograms, Unit 110-13, for Several Combinations of Current, I_c , and Tone Burst Stimulus Level

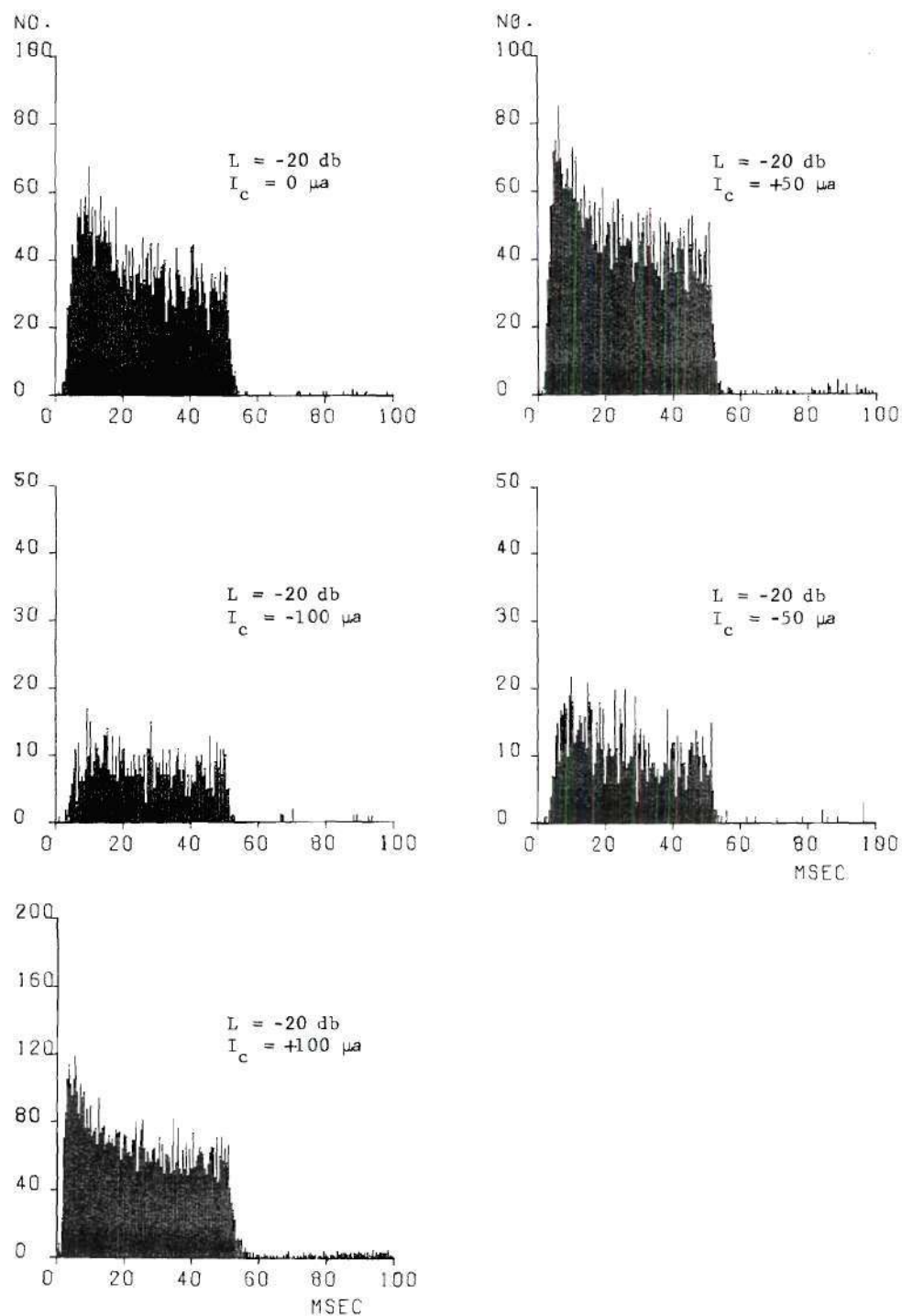


Figure 31. (Continued)

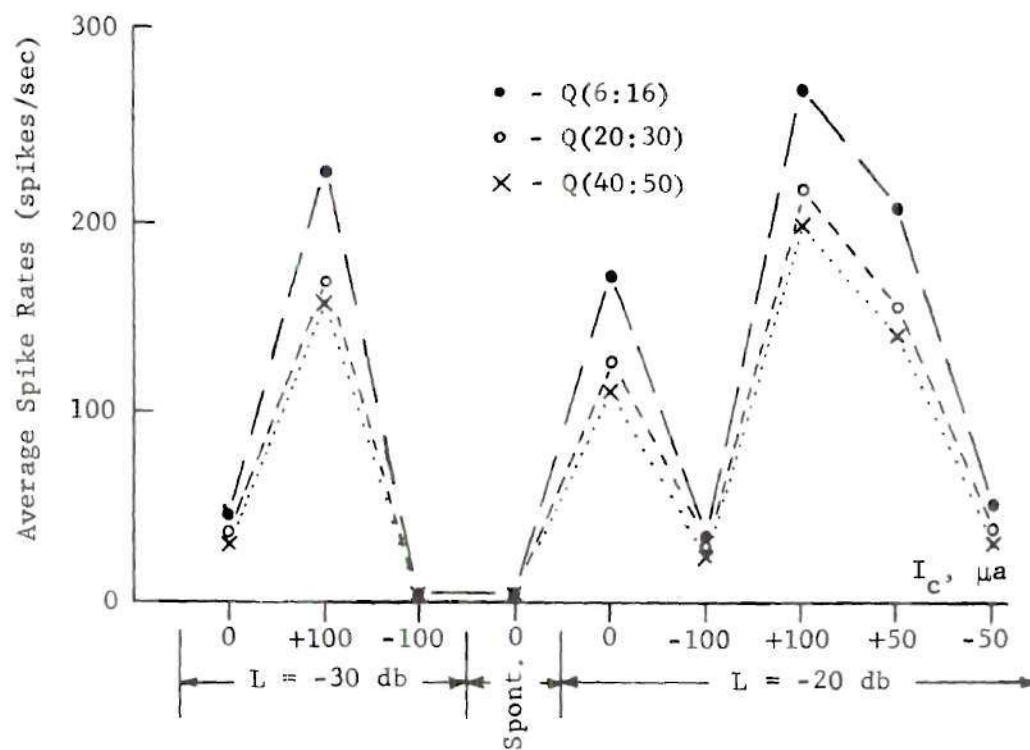


Figure 32. Average Spike Rates, $Q(6:16)$, $Q(20:30)$, and $Q(40:50)$ for Data of Fig. 31

of I_c in changing spike rates increases with current magnitude. Furthermore, the difference in the beginning and ending average rates, $Q(6:16)$ and $Q(40:50)$, is greater (indicating increased initial envelope peaks) as overall response is elevated by positive I_c , and the reverse holds for negative I_c .

It will be recalled from tone burst intensity results presented earlier that the general effect of increasing burst intensity from near threshold is to elevate the steady-state portion of the PST envelope and make the initial histogram peaks more pronounced. Figures 31 and 32 indicate that PST response changes due to I_c follow the same general pattern. In other words, it appears that vestibuli-tympani currents (which increase CM) cause the fiber sound response to change as if the acoustic stimulus level had been increased; and tympani-vestibuli currents (which decrease CM) appear to have the opposite effects. These results are interpreted as supporting of the microphonic theory, since they show that increased microphonic levels are accompanied by increased fiber response, and that decreased spike response accompanies decreased CM. Concurrent results were obtained by Konishi et al. in their work with prolonged dc and ultra-low-frequency alternating currents (26).

The effect of I_c on spontaneous response during the silent portions of the Figure 31 histograms is indicated in Figure 33, which shows $Q(60:100)$ for each histogram. Note that for both values of L , $Q(60:100)$ is increased by positive I_c and decreased by negative I_c . Hence, in this case, the effect of I_c on spontaneous behavior is similar to its effect on sound-evoked activity. Konishi et al. (26) interpreted similar

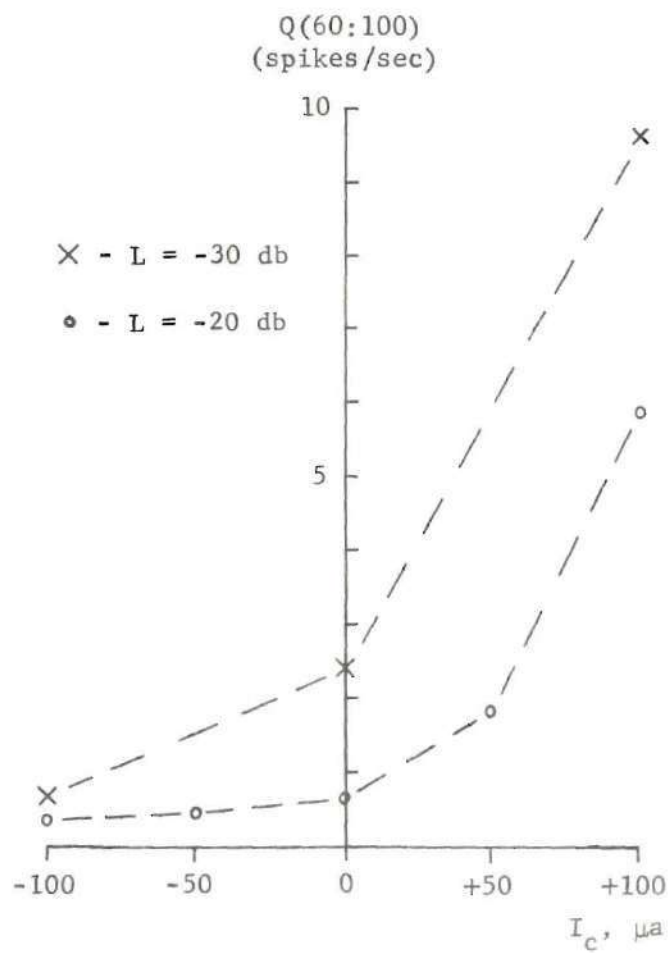


Figure 33. Effect of I_C on $Q(60:100)$ for Data of Fig. 31.

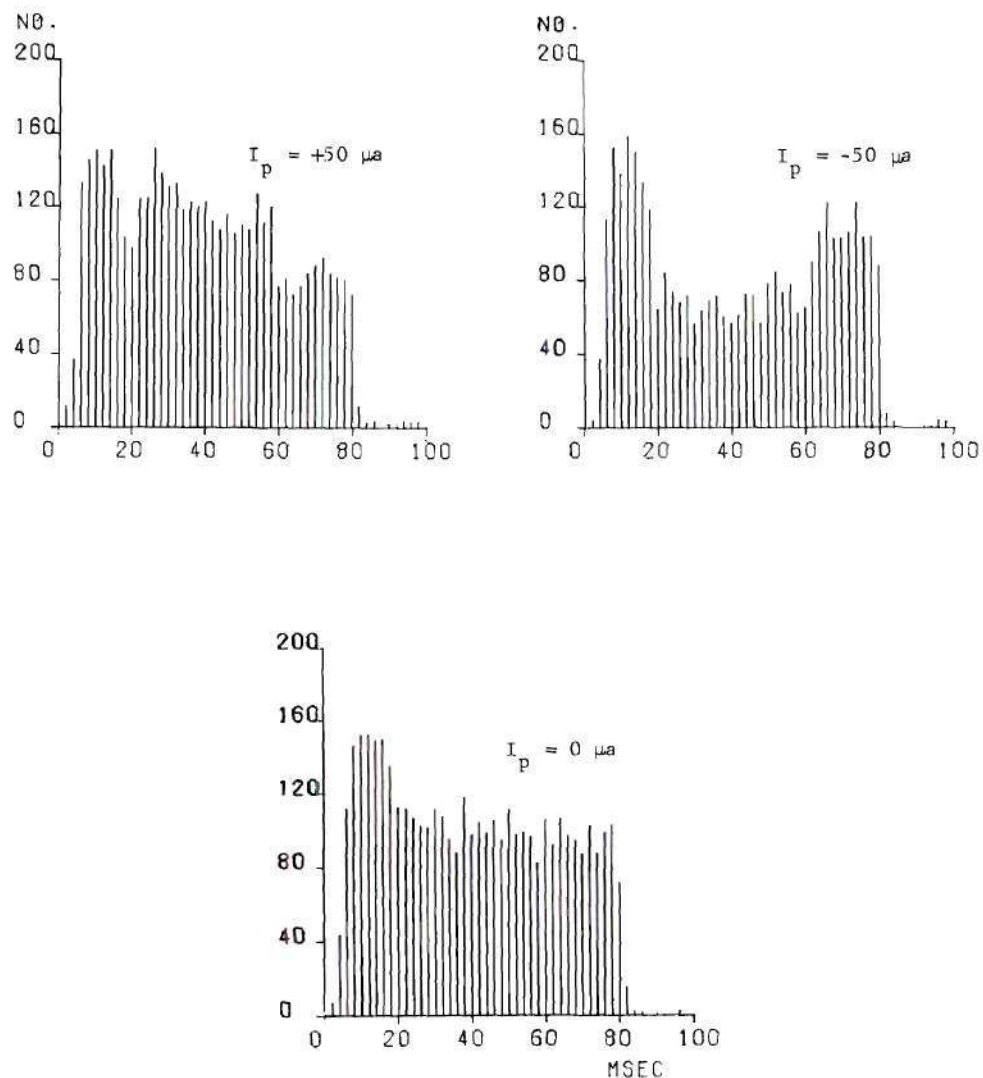
results to mean that spontaneous activity probably arises from random electrical effects in hair cells. The implication is that such effects increase (decrease) in magnitude with positive (negative) I_c and lead to alterations in spontaneous behavior. Since CM also changes with current, it is reasonable that those random effects might result from noise (both electrical and electrophysiological) on the CM signal.

The preceding results are indicative of those obtained in all units which showed response changes with current passage. In every case vestibuli-tympani currents produced increased fiber activity during the tone bursts, and tympani-vestibuli currents had the opposite effect. In most instances, spontaneous activity for silent periods was also changed by I_c in the same direction as response activity, but a few units were seen in which spontaneous rates were not appreciably altered.

Effect of Short Current Pulses. Even though the experiments with long-term direct current passage demonstrate the general effects of externally applied cochlear currents, they give no indication as to how rapidly such currents act. Neither do they show whether or not the nerve responses exhibit any adaptation tendencies associated with increased activity during the passing of positive current. It is known (25) that CM responds immediately at the beginning of polarizing current, so that if the microphonic is directly involved in stimulation, spike activity should in general also change as soon as current begins. Also, adaptation tendencies should be detectable in the early portions of elevated response during the positive current passage, just as they are during fiber response to tone bursts.

To determine how rapidly current effects are manifested and to detect if adaptive tendencies are present during initial current passage, experiments were run in which 40-msec current pulses were applied across the basilar membrane. They were synchronized with the stimulus waveform generator to begin 20 msec after the start of 80-msec tone bursts. The artifact associated with current make and break was considerable, but because the current electrodes were electrically shielded and the pulse edges were smoothed slightly (see Chapter III), the artifact impaired detection of nerve responses for at most 1-2 msec after current switching. In several runs, the measured spike amplitude was great enough so that the artifact was actually below the spike detector level of the signal conditioner.

Pulse current effects were studied in thirty units, all of which gave similar results. Figure 34 shows PST responses for an experiment in which stimulus level, L , was set at 5 dB above the tone burst threshold ($f = CF$; $SP = 100$ msec) and histograms were obtained for pulse currents, I_p , of $+50 \mu A$, $-50 \mu A$, and zero. Response elevation for $I_p = +50 \mu A$ and response depression for $I_p = -50 \mu A$ are clear-cut from the figure. Both effects occur as soon as current is turned on and terminate immediately after current stops. Also, there is a definite adaptation during the response associated with positive I_p . In this case, there is little evidence of adaptation for negative I_p , but four fibers were encountered in which adaptation in the reverse direction occurred for negative I_p , as indicated in Panel B of Figure 36. The positive- I_p adaptation of Figure 30 was seen in all cases where stimulus level was close enough to threshold to allow marked response increase



ABW = 2.0 msec; T = 30 sec

Unit 181-2

Pulse current was turned on at 20 msec and off at 60 msec.

Stimuli: Tone Bursts; D = 80 msec; f = 20 kHz (CF)
L = -40 db; T_e = 2.5 msec

Figure 34. PST Histograms Showing the Effect of Pulse Current, I_p , on Tone Burst Response

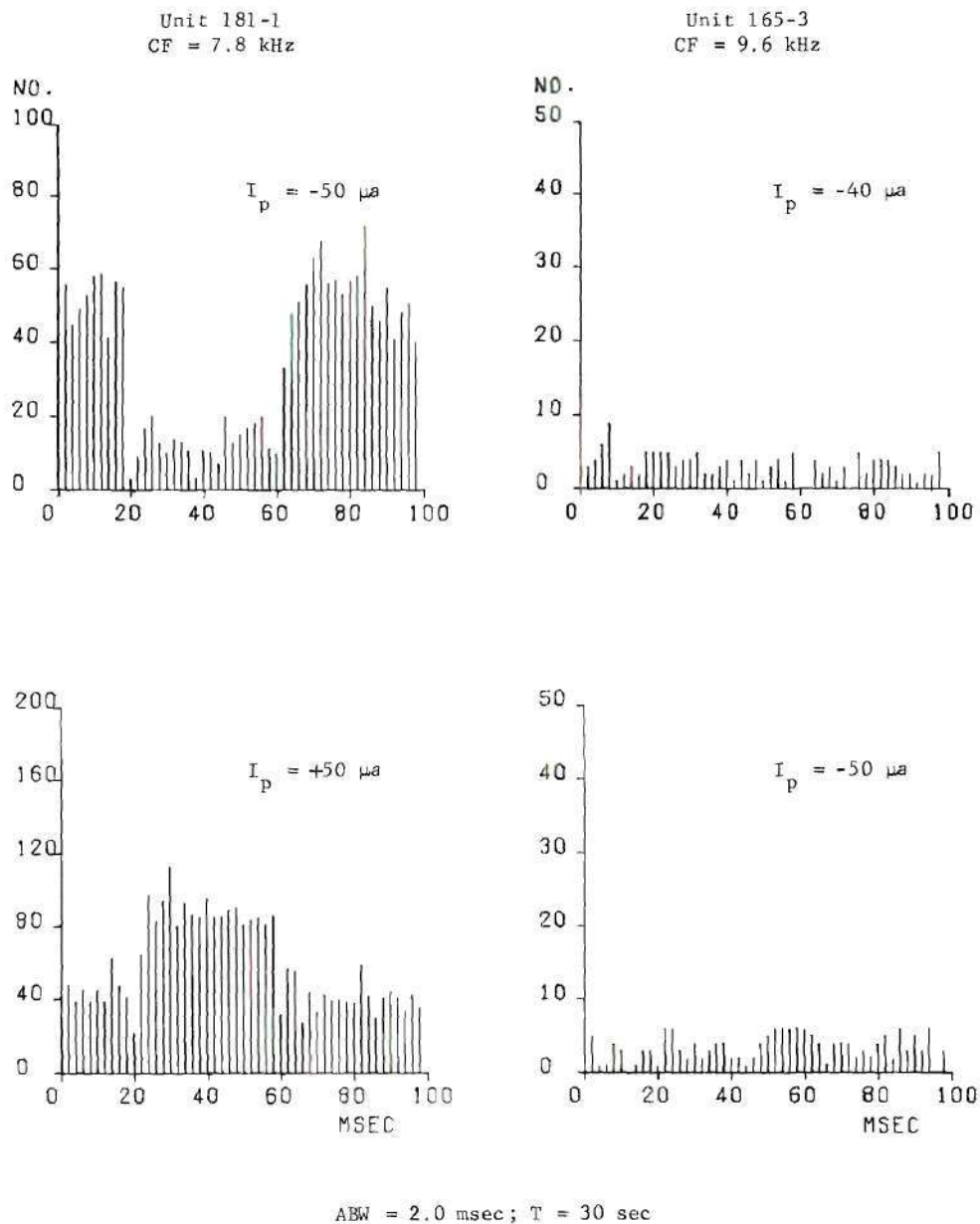
during I_p .

The effect of pulse currents on spontaneous activity was examined in a few units. As in the case of prolonged polarization, not all units responded, but those that did showed immediate current effects. Figure 35 gives results from two units which both had clear pulse current alterations to tone burst stimuli. Spontaneous behavior for unit 181-1 was immediately enhanced for $I_p = +50 \mu\text{a}$ and depressed for $I_p = -50 \mu\text{a}$, while practically no effect can be detected for the other fiber. Due to the low absolute level of the current-produced responses, no adaptation is evident.

These results indicate that the temporal characteristics of response changes accompanying sudden CM shifts due to short currents are consistent with the microphonic trigger theory.

An attempt was also made to compare the effects of equal-magnitude pulse and prolonged direct currents by comparing Q(50:60) for the two conditions under near-threshold tone burst stimulation. No consistent relationship was found. This reflects the observations of Konishi et al. (26) that even though prolonged direct current polarization does have the general results described above, such currents tend to cause time-varying changes in overall firing characteristics. Those authors, however, also showed that 5-sec, dc pulse trains (off time also 5 sec) produce stable responses (27). Hence, the 40-msec pulses of the present study may be assumed to produce no serious long-term alterations in fiber response.

Two additional experimental observations which are consistent with the microphonic trigger theory are now presented.

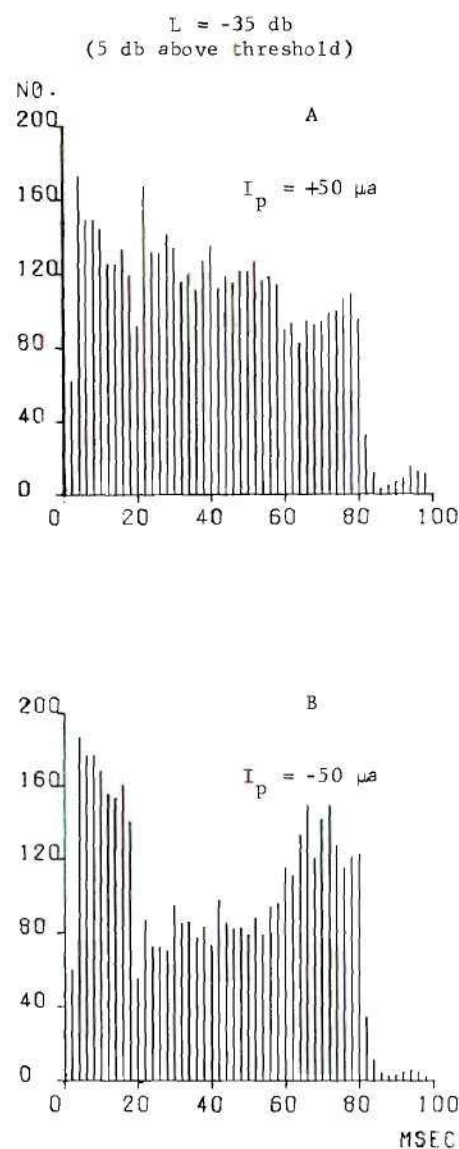


Pulse current was turned on at 20 msec and off at 60 msec.

Figure 35. PST Histograms Showing the Effect of Pulse Current, I_p , on Spontaneous Activity for Two Units

Experiments were performed to contrast the effects of pulse currents at low and high stimulus levels relative to the tone burst threshold, TBT, for a particular unit. Figure 36 shows such a series in which positive and negative 50- μ a pulses were introduced during tone bursts at -35 dB (5 dB above threshold) and at -5 dB. Panels A and B show the expected pulse current effects for low-level stimulation. Average spike rate during current passage, $Q(20:60)$, is 206/sec for $I_p = +50 \mu$ a and 137/sec for -50 μ a. Panels C, D, and E show, however, that the PST envelope is scarcely affected when the same currents are used under much more intense sound stimulation ($L = -5$ dB). At this level, $Q(20:60)$ for both pulse polarities is 171/sec. Histograms not shown indicate that for $L = -5$ dB, this unit is effectively saturated. Thus, it appears that pulse currents which cause response changes at low stimulus levels become ineffective at levels corresponding to maximal fiber stimulation. That is, polarizing currents cannot drive fiber response rates above maximum rates associated with intense sound. This result implies that the effect of polarization currents is to alter a unit's sensitivity to sound so that maximal response rates are reached for lower or higher SPL (depending on I_p polarity) but the attainable rate remains the same, regardless of the current. This suggests that under vestibuli-tympani current (increased CM), the fiber reacts primarily as if the sound level were increased and that the opposite holds for tympani-vestibuli current (decreased CM).

Another example of the similarity between current-controlled sound response and purely acoustic response is that the presence of I_p affects the spike activity outside the current interval. This is



Unit 181-1; ABW = 2.0 msec; T = 30 sec

Pulse current was turned on at 20 msec and off at 60 msec.

Stimuli: Tone Bursts; D = 80 msec; f = 7.8 kHz (CF)
SP = 100 msec; T = 2.5 msec

Figure 36. PST Histograms Showing the Effect of I_p on Response to Tone Bursts at High and Low Levels Relative to Threshold

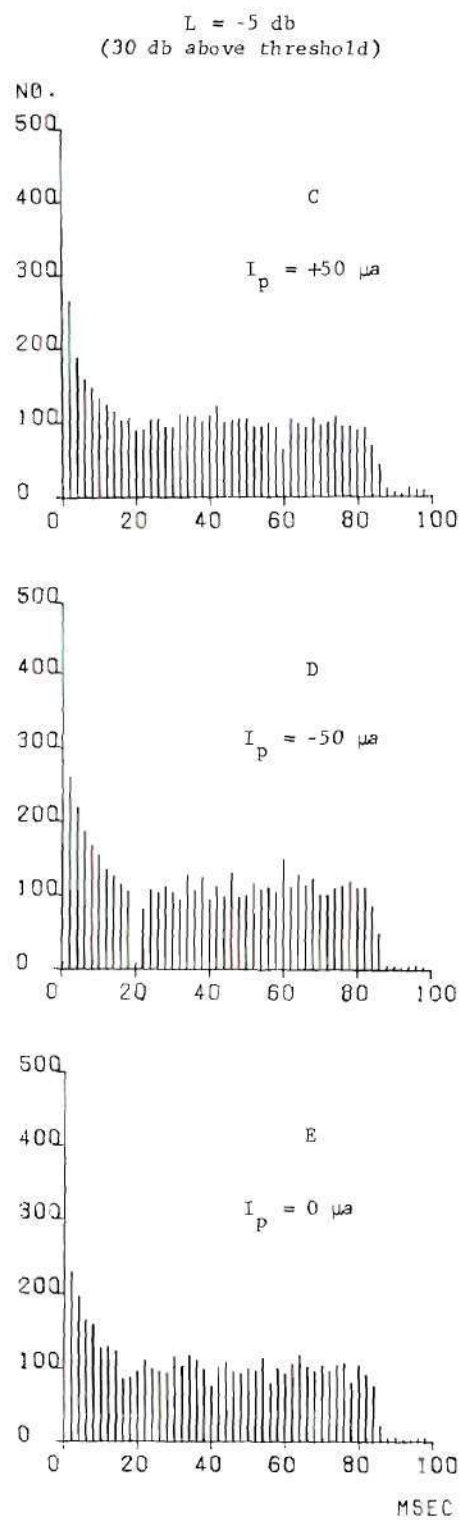


Figure 36. (Continued)

demonstrated, for instance, in the data of Figure 36 (Panels A and B) by comparing the average rates $Q(6:16)$ and $Q(70:80)$ for the two I_p polarities. As I_p changes from $+50 \mu a$ to $-50 \mu a$, $Q(6:16)$ increases from 231/sec to 277/sec, and $Q(70:80)$ increases from 170/sec to 218/sec. In nine of the thirteen units for which similar comparisons are available, these rates shifted correspondingly. The average increases as polarity changed from positive to negative were 12.6/sec for $Q(6:16)$ and 22.2/sec for $Q(70:80)$. Thus, the probability of a sound-evoked response outside the current interval is greater after a short tympani-vestibuli current than after the opposite current. This reflects the fact that the negative current suppresses responses that normally would occur in the current interval. Therefore, when I_p terminates, the fiber is more likely not to have fired recently and is more easily excited by sound in the 70:80 and 6:16 intervals. Likewise, a positive current makes it more likely that the fiber fired recently in the current interval so that there is somewhat less likelihood of response outside. This is the same sort of behavior that would be expected if a shift in sound stimulus level were present in the 20:60 interval instead of current.

Effect of Alternating Currents in the Cochlea. The experiments detailed above show that CM changes produced by currents across the cochlear partition are accompanied by fiber response shifts generally consistent with the trigger hypothesis. Another test of the theory is to subject the fiber endings to completely external audio-frequency current bursts (with no acoustic stimulation) and search for fiber responses to such an "artificial microphonic." This procedure was

attempted using currents of up to 50 μa (p-p), but it produced negative results. Stimulation frequencies varied from a few hundred Hz to 30 kHz, and each of the subjects had been previously employed in successful pulse current experiments, so that they were known to possess fibers responsive to current passage.

As an alternative to pure alternating current stimulation, the stimulator was modified by placing a battery in series with the output so that a 50- μa bias could be added to the alternating current. With this system units were monitored whose tone burst responses were clearly affected by the bias current. Nevertheless, when the sound was turned off and a 50- μa (p-p) alternating signal was added to the bias, no responses associated with the current bursts were found.

Teas et al. (27) also obtained negative results for audio-frequency current stimulation with 100- μa currents (p-p or rms not specified), and they suggest that even larger currents may be necessary to produce stimulation. However, Honrubia and Ward (36) indicate that with no acoustic stimulation the actual direct currents passing naturally through about a 4-mm segment of the organ of Corti are on the order of 6 μa . Direct currents applied from the scala vestibuli to the scala tympani affect about a 4-6 mm segment (25). Thus, if alternating current takes about the same path as direct current, then the densities resulting from 50- or 100- μa currents should be adequate for stimulation, if such currents are the fiber trigger. It is possible that because of distributed capacitances associated with the basilar membrane (2), the current path for alternating currents is different than for direct stimulation, but the rapid effects produced by current

pulses seem to contradict this assumption. Therefore, these results do not seem to substantiate the CM trigger hypothesis, but additional research is needed before a final conclusion can be reached.

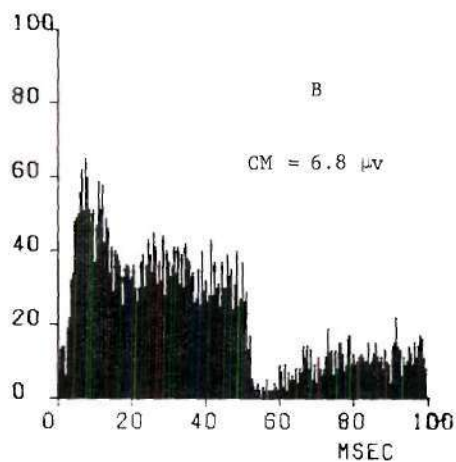
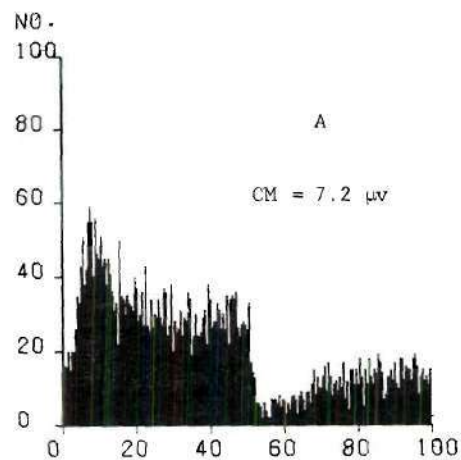
A more definitive experiment would be to introduce the ac stimulation closer to the cochlear partition by moving the scala tympani current electrode up next to the basilar membrane and by moving the other electrode from the scala vestibuli to the scala media and placing it close to the organ of Corti. Presumably this procedure would concentrate current activity in a more restricted segment of the basilar membrane so that a relatively small fraction of fibers would receive increased current densities. Thus, very careful searching for fiber current responses would be necessary.

Microphonic Modification by Cochlear Heating

The second method of CM modification via non-acoustic means was by the application of heat directly to the cochlea. The heat was generated by current passage in a small nichrome coil mounted at the focal point of a spherical reflector. Since no provision was made to measure cochlear temperature, no data were obtained quantifying the relation between hyperthermia and CM change, but in each of four animals investigated, it was found that CM was reduced by infra-red radiation. This reduction could be seen usually within 10-20 seconds after coil current was applied, and, depending on how well the coil was focused, microphonic response to tonal stimulation continued to decline as long as heating current was present. When heating was terminated, CM response always recovered, but recovery generally took longer than the original decline.

Two experiments were performed to study the relation between heat-produced CM loss and fiber activity. In the first, histograms were obtained for 50-msec tone burst stimulation at the CF before, during, and after heat application. Burst level, L, was set at about 5 dB above normal threshold. One shortcoming of this procedure was that during and after heating, CM could not always be held constant for the entire 30-second recording period of a given histogram. Also, because of the low signal-to-noise ratio of the microphonic signal at near threshold stimulation, it was necessary to measure CM with the GR 1900 wave analyzer (using continuous tones at the same level as the bursts). Hence, CM data were available only between histogram runs.

An example of a unit for which CM attenuation remained fairly constant during heating is given in Figure 37. Panel A shows the normal burst response before heat was applied. After these data were recorded, heating current began, and CM for continuous stimulation at the intensity of the tone bursts dropped from 7.2 $\mu\text{v}(\text{rms})$ to 6.8 μv . Heat was then maintained while data for Panel B were recorded, after which CM was still about 6.8 μv . Note that the B histogram is actually somewhat larger than the previous one, which was obtained with a larger CM, a result which would seem to cast some doubt on the microphonic trigger hypothesis. However, after the heating coil was turned off, CM continued decreasing, going down to 5 μv , and at this time, data were taken for Panel C, which shows a severely attenuated fiber response. Afterwards, CM slowly recovered, and the histograms of Panels D and E were generated for initial CM's of 5.5 μv and 6.5 μv .



Unit 172-4; ABW = 0.5 msec; T = 30 sec

Heat was applied only during time that data for Panel B were recorded. Microphonic voltage (CM) at the beginning of each histogram sample period is indicated. See text for further details.

Stimuli: Tone Bursts; SP = 100 msec; $f = 19$ kHz (CF)
 $D = 50$ msec; $L \approx -35$ db; $T_e = 2.5$ msec

Figure 37. PST Response Patterns as CM is Modified by Cochlear Heating

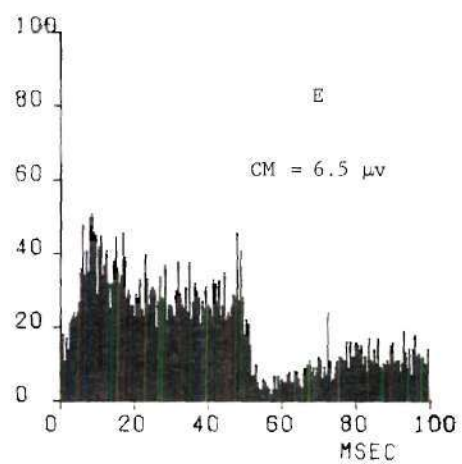
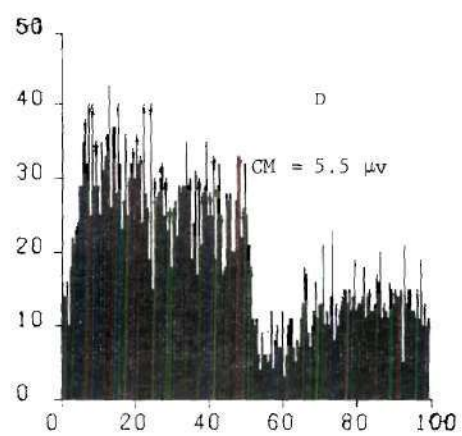
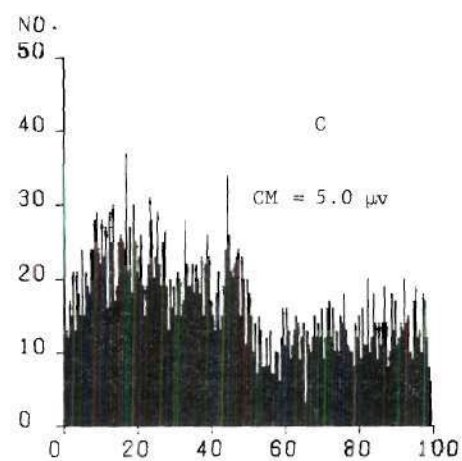
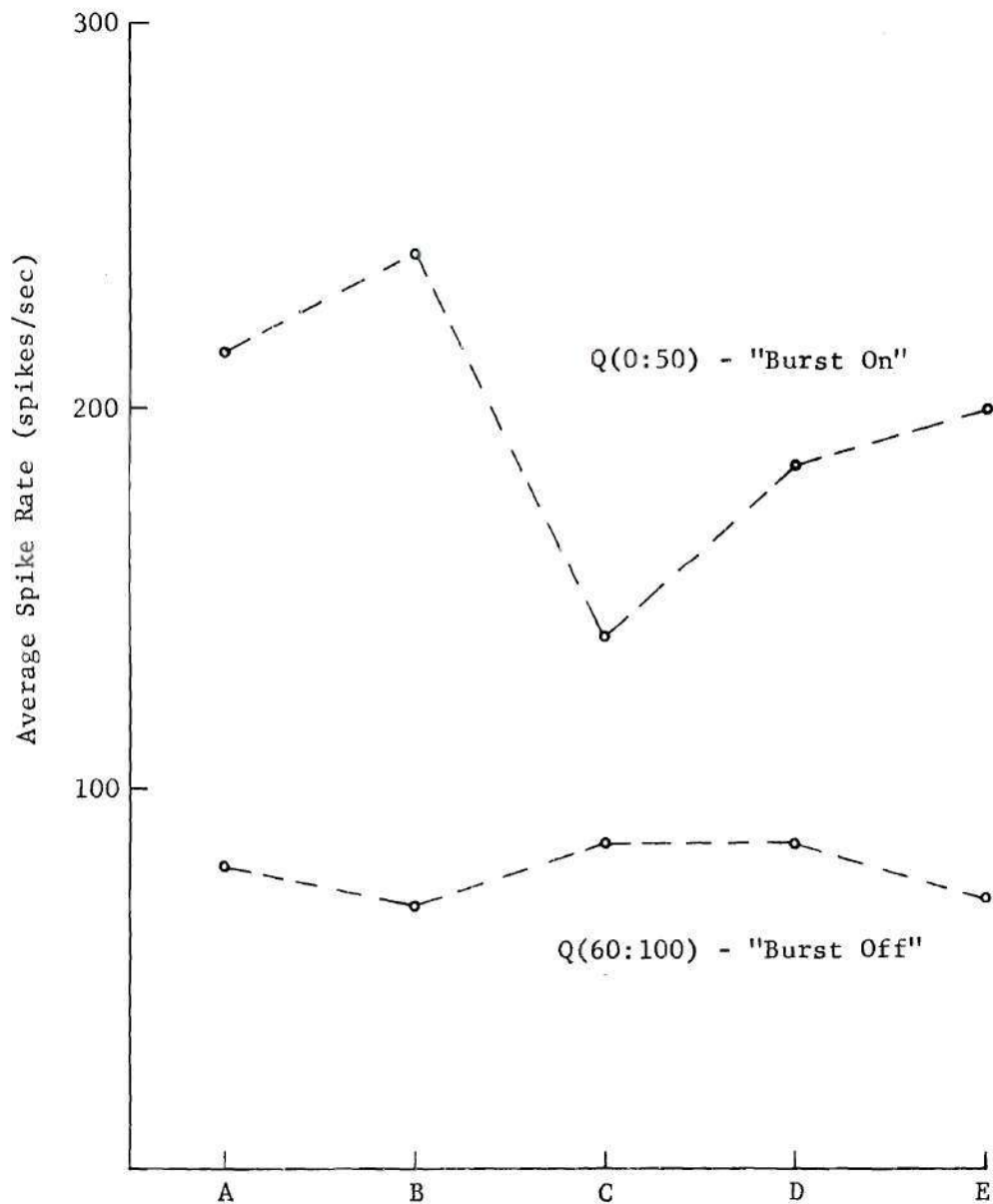


Figure 37. (Continued)

respectively. These show clearly that the fiber response also recovered with the microphonic. These data, then, indicate that when heat is first applied to the cochlea, nerve activity actually increases in spite of small initial drops in CM (0.5 dB, in this case). However, larger heat-produced CM decreases are accompanied by significant reductions in neural activity.

Additional insight into the overall effect of heat on the fiber of Figure 37 is gained by comparing the average spike discharge rates $Q(0:50)$ ("burst-on") and $Q(60:100)$ ("burst-off") for each histogram. These rates are plotted in Figure 38. Response during burst stimulus rose by 13 per cent, but activity during silent periods decreased by about 15 per cent when heat was initially applied and CM loss small. As CM dropped to 5 μ v and recovered, burst-on response decreased and then increased, while burst-off rates changed by small amounts in the opposite directions. This type of behavior is typical of what would be expected if the fiber response changes had been produced by altering only the sound stimulus level. (Recall that increasing burst levels yield increased burst-on responses at the expense of burst-off, or spontaneous, activity.)

Since thermally-induced CM loss could not easily be held constant for complete histogram run periods (30 seconds), another (simpler and more direct) approach was taken for the second heat effect experiment. In this procedure, continuous tone stimulation at near threshold was employed, and average fiber response rates were measured with a GR 1150-BP frequency meter over 10-second intervals as heat was turned on and off. Since the tone stimulus was derived from the wave analyzer,



Histogram of Fig. 37 from Which Rates are Computed

Figure 38. Average Spike Rates $Q(0:50)$ and $Q(60:100)$ for Histograms of Fig. 37

CM level was continuously monitored and recorded at the same time intervals for which average response rates were computed. Stimulating frequency, f , in many of these runs was not the same as the characteristic frequency because of the relatively low thresholds of some fibers (about -60 dB for tone bursts at CF). If these fibers had been stimulated at CF near threshold, the resulting CM would have been too small for reliable measurement, even with the wave analyzer. Good measurements required sound levels of about -35 dB, a level which caused the fiber spike response at CF to become saturated. Therefore, in these cases, a lower stimulus frequency, for which the unit's threshold was near -35 dB, was selected.

Results from one such experiment are depicted in Figure 39. This run is of particular interest since the fiber was held long enough to record time histories of CM and response rate for two different heating periods. In the first run, heating current was on for 60 seconds, which was sufficient to decrease CM by about 3 dB (11.5 μ v to 8 μ v). During this time, though, the fiber response rate increased by about 11 per cent. When heating stopped, CM returned (after some overshoot) to near its initial value, at which time fiber response had fallen almost to its original level. Approximately five minutes later, heat was applied for 120 sec. Both CM and response rate curves began as before (CM decrease; response rate increase), but because of the longer heating time, CM ultimately decreased by 7 dB. During this run, there was a definite lessening of fiber response as CM fell, the effect being first noticeable for about 4 dB of CM decrease.

All but one of the seven fibers studied for the conditions

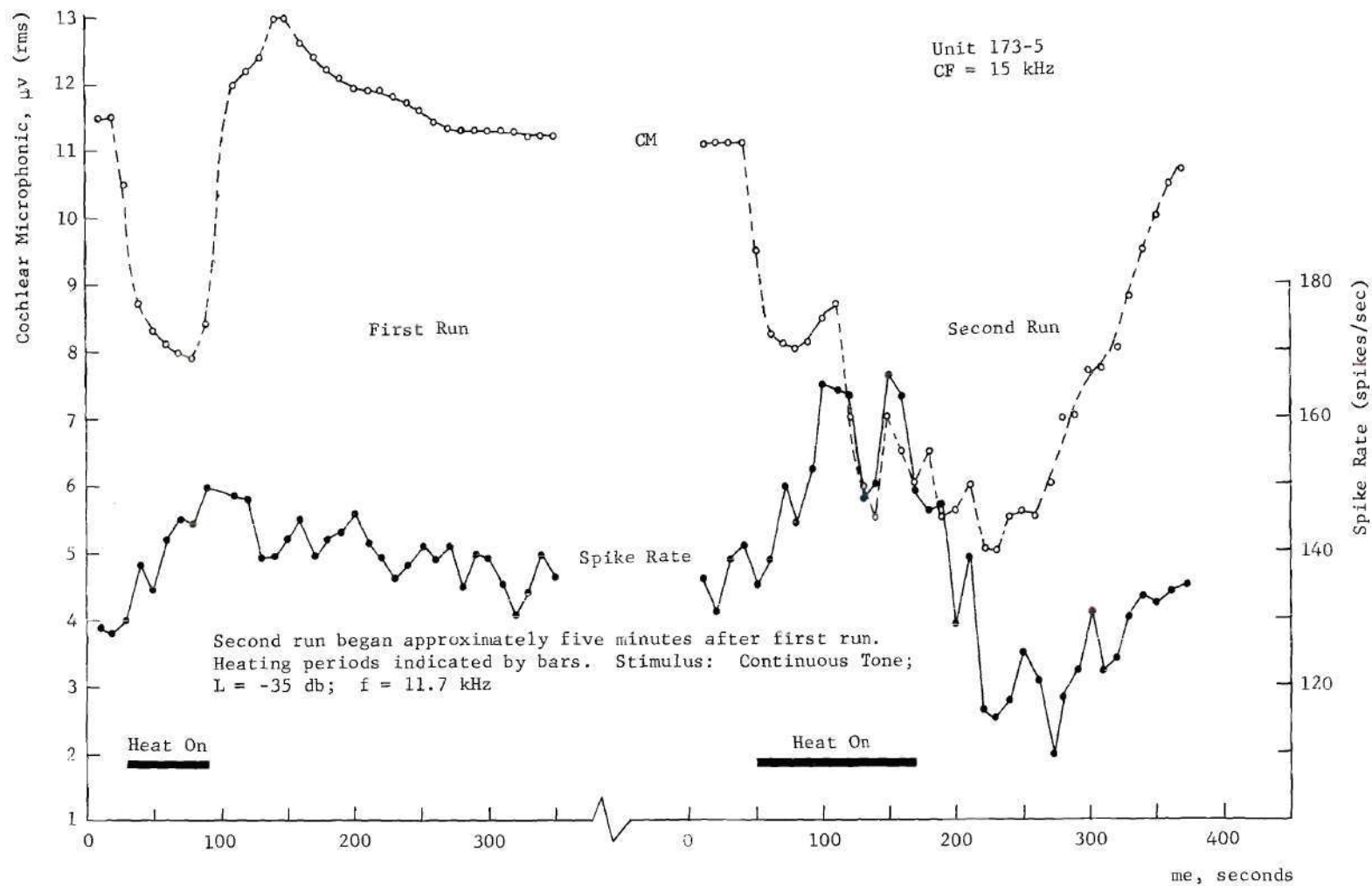


Figure 39. Effect of Heat Applied to Cochlea on CM and Average Fiber Response Rate

described above showed these same general characteristics for the combination of tonal stimuli and direct cochlear heating. Thus, both heating experiments indicate consistent results; i.e., that small heat-produced CM loss (say, 3 dB or less) is usually accompanied by moderate fiber response increase, but larger losses (say, more than 6 dB) can affect the initial fiber response increase and result in overall reduction of fiber activity. It is difficult to be more specific about the exact degree of microphonic attenuation necessary for spike response rate changes to occur because CM as measured in these experiments probably reflects the activity of only a few millimeters of the basilar membrane in the basal turn (25). Hence, there can be little certainty about how the microphonic is reacting to heat in the immediate region innervated by a particular fiber under study. It is assumed that CM shifts in the same direction for the entire cochlea, but it is possible that the non-radiated portions of the turns are affected to a lesser degree than the remainder.

At first glance, the thermal effects described above appear inconsistent with the microphonic trigger theory because spike activity can in fact increase while CM is decreasing. One possible explanation which accounts for this phenomenon and yet leaves intact the CM trigger hypothesis is that the heating effects result from two opposing reactions. The first reaction would be general increase in fiber sensitivity to its final excitatory agent. This would be in agreement with generally accepted principles concerning the excitability changes of neural elements for temperature increase. The second reaction would be a decrease in the magnitude of the excitatory agent. The first

process would lead to fiber response changes indicative of stimulus increase, while the second should produce changes associated with stimulus decrease. It is not difficult to envision time structures for these two reactions which together would account for fiber response changes like those seen in Figures 38 and 39. The fact that CM does indeed decrease with heating leaves open the possibility that it is actively involved in the ultimate excitatory process of spike initiation. Therefore, the effects of cochlear heating can be interpreted as supporting the CM trigger theory.

Summary of Results

The results presented above may be summarized as follows:

Two types of experiments were performed. The goal of the first was to characterize the way that single auditory fibers in the guinea pig respond to tone bursts and clicks of varying parameters.

It was found that the PST responses to tone burst stimuli possess certain characteristics, and that those characteristics reflect changes in stimulus parameters such as intensity and stimulus period. In general, the PST tone burst envelope shows that the probability of a spike occurrence is greatest at the beginning of the burst, falls to a fairly constant value for the remainder of the burst, and then becomes very small immediately afterwards. The probability then begins to recover to the level associated with spontaneous behavior. The effect of changing burst duration is usually just to prolong the steady-state portion of the envelope, but cases were seen in which steady-state level and initial envelope peaks were reduced under long bursts. Burst

intensity tests showed that as burst level is increased, initial peaks become more pronounced and the spontaneous activity between bursts becomes suppressed. Also the steady-state envelope level increases with SPL, but only over about a 20-40 dB range above threshold. The saturation level is not exceeded as sound grows more intense. Experiments with bursts of increasing repetition rate (decreasing SP) showed that tone burst response does not appreciably depend on repetition rate as long as burst rate is 10/sec or less. However, if stimuli appear more rapidly than 15-20/sec, the average response rate during the bursts declines and initial envelope peaks are diminished.

Other results obtained with tone burst stimuli include the demonstration of phase-locking of fiber responses to individual cycles of the tone, which was seen for frequencies up to about 2 kHz. Also, a few tuning curves were generated. They reflect the fact that fibers respond to practically all frequencies below the CF if the level is great enough, but that response falls rapidly for stimulation frequencies above the CF.

PST response patterns for click stimuli were shown to depend on CF; i.e., high-CF units show single peaks that grow with click level, and low-CF units exhibit multiple peaks separated approximately by $1/CF$. Also the latency of the first histogram peak decreases as CF increases, a result which verifies the fact that high-CF fibers innervate the basal portion of the cochlea and low-CF units the more apical portions. Finally, comparison of low-CF fiber responses to opposite click polarities indicates that the direction of basilar membrane motion associated with rarefaction clicks is excitatory, and that the other direction is

inhibitory. All these response characteristics are in agreement with those obtained under similar stimulus conditions with cats and monkeys.

The goal of the second type of experiment was to test the cochlear microphonic trigger theory by altering microphonic responses through non-auditory means and showing that concomitant changes in fiber response occur.

It was found that CM modification by direct current passage across the cochlear partition is accompanied by marked changes in fiber response for high-CF units. In general, vestibuli-tympani currents (which increase CM) result in increased fiber activity (both sound-evoked and spontaneous), and tympani-vestibuli currents decrease fiber response. The phenomena occur for both prolonged current passage and for 40-msec current pulses. However, prolonged current application tends to cause time-varying overall response patterns, whereas current pulses produce stable long term response behavior.

PST histograms obtained with tone bursts accompanied by current pulses show that the effect of the current is immediate, and that the fiber response during current action shows an adaptive tendency similar to the adaptation which marks the beginning of a normal tone burst response. It was also shown that when a unit is responding maximally to intense stimulation, the polarization current has little or no effect. Furthermore, tympani-vestibuli pulses tend to increase fiber activity outside the current interval, and the reverse current has the opposite effect.

In contrast to the striking effects of dc currents, the attempt

to stimulate nerve fibers directly with audio-frequency alternating current bursts produced negative results. Even when the ac signal was added to a dc bias which was capable of changing response, no spike behavior associated with the ac bursts was detected.

Finally, CM levels were altered by the application of heat directly to the cochlea. This procedure results in a reduction in CM. It was demonstrated that fiber activity, as measured by PST response patterns and by average spike rates, actually increases with small heat-produced loss, but that if the loss is greater than, say, 4-6 dB, the fiber response is inhibited.

The results from CM modification by direct current and by cochlear heating are interpreted as strengthening the microphonic trigger hypothesis, since both types of modification are accompanied by fiber response changes that would be expected if the CM change had been produced by sound level changes. The lack of response to pure current stimulation does not support the hypothesis, but additional experimentation with more concentrated current application is needed before definite conclusions can be reached in this regard.

CHAPTER V

CONCLUSIONS AND RECOMMENDATIONS

It is concluded that:

(1) Response patterns of individual primary auditory nerve fibers in the guinea pig for tone burst and click stimuli have been characterized and shown to exhibit the same general characteristics as those that have also been generated with cat and monkey fibers. This is based on the comparison of PST and ISI histograms, tuning curves, and phase-locking results from guinea pig fibers with the same response measures in the other species.

(2) Prolonged and pulsed direct currents in the cochlea produce concomitant cochlear microphonic and fiber response changes consistent with the microphonic trigger hypothesis. That is, fiber response increase (decrease) accompanies current-produced CM increase (decrease).

(3) Heat applied to the cochlea alters microphonic and fiber activity in a manner which may also be interpreted as supporting the microphonic theory. Heat-produced CM loss, if great enough, is accompanied by a reduction in fiber spike response.

It is recommended that the investigation into the effects of electric currents and cochlear temperature modification be continued and extended. Possible studies related to current effects include the following:

(1) Parametric studies relating the effects of current application for a wider range of current level and sound intensity.

(2) Experiments to determine the effects of polarizing currents on responses to frequencies other than the CF.

(3) Additional tests with alternating current stimulation in which the current electrodes are closer to the organ of Corti.

(4) Experiments to determine the effects of polarizing current on fiber responses to stimuli other than tone bursts and to multiple stimuli.

Additional investigations into temperature effects include the following.

(1) Determination of the effect of cochlear cooling on fiber activity.

(2) Measurement of the cochlear temperature changes caused by heating or cooling with small thermocouple or thermistor sensors.

It is also recommended that current and temperature procedures be combined to determine if the effects of one can be offset by the other.

BIBLIOGRAPHY

1. E. G. Wever, Theory of Hearing, John Wiley and Sons, Inc., New York, 1949.
2. Georg von Békésy, Experiments in Hearing, McGraw-Hill Book Company, Inc., New York, 1960.
3. Hallowell Davis, "Biophysics and Physiology of the Inner Ear," Physiological Reviews, Vol. 37, pp. 1-49, 1966.
4. N. Y. S. Kiang, "Stimulus Coding in the Auditory Nerve and Cochlear Nucleus," Acta Oto-Laryngologica, Vol. 59, pp. 186-200, 1965.
5. B. M. Johnstone, K. J. Taylor, and A. J. Boyle, "Mechanics of the Guinea Pig Cochlea," Journal of the Acoustical Society of America, Vol. 47, pp. 504-509, 1970.
6. J. L. Flanagan, "Computational Model for Basilar Membrane Displacement," Journal of the Acoustical Society of America, Vol. 34, pp. 1370-1376, 1962.
7. W. M. Siebert, "Models for the Dynamic Behavior of the Cochlear Partition," Quarterly Progress Report No. 64, Research Laboratory of Electronics, Massachusetts Institute of Technology, pp. 242-258, 1962.
8. H. Spoendlin, "Ultrastructure and Peripheral Innervation Pattern of the Receptor in Relation to the First Coding of the Acoustic Message," pp. 89-125 of Hearing Mechanisms in Vertebrates, ed. by A. V. S. De Reuck and J. Knight, Little, Brown, and Co., Boston, 1968.
9. R. Galambos and H. Davis, "Responses of Single Auditory Nerve Fibers to Acoustic Stimulation," Journal of Neurophysiology, Vol. 6, pp. 39-57, 1943.
10. I. Tasaki, "Nerve Impulses in Individual Auditory Nerve Fibers of Guinea Pig," Journal of Neurophysiology, Vol. 17, pp. 97-122, 1954.
11. Y. Katsuki, T. Sumi, H. Uchiyama, and T. Watanabe, "Electric Responses of Auditory Neurons in Cat to Sound Stimulation," Journal of Neurophysiology, Vol. 21, pp. 569-588, 1958.
12. A. Rupert, G. Moushegian, and R. Galambos, "Unit Responses from Auditory Nerve of the Cat," Journal of Neurophysiology, Vol. 26, pp. 449-465.

BIBLIOGRAPHY (Continued)

13. Y. Katsuki, N. Suga, and Y. Kanno, "Neural Mechanism of the Peripheral and Central Auditory System in Monkeys," Journal of the Acoustical Society of America, Vol. 34, pp. 1396-1410, 1962.
14. Y. Katsuki, T. Watanabe, and N. Suga, "Interaction of Auditory Neurons in Response to Two Sound Stimulation in Cat," Journal of Neurophysiology, Vol. 22, pp. 603-623, 1959.
15. M. Nomoto, N. Suga, and Y. Katsuki, "Discharge Pattern and Inhibition of Primary Auditory Nerve Fibers in the Monkey," Journal of Neurophysiology, Vol. 27, pp. 768-787, 1964.
16. J. E. Rose, J. F. Brugge, D. J. Anderson, and J. E. Hind, "Phase-Locked Response to Low-Frequency Tones in Single Auditory Nerve Fibers of the Squirrel Monkey," Journal of Neurophysiology, Vol. 30, pp. 769-793, 1967.
17. J. E. Hind, D. J. Anderson, J. F. Brugge, and J. E. Rose, "Coding of Information Pertaining to Paired Low-Frequency Tones in Single Auditory Nerve Fibers of the Squirrel Monkey," Journal of Neurophysiology, Vol. 30, pp. 794-816, 1967.
18. N. Y. S. Kiang, T. Watanabe, E. C. Thomas, and L. F. Clark, Discharge Patterns of Single Fibers in the Cat's Auditory Nerve, The M. I. T. Press, Cambridge, Massachusetts, 1965.
19. P. R. Gray, A Statistical Analysis of Electrophysiological Data from Auditory Nerve Fibers in Cat, Technical Report 451, Research Laboratory of Electronics, Massachusetts Institute of Technology, 1966.
20. G. R. Hanna, Neural Information Processing in the Peripheral Auditory System of the Guinea Pig, U. S. Air Force Technical Report AMRL-TR-66-87, 1966.
21. E. G. Wever, "Electrical Potentials of the Cochlea," Physiological Reviews, Vol. 46, pp. 102-127, 1966.
22. H. Davis, "Biophysics and Physiology of the Inner Ear," Physiological Reviews, Vol. 37, pp. 1-49, 1957.
23. I. Tasaki, H. Davis, and D. H. Elderedge, "Exploration of Cochlear Potentials in Guinea Pig with a Microelectrode," Journal of the Acoustical Society of America, Vol. 26, pp. 765-773, 1954.
24. I. Tasaki, H. Davis, and J.-P. Legoux, "The Space-Time Pattern of Cochlear Microphonics (Guinea Pig), as Recorded by Differential Electrodes," Journal of the Acoustical Society of America, Vol. 24, pp. 502-519, 1952.

BIBLIOGRAPHY (Continued)

25. I. Tasaki and C. Fernández, "Modification of Cochlear Microphonics and Action Potentials by KCl Solution and by Direct Currents," Journal of Neurophysiology, Vol. 15, pp. 497-512, 1952.
26. T. Konishi, D. C. Teas, and J. S. Wernick, "Effects of Electrical Current Applied to Cochlear Partition on Discharges in Individual Auditory-Nerve Fibers. I. Prolonged Direct-Current Polarization," Journal of the Acoustical Society of America, Vol. 47, pp. 1519-1526, 1970.
27. D. C. Teas, T. Konishi, and J. S. Wernick, "Effects of Electrical Current Applied to Cochlear Partition on Discharges in Individual Auditory-Nerve Fibers. II. Interaction of Electrical Polarization and Acoustic Stimulation," Journal of the Acoustical Society of America, Vol. 47, pp. 1527-1537, 1970.
28. R. A. Butler, T. Konishi, and C. Fernández, "Temperature Coefficients of Cochlear Potentials," American Journal of Physiology, Vol. 199, pp. 688-692, 1960.
29. G. L. Gerstein and N. Y. S. Kiang, "An Approach to the Quantitative Analysis of Electrophysiological Data from Single Neurons," Biophysical Journal, Vol. 1, pp. 15-28, 1960.
30. L. L. Beranek, Acoustic Measurements, John Wiley and Sons, New York, pp. 730-735, 1949.
31. D. W. Kennard, "Glass Microcapillary Electrodes used for Measuring Potential in Living Tissues," pp. 534-567 of P. E. K. Donaldson's book, Electronic Apparatus for Biological Research, Academic Press, Inc. New York, 1958.
32. O. F. Schanne, M. Lavallée, R. Laprade, and S. Gagné, "Electrical Properties of Glass Microelectrodes," Proceedings IEEE, Vol. 56, pp. 1072-1082, 1968.
33. P. Dallos, Z. G. Schoeny, D. W. Worthington, and M. A. Cheatham, "Cochlear Distortion: Effect of Direct-Current Polarization," Science, Vol. 164, pp. 449-451, 1969.
34. I. A. Silver, "Other Electrodes," pp. 568-581 of P. E. K. Donaldson's book, Electronic Apparatus for Biological Research, Academic Press, Inc., New York, 1958.
35. M. Lawrence, "Dynamic Range of the Cochlear Transducer," Cold Spring Harbor Symposia on Quantitative Biology, Vol. 30, pp. 159-176, 1965.

BIBLIOGRAPHY (Continued)

36. V. Honrubia and P. H. Ward, "Mechanism of Production of Cochlear Microphonics," Journal of the Acoustical Society of America, Vol. 47, pp. 498-503, 1970.

VITA

Huey Neal Nunnally was born in Atlanta, Georgia, on December 28, 1944. He is the son of M. E. Nunnally and Mary Petty Nunnally. He was married to Shirley Elaine Jones, also of Atlanta, on December 14, 1968.

He attended elementary school in Decatur, Georgia, and graduated from Avondale High School in June, 1962. In September of 1962, he entered the Georgia Institute of Technology and in June of 1966, received a Bachelor of Electrical Engineering. He was elected to membership in Eta Kappa Nu, Tau Beta Pi, and Phi Kappa Phi.

After holding a summer job with the Lockheed-Georgia Company, Marietta, Georgia, in 1966, he entered the Graduate Division of the Georgia Institute of Technology and received the M.S.E.E. degree in September, 1967.

He held a NASA Traineeship from September, 1966, through August, 1969, and a Graduate Research Assistantship from September, 1969, to March, 1971.